AFFDL-TR-76-133
ADA 048 847

GENERALIZED PROCEDURES FOR TRACKING CRACK GROWTH IN FIGHTER AIRCRAFT

MCDONNELL DOUGLAS CORPORATION
MCDONNELL AIRCRAFT COMPANY
P.O. BOX 516
ST. LOUIS, MISSOURI 63166

JANUARY 1977

TECHNICAL REPORT AFFDL-TR-76-133

FINAL REPORT FOR PERIOD 15 SEPTEMBER 1975 - 15 OCTOBER 1976

AIR FORCE FLIGHT DYNAMICS LABORATORY
AIR FORCE WRIGHT AERONAUTICAL LABORATORIES
AIR FORCE SYSTEMS COMMAND
WRIGHT-PATTERSON AIR FORCE BASE, OHIO 45433

NOTICE

When Government drawings, specifications, or other data are used for any purpose other than in connection with a definitely related Government procurement operation, the United States Government thereby incurs no responsibility nor any obligation whatsoever; and the fact that the government may have formulated, furnished, or in any way supplied the said drawings, specifications, or other data, is not to be regarded by implication or otherwise as in any manner licensing the holder or any other person or corporation, or conveying any rights or permission to manufacture, use or sell any patented invention that may in any way be related thereto.

This report has been reviewed by the Information Office (OI) and is releasable to the National Technical Information Service (NTIS). At NTIS, it will be available to the general public, including foreign nations.

This technical report has been reviewed and is approved for publication.

Terry D. Gray

TERRY D. GRAY, Proj Engr

FOR THE COMMANDER

R.M. Bader

ROBERT M. BADER, Chief
Structural Integrity Br

Howard L. Farmer

HOWARD L. FARMER, Colonel, USAF
Chief, Structural Mechanics Division

Copies of this report should not be returned unless return is required by security considerations, contractual obligations, or notice on a specific document.

AIR FORCE/56780/5 December 1977 — 500

UNCLASSIFIED

SECURITY CLASSIFICATION OF THIS PAGE *(When Data Entered)*

REPORT DOCUMENTATION PAGE		READ INSTRUCTIONS BEFORE COMPLETING FORM
1. REPORT NUMBER AFFDL-TR-76-133	2. GOVT ACCESSION NO.	3. RECIPIENT'S CATALOG NUMBER
4. TITLE *(and Subtitle)* GENERALIZED PROCEDURES FOR TRACKING CRACK GROWTH IN FIGHTER AIRCRAFT		5. TYPE OF REPORT & PERIOD COVERED Final Technical Report 15 Sept 75 - 15 Oct 76
		6. PERFORMING ORG. REPORT NUMBER
7. AUTHOR(s) G. S. Parker		8. CONTRACT OR GRANT NUMBER(s) F33615-75-C-3136
9. PERFORMING ORGANIZATION NAME AND ADDRESS McDonnell Aircraft Company P.O. Box 516 St. Louis, Mo. 63166		10. PROGRAM ELEMENT, PROJECT, TASK AREA & WORK UNIT NUMBERS 13670323
11. CONTROLLING OFFICE NAME AND ADDRESS Air Force Flight Dynamics Laboratory Wright-Patterson Air Force Base Dayton, Ohio 45433		12. REPORT DATE January 1977 13. NUMBER OF PAGES 167
14. MONITORING AGENCY NAME & ADDRESS*(if different from Controlling Office)* same		15. SECURITY CLASS. *(of this report)* Unclassified 15a. DECLASSIFICATION/DOWNGRADING SCHEDULE

16. DISTRIBUTION STATEMENT *(of this Report)*

Approved for Public Release: Distribution Unlimited

17. DISTRIBUTION STATEMENT *(of the abstract entered in Block 20, if different from Report)*

18. SUPPLEMENTARY NOTES

19. KEY WORDS *(Continue on reverse side if necessary and identify by block number)*

Crack Growth Tracking	Spectrum Development	Flight Loads Recorders
Individual Aircraft Tracking	Crack Growth Analysis	
Force Management	Crack Growth Retardation	
Damage Tolerance	Mathematical Models	
Durability	Flight Loads Data	

20. ABSTRACT *(Continue on reverse side if necessary and identify by block number)*

This study is composed of three major parts, (1) effects of usage parameters on crack growth, (2) development of generalized procedures, and (3) implementation of the tracking program.

During the development of generalized procedures, crack growth trends and alternate methods of tracking were established. In addition, the recorded data requirements have been evaluated.

The effort regarding implementation of a tracking program consisted of an evaluation of logistics and the identification of technical difficulties and potentially significant costs.

DD FORM 1 JAN 73 1473 EDITION OF 1 NOV 65 IS OBSOLETE

UNCLASSIFIED

SECURITY CLASSIFICATION OF THIS PAGE *(When Data Entered)*

FOREWORD

This report was prepared by McDonnell Aircraft Company (MCAIR), St. Louis, Missouri, for the Structural Integrity Branch, Structural Mechanics Division, Air Force Flight Dynamics Laboratory, Wright-Patterson Air Force Base, Ohio under contract F33615-75-C-3136, Project 1367, "Structural Integrity for Military Aerospace Vehicles," Task 136703, "Fatigue, Fracture and Reliability Analysis and Design Methods for Aerospace Vehicles," Work Unit 13670323, "Generalized Procedures for Tracking Crack Growth in Individual Fleet Aircraft." Mr. Terry D. Gray (AFFDL/FBE) served as technical monitor.

The program manager for MCAIR was Mr. E.D. Bouchard. The MCAIR Principal Investigator was Mr. Grant S. Parker. A major MCAIR contributor was Dr. Richard E. Pinckert.

This report covers work accomplished during the period 15 Sep 75 to 15 Oct 76.

This report was released by the author in February 1977.

TABLE OF CONTENTS

TABLE OF CONTENTS (Continued)

LIST OF ILLUSTRATIONS

LIST OF ILLUSTRATIONS (Continued)

LIST OF ILLUSTRATIONS (Continued)

LIST OF TABLES

LIST OF ABBREVIATIONS AND SYMBOLS

Symbol	Definition
A-A	Air-to-Air Mission Type
A-G	Air-to-Ground Mission Type
A/C	Aircraft
a_i	Equivalent Initial Flaw Depth
BL44	Wing Main Spar Lower Kickpoint
D.C.	Double Crack
D.I.	Damage Index
DLS	Design Limit Stress
f_{MAX}	Positive Peak Stress in a Cycle or Maximum Spectrum Stress
Inf.	Infinite
Ksi	1000 Pounds per Square Inch
K_T	Stress Concentration Factor
lb.	Pounds
LRS	Load Reference Station
LRS 70	Wing Main Spar Lower Kickpoint
MAX.	Maximum
N-T	Non-Tactical Mission Type
SBA	Side Brace Actuator
S.C.	Single Crack
Str.	Stringer
σ	Stress
σ_{MAX}	Maximum Spectrum Stress
TLL	Test Limit Load
VGH	Velocity, Load Factor, Altitude

1. INTRODUCTION

Tracking of crack growth is a relatively new requirement and techniques have not been developed to relate changes in usage to change in growth rate for complex spectra. Limited instances of monitoring crack growth on older systems can be cited, however, no general procedures have been generated for a specific class of aircraft. Requirements to develop parametric fatigue analysis methods have existed for some time but have primarily considered the concept of cumulative damage and the expected time to crack initiation.

Fleet tracking is the responsibility of the Air Force and is accomplished as part of the Force Management Task (Task V) of MIL-STD-1530. For each new system, the contractor is required to develop a tracking program consisting of the necessary data acquisition and data reduction devices, analysis techniques, and procedures. These will be used to provide an index of usage severity that can be used for estimating probable crack growth rates at all critical locations within the airframe. Maintaining damage tolerance and durability is dependent on the capability of the appropriate Air Force commands to perform specific inspection, maintenance, and possibly modification/replacements tasks throughout the service life of the particular fleet. The Air Force must have detailed knowledge of the required actions. In order to know when to inspect/repair fleet aircraft, an individual tail tracking program is required because each particular fleet experiences unique usage, and individual aircraft within that fleet exhibit wide variations in usage severity. Continual adjustments to initially determined safe crack growth intervals must be made for individual fleet aircraft to protect safety and to allow for retrofit and repair on an acceptable economic basis.

The essential purpose of this study is to provide general tracking procedures for fighter class aircraft. The study is composed of three major parts;

(1) effect of usage parameters on crack growth, which will establish the significant parameters that should be tracked,

(2) development of generalized procedures, which provides several tracking schemes, and

(3) implementation of the tracking program, which will include procurement of necessary instrumentation, maintenance of the equipment, and provision for supplemental data sheets, as well as a facility for calculating crack growth on critical areas of in-

dividual fleet aircraft and providing tabulated damage summaries of same to the using command periodically.

The purposes for tracking crack growth are to establish:

(1) when to inspect,

(2) when to repair,

(3) when and where to rotate aircraft, and

(4) when to retire an aircraft.

Economic limits are associated with the time to repair or modify an aircraft, while safety limits are associated with the useful life of the aircraft. Inspection intervals may be tied to either an economic or a safety limit. Rotation of aircraft to bases of different usage can prolong aircraft life.

In the F-4C/D and F-4E(S) Damage Tolerance Assessment Programs (References 10 and 2) an economic repair limit was defined as the opportune time for retrofit incorporation. The following assumptions were made:

(1) Any individual hole can have an initial flaw size (a_i) = 0.010 inch

(2) Flaw shape parameter Q - best estimate of average Q

(3) Air environment

The safety limit was defined as the life beyond which a failure potential is believed to exist if no inspection and/or repair is accomplished. The following assumptions were made:

(1) Any individual hole can have a_i = 0.03 inch

(2) Severe flaw shape

(3) Severe environment of 1/2 air, 1/2 water

(4) Average retardation

The F-4E slatted airplane (F-4E(S)) was selected as the baseline multimission fighter to be used for mission and design parameter variations. Spectra were developed for each variation and crack growth was predicted. As a result of this effort, it was possible to determine which of the mission and design parameters are the most significant.

In addition to the F-4E(S), the F-15 was chosen as a variant from the baseline because its differential tail augmented roll could require tracking of different parameters than for a conventional type fighter.

During the development of generalized procedures, crack growth trends and alternate methods of tracking were established. In addition, the recorded data requirements have been evaluated.

The effort regarding implementation of a tracking program consisted of an evaluation of logistics and the identification of technical difficulties and potentially significant costs.

2. EFFECTS OF USAGE PARAMETERS ON CRACK GROWTH

The effects of usage parameters on crack growth were evaluated for two types of fighter aircraft that experience different types of usage and hence require a significant difference in the number of parameters being tracked.

Fighter wings are designed primarily by airloads resulting from positive, negative, and unsymmetrical maneuvers performed during training and/or combat. The important flight parameters are normal load factor, airspeed, and gross weight.

Fighter fuselages are designed by a combination of airloads and inertia loads. The important flight parameters are normal load factor, airspeed, gross weight, yaw rate, roll rate and pitching acceleration.

Unsymmetrical loads are not significant in crack growth calculations for fighters such as the F-4 because its primary mission is air-to-ground (close air support) which entails a minimum of unsymmetrical maneuvering. In the case of the F-15 which has a high power to weight ratio as well as differential tail augmented roll, unsymmetrical maneuvers are significant for the horizontal tail and aft fuselage, as well as the wing.

The important inputs to the development of fighter stress spectra are (1) frequency of occurrence of normal load factor, (2) airspeed, (3) altitude, (4) gross weight, (5) mission mix, (6) distribution of load factor occurrences to various airspeed/altitude combinations, and ground cycle.

2.1 Multi-Mission Fighter - Baseline Aircraft

The F-4E(S) was selected as the baseline fighter mainly because of the recent large data base established during the ASIP damage tolerance program. In addition, the F-4 has:

- 15 years of individual aircraft tail tracking
- 3,500,000 counting accelerometer hours
- 40,000 VGH hours
- 6 full scale fatigue tests
- 1,500 element tests
- 15 years of service experience
- tail tracking program operational at ASIMIS

During the F-4E(S) ASIP program a comprehensive teardown inspection of the slatted full scale fatigue test article was performed in which:

- 38,500 holes were inspected
- cracks were exposed in 400 holes and crack size and shape measured
- 157 cracks traced fractographically

The F-4E(S) ASIP spectrum development resulted in spectra based on:

- 22,208 hours of counting accelerometer data
- 1,527 hours of VGH data
- Multiple Mach/altitude points (all points in the sky) for three missions - air-to-air, air-to-ground, and non-tactical
- Random distribution of high positive peaks and all negative peaks
- Flight-by-flight sequencing of maneuvering and landing cycles

2.1.1 Mission Parameter Variations - Mission parameter variations were evaluated at two locations on the aircraft - one wing location and one fuselage location. Included were variations of mission mix, load factor exceedance, airspeed, gross weight, altitude, and mission duration.

- 3 Mission Mix Variations (Figure 1)
- 6 Load Factor Exceedance Variations (Figure 2)
- 4 Airspeed Variations (Figure 3)
- 4 Gross Weight Variations (Figure 4)
- 2 Altitude Variations (Figure 5)
- 4 Mission Duration Variations (Figure 6)

Mix		Air-to-Air	Air-to-Ground	Non-Tactical
Baseline	(1)	26%	49%	25%
Variation 1	(2)	75%	0%	25%
Variation 2	(3)	29%	56%	15%
Variation 3	(4)	49%	26%	25%

(1) From F-4E(S) damage tolerance assessment (Reference 2)

(2) Replace air-to-ground with air-to-air

(3) Reduce non-tactical - air-to-air/air-to-ground ratio same as baseline

(4) Transpose air-to-air and air-to-ground

FIGURE 1 MISSION MIX VARIATIONS

Variation	Air-to-Air	Air-to-Ground	Non-Tactical
1	Severe	Baseline	(1)
2	Mild	Baseline	(1) (2)
3	Baseline	Severe	↓
4	Baseline	Mild	
5	Severe	Severe	(1)
6	Mild	Mild	(1)

(1) Baseline for all variations

(2) This variation for wing location only

FIGURE 2 LOAD FACTOR EXCEEDANCE VARIATIONS

Variation	Air-to-Air	Air-to-Ground	Non-Tactical
1	15% Faster	Baseline	(1)
2	15% Slower	Baseline	(1)
3	Baseline	15% Faster	(1) (2)
4	Baseline	15% Slower	(1) (2)

(1) Baseline for all variations

(2) This variation for wing location only

FIGURE 3 AIRSPEED VARIATIONS

Variation	Air-to-Air	Air-to-Ground	Non-Tactical
1	3,000 Lb Heavier	Baseline	(1), (2)
2	3,000 Lb Lighter	Baseline	(1)
3	Baseline	3,000 Lb Heavier	(1)
4	Baseline	3,000 Lb Lighter	(1), (2)

(1) Baseline for all variations

(2) This variation for wing location only

3 Baseline gross weights: Air-to-Air, 40,000 lb; Air-to-Ground, 43,000 lb; Non-Tactical, 42,000 lb

FIGURE 4 GROSS WEIGHT VARIATIONS

Variation	Air-to-Air	Air-to-Ground	Non-Tactical
1	30% Higher	Baseline	Baseline
2	30% Lower	Baseline	Baseline

For both locations on aircraft

FIGURE 5 ALTITUDE VARIATIONS

Variation	Air-to-Air	Air-to-Ground	Non-Tactical
1	22% Longer Flight	Baseline	(1) (2)
2	22% Shorter Flight	Baseline	
3	Baseline	20% Longer Flight	
4	Baseline	20% Shorter Flight	

(1) Baseline for all variations

(2) This variation for wing location only

3 Baseline flight lengths: Air-to-Air, .74 hours; Air-to-Ground, 1.32 hours; Non-Tactical, 1.56 hours

FIGURE 6 MISSION DURATION VARIATIONS

As the study progressed, additional mission parameter variations were evaluated. These included two mission mix variations, one load factor variation, one gross weight variation, and two special variations.

The additional mission mix variations (Figure 7) were chosen to further bound the problem. This provides a set of mission mixes in which each mission is set to zero percent while each of the other two missions retains a finite percentage. It should be noted that it is unlikely that any fleet aircraft would accumulate zero flight hours in one mission category during its lifetime.

Variation	Air-to-Air	Air-to-Ground	Non-Tactical
1	0%	75%	25%
2	35%	65%	0%

Wing location only

FIGURE 7 ADDITIONAL MISSION MIX VARIATIONS

The gross weight variations were evaluated for ±3,000 pounds of mission gross weight. While a 3,000 pound variation is considered to be sufficient for bounding the problem, it is felt that a variation of 1,000 pounds is more realistic while still retaining some degree of conservatism. Therefore, a +1,000 pound variation in air-to-air gross weight was evaluated.

An additional load factor variation was defined in an attempt to evaluate an aircraft experiencing the lower bound of load factor exceedance as well as truncation of the upper end of the spectrum at about 6g.

A special variation was run in which gross weight, airspeed, and mission mix were varied simultaneously. These variations are individually less conservative than those used during the primary effort. Using the baseline spectrum, the following variations were made:

+ 500 lb air-to-air gross weight
+ 500 lb air-to-ground gross weight
+ 5% air-to-air airspeed
+3% air-to-ground gross weight
+ 10% air-to-air altitude
30% air-to-air, 45% air-to-ground, 25% non-tactical

Variations of maximum spectrum stress were run to evaluate differences in retardation. The following stress levels were used:

F-4E(S) baseline max. σ =	32.5 Ksi
Variation 1	28.7 Ksi
Variation 2	26.3 Ksi

2.1.2 Design Parameter Variations - Design parameter variations were evaluated at two locations on the aircraft - one wing location and one fuselage location. Included were variations of design limit stress and material (Figure 8), load transfer (Figure 9), geometric K_T (Figure 10), and fastener size (Figure 11).

Variation	Location	Material
1.2 X Baseline	Wing	7075-T651 Plate
	Wing	4340 Steel
	Fuselage	7178-T6 Extrusion
	Fuselage	Ti 6Al-4V
.80 X Baseline	Wing	7075-T651 Plate
	Wing	4340 Steel
	Fuselage	7178-T6 Extrusion
	Fuselage	Ti 6Al-4V

FIGURE 8 DESIGN LIMIT STRESS

Variation	Location	Material
Δf_{br} = +.25 DLS	Wing	7075-T651 Plate
-.25 DLS	Wing	7075-T651 Plate
+.25 DLS	Fuselage	7178-T6 Extrusion
-.25 DLS	Fuselage	7178-T6 Extrusion

FIGURE 9 LOAD TRANSFER

Baseline: Neat fit, single crack, 2D edge distance

K_T Increase: Clearance fit, single crack, 2D edge distance

K_T Decrease: Clearance fit, single crack, infinite plate

At Two Locations on the Aircraft

FIGURE 10 GEOMETRIC K_T

Variation	Location	Fastener Diameter
1	Wing	+ one size, 5/8 In.
2	Wing	- one size, 3/8 In.
3	Fuselage	+ one size, 1/4 In.
4	Fuselage	- one size, 5/32 In.

FIGURE 11 FASTENER SIZE

2.1.3 Development of Stress Spectra - The baseline spectra developed during the Reference 2 F-4E(S) damage tolerance assessment are the references from which variations in this study are defined and evaluated.

The spectrum used for crack growth predictions utilizing the modified Wheeler prediction method is a so-called block spectrum composed of three mission types: air-to-air, air-to-ground, and non-tactical. An example for an individual mission type is shown in Figure 12.

MAX. STRESS (KSI)	MINIMUM STRESS (KSI)					
	4.05	.488	-1.23	-3.76	-6.25	-8.76
8.76	2358	162	74	6	1	1
11.25	1131	413	189	15	3	3
13.75	816	188	86	7	2	1
16.22	415	63	29	3	1	
18.75	215	27	12	1		
21.22	131	18	8	1		
23.75	88	13	6			
26.25	38	13	6			
28.70	16					
32.50	.3					

FIGURE 12 F-4E(S) ASIP BASELINE
Air-to-Air Occurrences per 260 Hours

Mission profiles were not used in the development of F-4 stress spectra because of the available data base of counting accelerometer data and VGH data.

The air-to-air mission consists of air-to-air training (air combat maneuvering and air intercept) which involves "dog fighting" with one or more "enemy" aircraft or firing missiles at an airborne target.

The air-to-ground mission consists of air-to-ground training which involves dropping practice bombs on a designated target and/or gunnery practice.

The non-tactical mission consists of instrumentation, navigation, and test missions.

The basic stress sequence is a 1000 hour repeatable block consisting of 1000 hour segments which are repeatable except for cycles that occur less than once per 1000 hours. Each 1000 hour segment has a sequence of 350 air-to-air flights (260 hours), 370 air-to-ground flights (490 hours), and 160 non-tactical flights (250 hours). The individual flights are arranged in a lo-hi-lo sequence with a ground cycle at the end of each flight. Cycles occurring at least once per flight are ordered at the beginning and end of the flight. These cycles represent generally load factors of less than 4g. Cycles occurring less than once per flight were randomly distributed in the middle portion of the flight. All negative cycles were randomly distributed.

2.1.3.1 Mission Mix - The spectra for mission mix variations were readily obtained by ratioing the counts in the block spectra by the mission mix percentages. For example, to get the number of counts in the air-to-air block of variation 1 (Figure 1) ratio up the baseline air-to-air counts by 75/26.

2.1.3.2 Load Factor Exceedance - The spectra for load factor exceedance are obtained by mixing a severe (or mild) block with two baseline blocks, i.e., for variation 1 (Figure 2), use the severe air-to-air block with a baseline air-to-ground block and a baseline non-tactical block.

2.1.3.3 Airspeed - Using the computer printout of the F-4E(S) stress spectra (Table A-1 in the Appendix), curves of stress vs airspeed were plotted for a family of load factors by mission and altitude, an example of which is shown in Figure 13. For a 15% increase in baseline airspeed, a % increase in stress was obtained for each load factor level. A curve was then plotted of % change in stress level vs stress (Figure 14). From Figure 14, for each % max stress of the block spectrum, a % change in stress level was read (Figure 15). When making the crack growth prediction, use this air-to-air block spectrum with baseline blocks of air-to-ground and non-tactical.

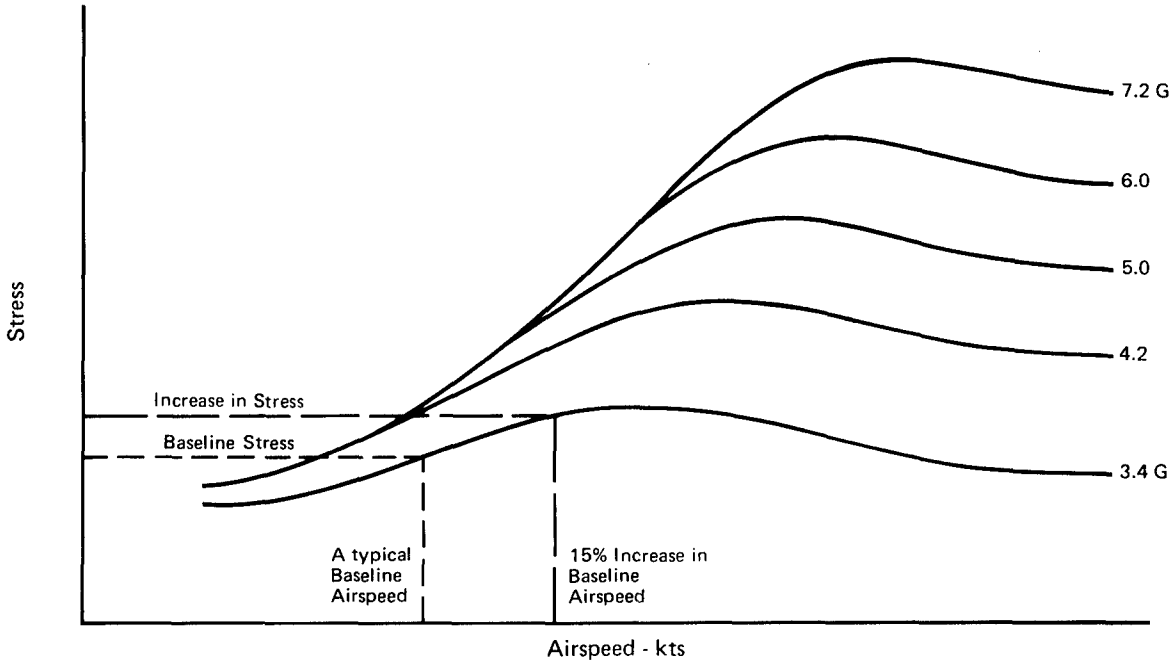

FIGURE 13 AIRSPEED VARIATION
Air-to-Air BL 44 25 000 Ft

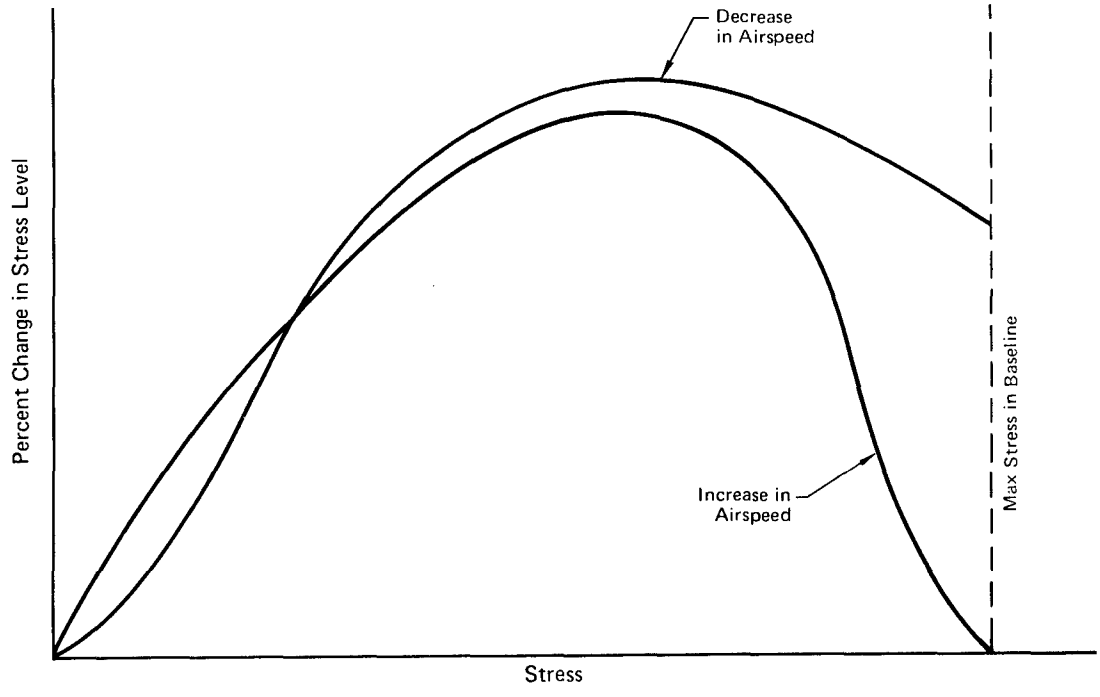

FIGURE 14 AIRSPEED VARIATION

Max Stress (ksi)	Minimum Stress (ksi)						+15% Airspeed Variation Increase in Stress (%)
	4.05	0.488	−1.23	−3.76	−6.25	−8.76	
8.76	2358	162	74	6	1	1	0.00
11.25	1131	413	189	15	3	3	7.10
13.75	816	188	86	7	2	1	8.40
16.22	415	63	29	3	1		8.80
18.75	215	27	12	1			8.70
21.22	131	18	8	1			7.90
23.75	88	13	6				5.60
26.25	38	13	6				0.90
28.70	16						0.20
32.50	0.3						0.00

FIGURE 15 F-4E(S) ASIP BASELINE SPECTRUM AIR-TO-AIR MISSION
Occurrences Per 260 Hours

2.1.3.4 Altitude - The approach was similar to that used for airspeed, except curves of stress vs altitude were plotted for a family of load factors by mission and airspeed.

2.1.3.5 Gross Weight - The baseline stress spectra were modified by merely increasing/decreasing the stress by a constant ratio of variation gross weight to baseline gross weight, however, this caused enough increase in retardation to result in greater lives even for the cases where the mission gross weight was increased. In actual F-4E(S) fleet usage an increase in the maximum stress in the spectrum is not possible due to tip stall effects, therefore, an additional variation was run for 3,000 lb greater air-to-air gross weight for no increase in maximum spectrum stress. For this case, there was about a 10% decrease in life.

2.1.3.6 Mission Duration - The spectra were obtained in a fashion similar to that used for mission mix, i.e., ratioing the counts in the block spectrum in proportion to the flight length.

2.1.4 Crack Growth Predictions - The Wheeler retardation model as modified by MCAIR is the crack growth prediction method chosen for the evaluation of mission and design parameter variations.

2.1.4.1 Basic Method - The Wheeler model is a cumulative crack growth approach which accounts for retardation of crack growth caused by peak loads in the spectrum. In the basic Wheeler method, crack growth is predicted on a cycle by cycle basis, whereas in the MCAIR modified Wheeler method crack growth is predicted on a block by block basis. The block by block basis is used in order to reduce the amount of computer time required for each prediction.

A summation of the crack growth caused by each load application within the loading block is made to obtain the total change in crack depth resulting from the block of loads. The change in crack depth, Δa, is then added to the initial crack size to obtain a new crack depth to be used for prediction with the next block of loads. The above process is continued until the crack depth reaches critical size, and failure is predicted.

The constant amplitude crack growth rate, da/dN, is used in this technique to account for the effects of changes in the stress intensity, ΔK. The effects of stress ratio, R, on the crack growth rate, da/dN, are determined by using Forman's equation (Reference 3) in conjunction with the tabulated input of the da/dN versus ΔK curve for $R = 0$.

The effect of retardation caused by peak loads in the spectrum was incorporated by a change to the Wheeler model. Wheeler introduced a factor, C_p, which is multiplied by the constant amplitude crack growth rate to obtain the crack growth rate for a given load cycle in a spectrum. Thus, when peak tension loads in the spectrum are followed by lower load levels, the following equation is used to determine the effect on crack growth rates:

$$\left(\frac{da}{dN}\right)_{\substack{\text{Spectrum}\\\text{Loading}}} = C_p \left(\frac{da}{dN}\right)_{\substack{\text{Constant}\\\text{Amplitude}\\\text{Loading}}} \qquad (1)$$

In the MCAIR prediction technique, C_p is defined as:

$$C_p = \left(\frac{r_y}{r_{peak}}\right)^m \qquad (2)$$

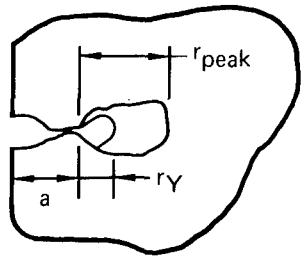

The plastic zone size, r_y, ahead of the crack tip is due to a given load in the spectrum, and r_{peak} is the plastic zone size produced by the application of the peak load prior to the given smaller load. The exponent m is an empirically determined retardation factor which regulates the amount of retardation required to bring the predicted crack growth into agreement with the experimental spectrum data. If m = 0, C_p = 1 and there is no retardation. Also, if r_y is greater than r_{peak}, C_p is set equal to one. The value of r_y is determined from the following equation for plane strain conditions:

$$r_y = \frac{1}{4\pi\sqrt{2}}\left(\frac{K_I}{F_{ty}}\right)^2 \qquad (3)$$

where K_I is the stress intensity corresponding to a given load level in the spectrum. Since the stress intensity, K_I, is proportional to the stress, f, the following equation results for C_p:

$$C_p = \left[\left(\frac{f}{f_{peak}}\right)^2\right]^m \qquad (4)$$

where f is the maximum tension stress for a given load cycle in the spectrum, and f_{peak} is the maximum tension stress for a preceding peak load.

In order to account for the sequencing of peak tension loads in the spectrum, an effective C_p factor is determined. This factor is an average of the individual C_p factors for the peak loads in the spectrum which are considered to contribute to the retardation of smaller magnitude loads. If it were determined in the crack growth analysis that the crack was propagating beyond the plastic zone of one of the above peak loads before the next peak load was applied, then the effective C_p factor was modified to include the next lower peak loads in the spectrum.

Crack growth predictions are based on multiple hour increments (blocks) in which the change in crack growth caused by each load level in the spectrum is summed to establish the incremental crack growth for a block. The crack depth at the end of the block is obtained by adding the incremental crack growth to the initial crack depth as follows:

$$a_n = a_o + \sum_{i=1}^{n} (C_{p_{EFF}})_i \times (da/dN)_i \times (\Delta N)_i \qquad (5)$$

where:

a_n = crack depth at the end of the block

a_o = crack depth at the beginning of the block

i = a given load level in the spectrum

n = total number of load levels in the spectrum

ΔN = number of cycles for a given load level in a 100 hour block

The above process is iterated until a_n is equal to a_{cr}, the critical crack size for the specific geometry and loading conditions. The fracture toughness of a given material, K_c, is determined for a particular thickness. The determination of the retardation factor, m, to be used for a prediction is discussed in Section 2.1.4.3.

2.1.4.2 Modification for Load Transfer Analysis - The stress intensity solutions for cracks in fastener holes without load transfer have been developed for both open holes and neat fit fastener holes. The open hole analysis used is that given by Bowie, Reference 4; the neat fit fastener solution was derived in a MCAIR IRAD program and is presented in Reference 5. The function $F(\frac{a+r}{r})$ versus (a+r)/r is developed from both methods and presented in Figure 16. This

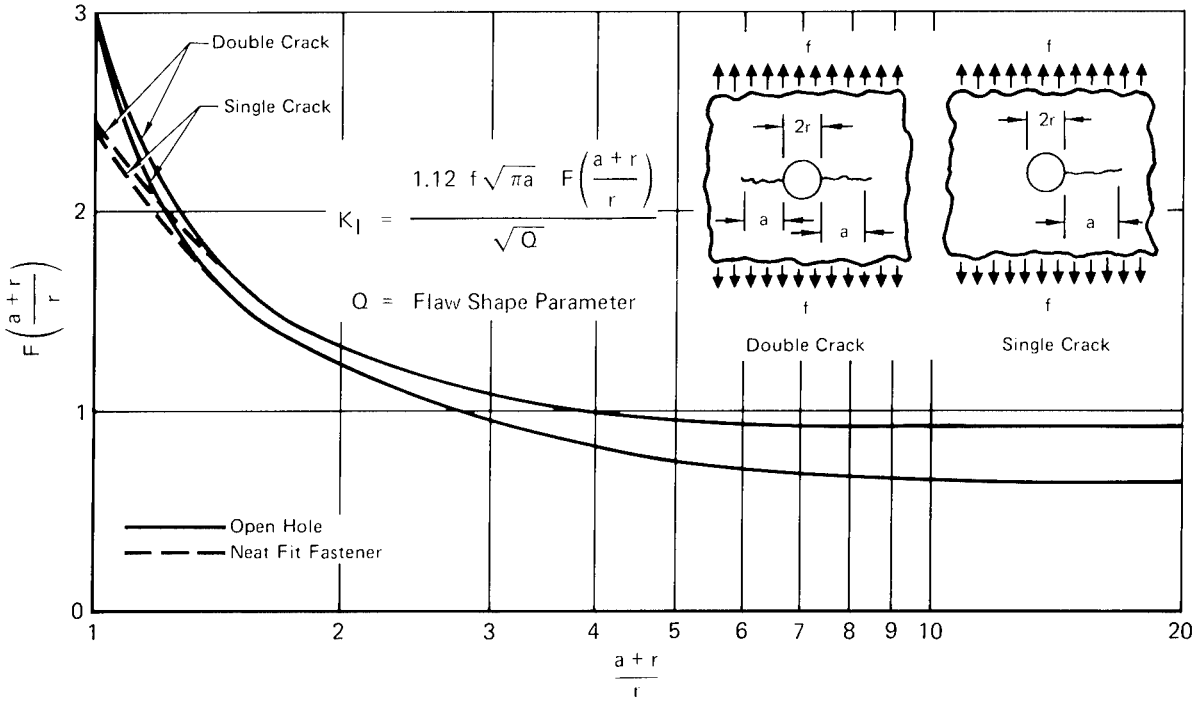

FIGURE 16 STRESS INTENSITY SOLUTION FOR CRACKS ORIGINATING AT A FASTENER HOLE

function is used in the stress intensity equations for cracks in holes, including through the thickness cracks, surface cracks in the bore of the hole, and corner cracks. Edge effects and finite width effects are accommodated using Isida's solution (Reference 6).

Load transfer effects are considered by modifying the stress intensity solution to account for bearing stress. For the bearing stress in the fastener hole, it was assumed that a uniform load was applied over a distance equivalent to the hole diameter. The stress intensity solution for a uniform stress on part of a crack surface is given by Paris and Sih in Reference 7:

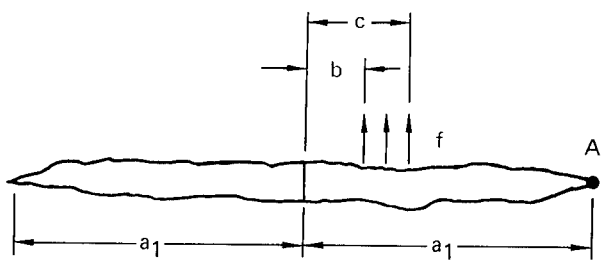

At Point A:

$$K_I = \frac{f}{2}\sqrt{\frac{a_1}{\pi}}\left[\sin^{-1}\frac{c}{a_1} - \sin^{-1}\frac{b}{a_1} - \left(1 - \frac{c^2}{a^2_1}\right)^{1/2} + \left(1 - \frac{b^2}{a^2_1}\right)^{1/2}\right] \quad (6)$$

The total stress intensity is then the sum of the through stress and bearing stress as shown in Figure 17.

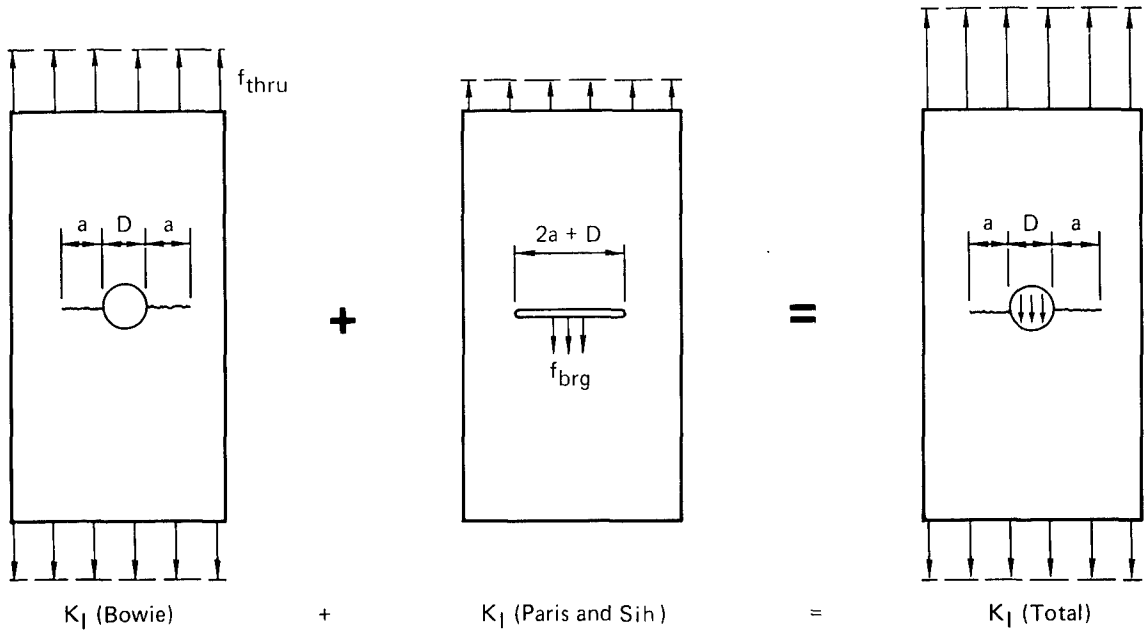

FIGURE 17 LOAD TRANSFER ANALYSIS

For the case of a double crack from a hole with depth "a", b is set equal to -r in Equation (6), c is equal to r, and a_1 is equal to a+r. Thus $K_{I_{brg}}$ is:

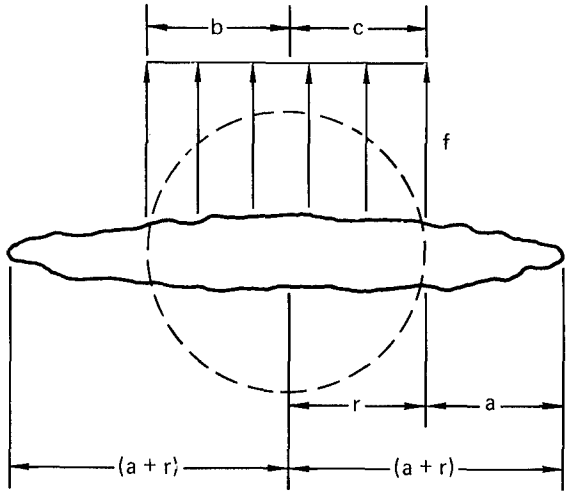

$$K_{I_{brg}} = f\sqrt{\frac{a+r}{\pi}}\left[\sin^{-1}\left(\frac{r}{a+r}\right)\right] \quad (7)$$

For the case of a single crack from a hole with depth "a", the following equation is derived:

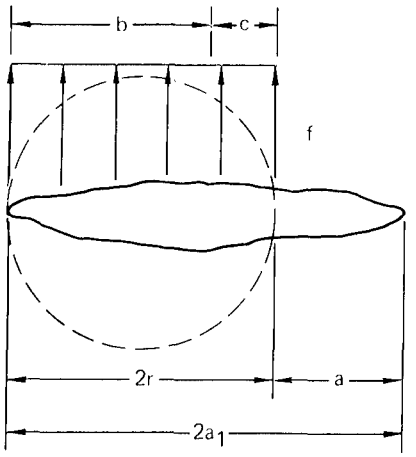

$$c = 2r - a_1$$
$$b = -(2r - c) = -a_1$$
$$a_1 = \frac{a + 2r}{2}$$

$$K_{I_{brg}} = \frac{f}{2}\sqrt{\frac{a + 2r}{2\pi}}\left\{\sin^{-1}\left(\frac{2r - a}{a + 2r}\right) + \frac{\pi}{2} - \left[1 - \left(\frac{2r - a}{a + 2r}\right)^2\right]^{1/2}\right\} \quad (8)$$

Notice in Equations (7) and (8) that when the crack depth, a, is equal to zero, a finite value exists for $K_{I_{brg}}$. In reality, the stress intensity should be equal to zero for a zero crack depth. To reduce the error in $K_{I_{brg}}$ for small crack sizes, a stress intensity solution for cracked holes in lugs was used. The solution, shown in Figure 18, was developed using Buechner's weight function along with a finite element analysis for a lug, and is presented in Reference 8.

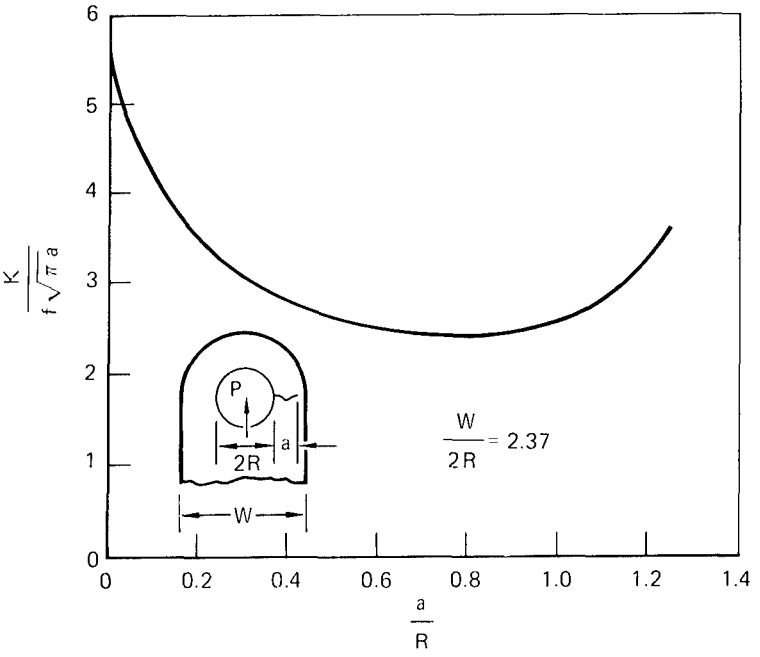

FIGURE 18 STRESS INTENSITY SOLUTION FOR A THROUGH CRACK IN A LUG

By converting the results of the above two stress intensity solutions into similar parameters for comparison, the results are plotted as shown in Figure 19.

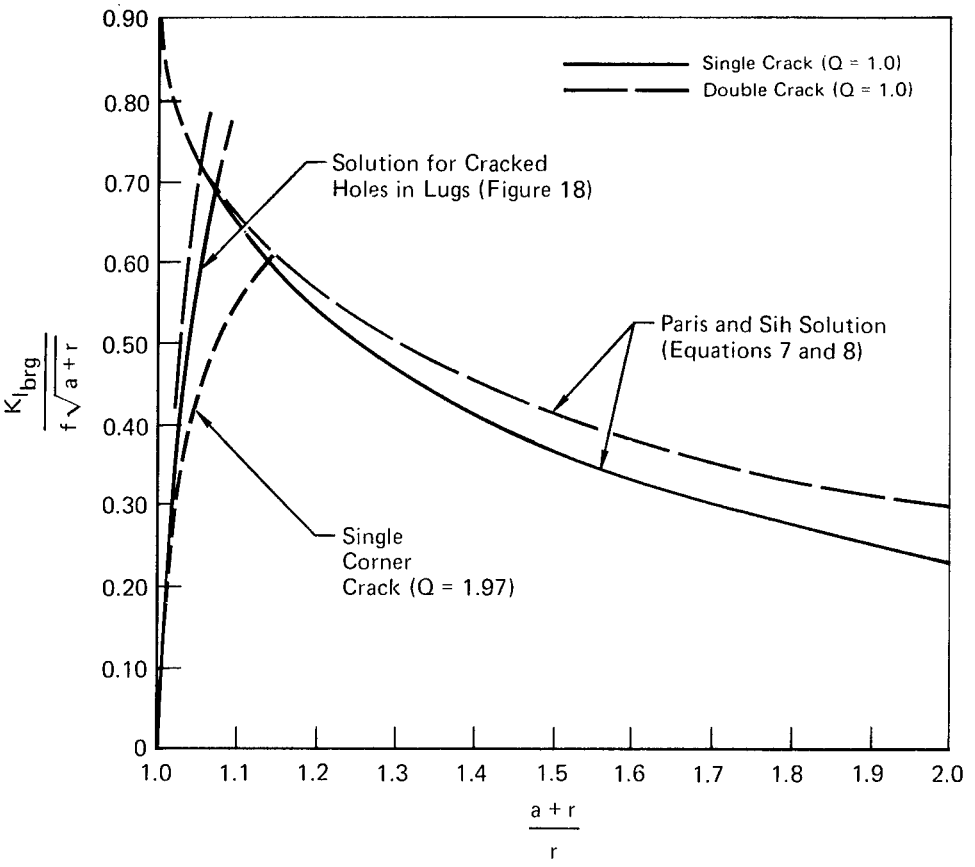

FIGURE 19 STRESS INTENSITY FOR BEARING STRESS IN A FASTENER HOLE

In the region where the Paris and Sih solution becomes inaccurate (small crack sizes), the solution for cracked holes in lugs is used. The intersection of the two solutions exists at $\frac{a+r}{r} = 1.06$ for single through thickness cracks, and 1.04 for double through thickness cracks.

For loaded holes with corner cracks, the stress intensity factors $\left(\frac{K_{I_{brg}}}{f\sqrt{a+r}}\right)$ for the lug solution are divided by $\sqrt{Q}$. An example is given for a single corner crack with Q = 1.97. After the crack increases in size beyond the intersection of the lug curve and the Paris and Sih curve, the Paris and Sih solution is used for analysis. Thus, the depth of the corner crack, a, is added to the diameter of the hole, 2r, to obtain the effective crack length for use in the Paris and Sih solution.

In general, the two stress intensity solutions for through stress (Figure 16) and bearing stress (Figure 19) are added together as shown in Figure 20.

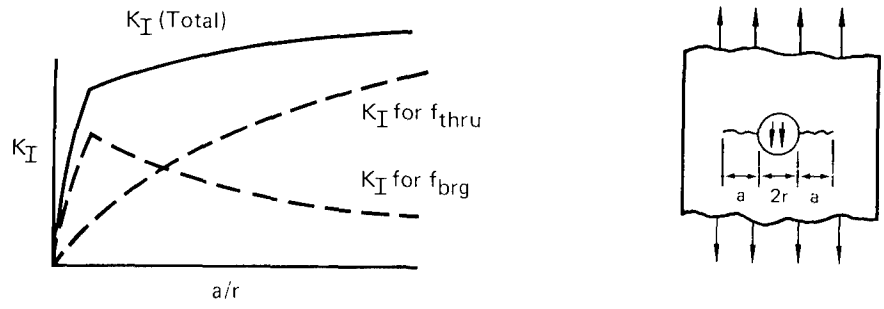

FIGURE 20 STRESS INTENSITIES NEAR A LOADED FASTENER

The stress intensity due to the bearing stress is greatest for relatively small crack sizes (about .01 inch) and is reduced as the crack size increases. The opposite is true for the through stress. The combination of the two solutions gives a total stress intensity which becomes nearly constant as the crack size increases. This explains why a crack propagating from a loaded fastener hole can in some cases grow at almost a constant rate.

In an area where high bearing stress (relative to the through stress) is encountered, initial crack growth is often very rapid. Once the influence of the bearing stress is diminished, the crack growth rate stabilizes and in some cases decreases. This phenomenon often results in an apparent discrepancy between the evaluations of relative criticality of two areas being analyzed. As an example, area "A" has a large bearing stress and a small through stress. Area "B" has a larger through stress and zero bearing stress. If a comparison is made of the time to grow from an initial flaw size to a relatively small flaw, say from .01 inch to .03 inch, area "A" is shown to be more critical. If however, the time to failure is calculated, area "B" is more critical. Thus, the evaluation of relative criticality must be made for the criteria of interest - initial crack growth or total crack growth.

2.1.4.3 Determination of m Values - After fractographic traces are obtained for the cracks in full scale fatigue test articles and in element specimens, crack growth is predicted for each by the method discussed in Section 2.1.4.1. The retardation factor, m, is determined for each crack growth curve using different values of m until a good correlation of prediction with test results is obtained. As an example, in Figure 21 an m of 2.05 gave the best fit.

In order to compare the MCAIR modified Wheeler crack growth prediction method with test results on a cycle by cycle basis, an analysis was performed on an element specimen subjected to the ECP 613 block spectrum. As is shown in Figure 22, the prediction using an m value of 3.50 gave a good correlation with the test data over the entire length of the crack growth curve. To compare the crack growth prediction with the actual data on a cycle by cycle basis, a photomicrograph was taken of the fracture surface for the 100 hour block between 3400 and 3500 spectrum hours. The photomicrograph is shown in Figure 23. Individual cycles could be counted for the 111%, 103%, 95%, 85%, 75% and 65% TLL levels within the 100 hour block. Individual cycles could not be counted for the 55%, 45%, and 35% TLL levels, although the total crack growth resulting from those cycles was a small percentage of the total. A bar graph was then constructed as shown, indicating the actual percent of crack growth caused by each load level, and comparing those percentages with the analytical percent of crack growth for each load level.

A similar type of analysis was performed on a specimen subjected to a flight-by-flight spectrum tested during the F-4E(S) Damage Tolerance Assessment Program. The predicted and test fracture curves are presented in Figure 24. For that specimen, an m of 2.20 gave a good match of the data. A photomicrograph was taken of the fracture surface at 11,226 spectrum hours where the amount of crack growth for the different load levels was measured. Individual cycles could be counted for the 133.2%, 117.8%, 107.6%, 97.3%, and 87.1% TLL levels in the spectrum. Individual cycles could not be counted for the 76.8%, 66.6%, 56.4%, 46.1%, and 35.9% load levels because of the condition of the fracture surface and the complexity of the spectrum. The total measured crack growth for the 35.9% through 76.8% load levels was distributed by the predicted crack growth percentages for those load levels. The 35.9% through 76.8% load levels accounted for approximately 30% of the total crack growth. A bar graph was then constructed as shown in Figure 25 indicating the measured percent of crack growth caused by each load level, and comparing those percentages with the analytical percent of crack growth for each load level.

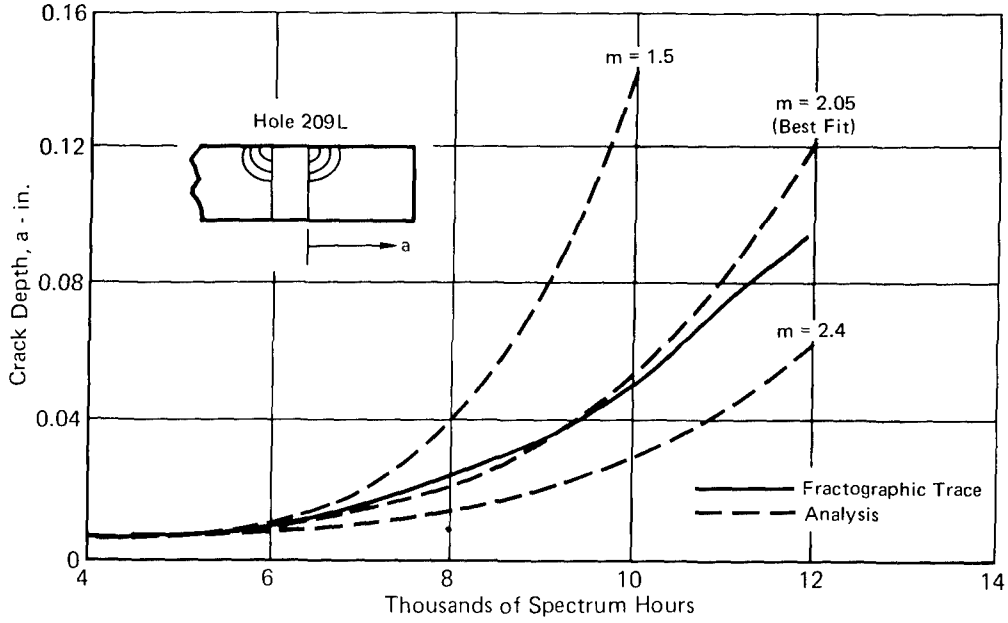

FIGURE 21 DETERMINATION OF RETARDATION FACTOR - m
F-4B/J Full Scale Test
Lower Torque Box Skin

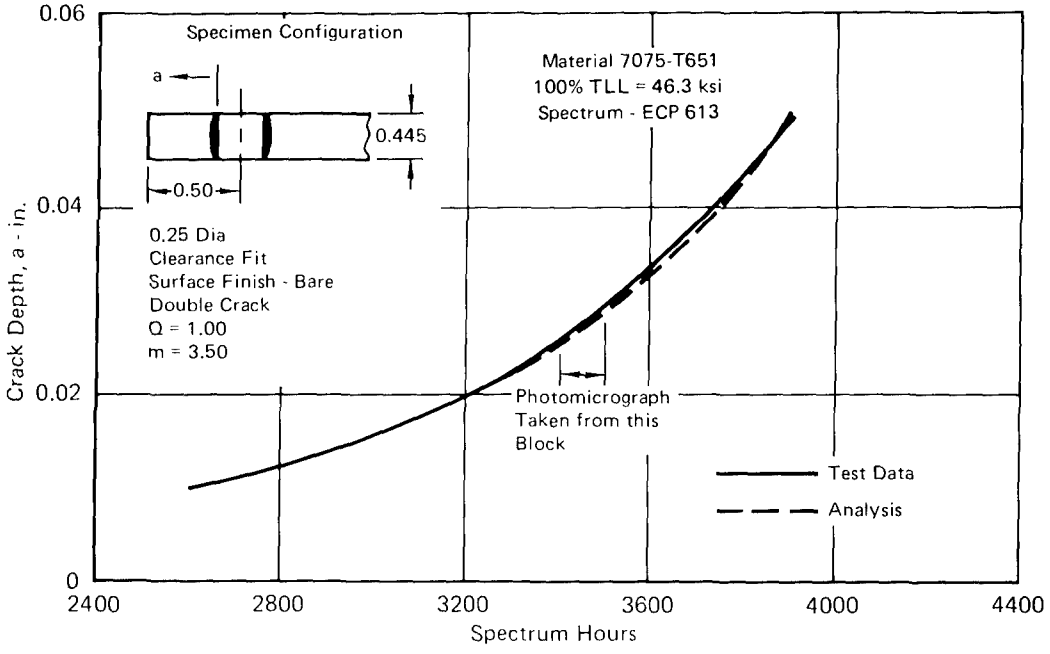

FIGURE 22 CRACK GROWTH ANALYSIS

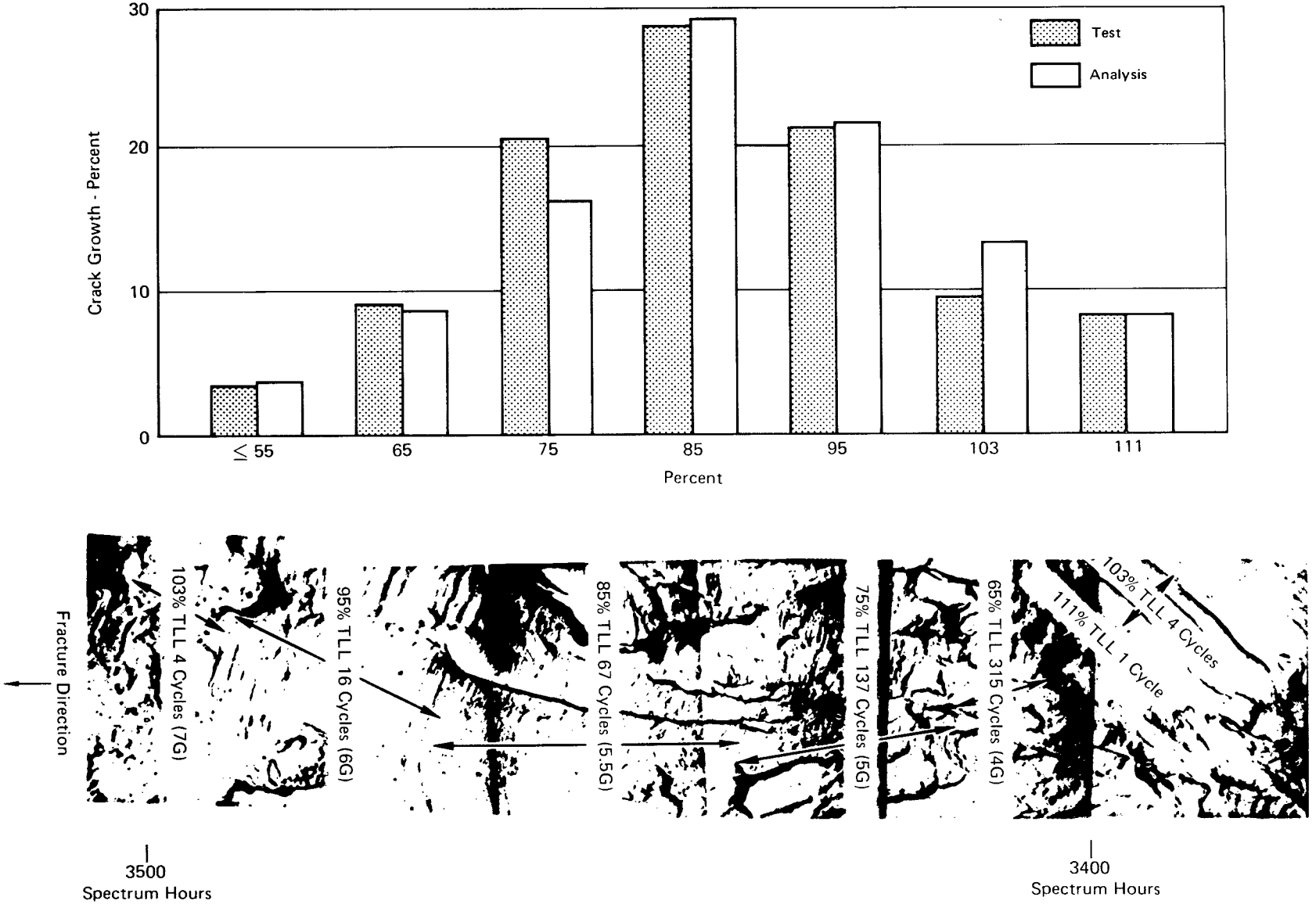

FIGURE 23 CORRELATION OF PREDICTIONS WITH PHOTOMICROGRAPH OF FRACTURE SURFACE

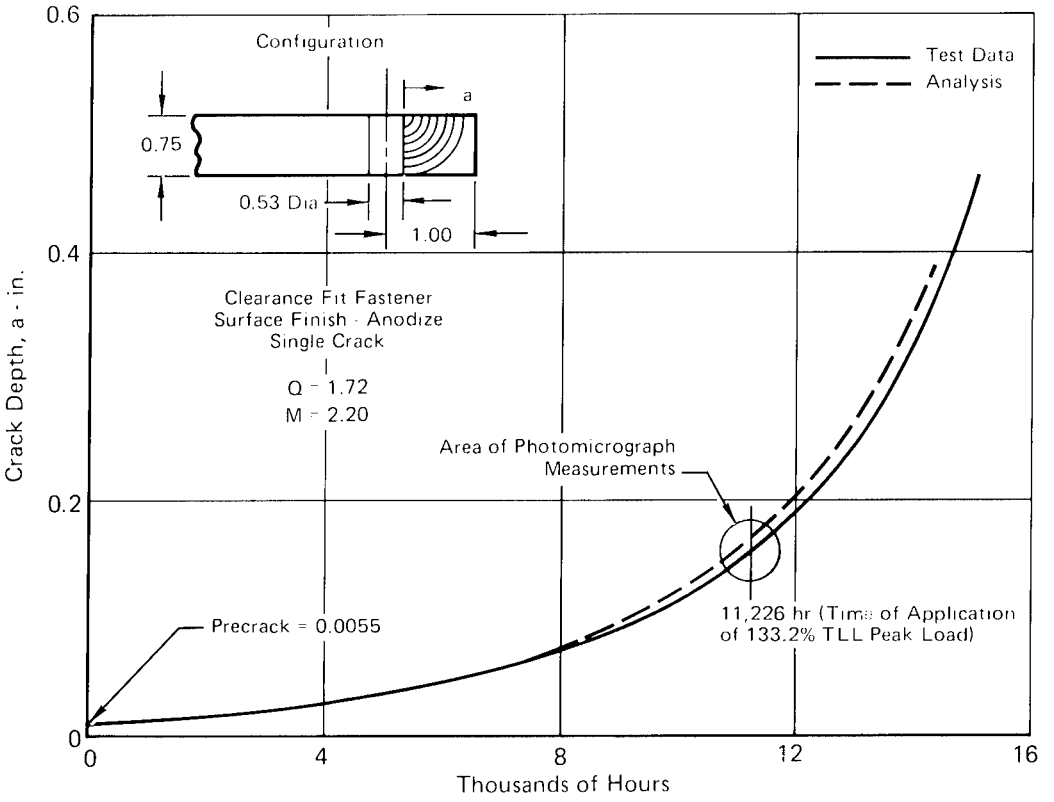

FIGURE 24 CRACK GROWTH ANALYSIS
Specimen for Photomicrographic Comparison
Specimen No. 445SKFRB-1
Material - 7075-T651
Spectrum - F-4E(s) Baseline
100% TLS-28 ksi

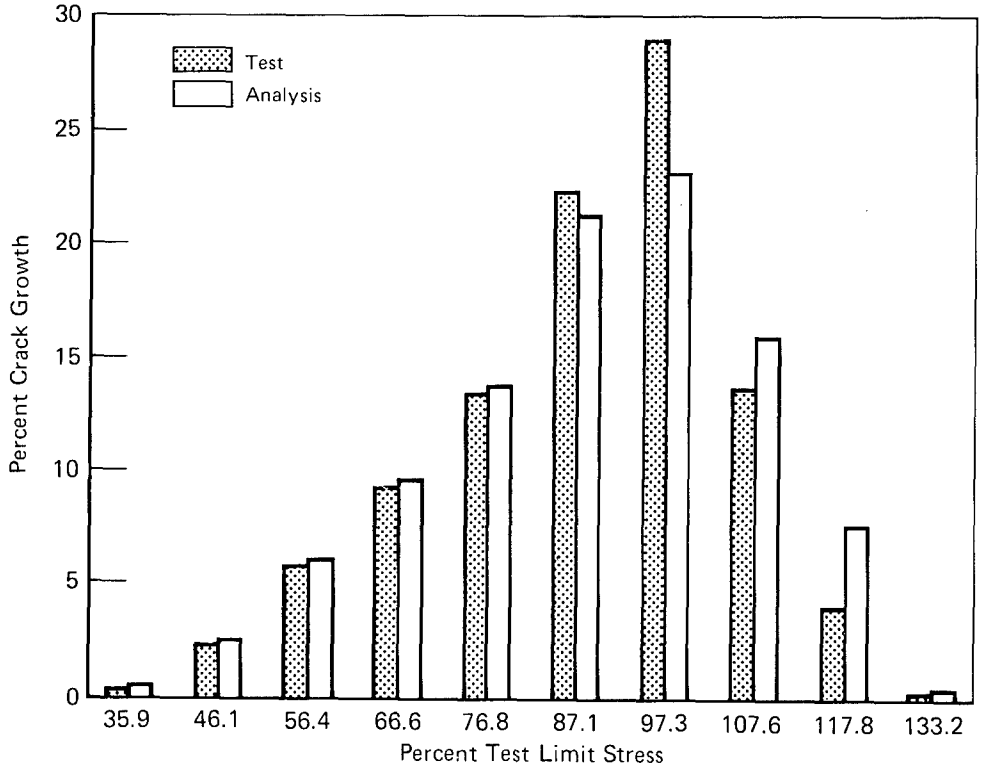

FIGURE 25 CORRELATION OF PREDICTIONS WITH PHOTOMICROGRAPH OF FRACTURE SURFACE

Both of the above examples (block loading and flight-by-flight loading) indicate that the MCAIR crack growth method gives reasonable predictions at the microscopic level as well as the macroscopic level. It also indicates that the method of establishing the C_p factors based on r_y/ r_{peak} is well founded.

2.1.4.4 Interrelationship of Stress, Flaw Shape, and Retardation - As a result of the predictions of crack growth for specimens and full scale tests, and determination of m values, it was found that there was an effect of stress and flaw shape on the retardation factor, m, and that there was an effect of stress on the flaw shape parameter, Q.

The value of m was larger for those specimens subjected to a fatigue spectrum with a relatively high maximum stress, and it was larger for those specimens which had a low value of the flaw shape parameter, Q. The value of Q varied between 1.0 for a through thickness crack at a fastener hole, and 2.4 for a 2 to 1 surface flaw at a fastener hole as shown below.

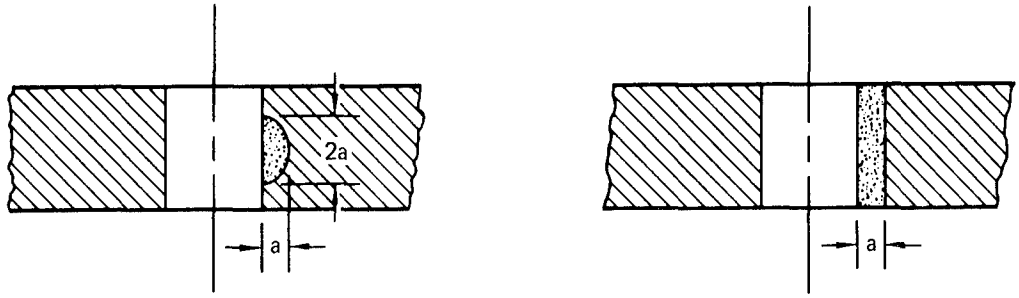

RANGE OF FLAW SHAPE PARAMETER Q

The wide variation in flaw shape resulted from the fact that the cracks were allowed to develop naturally during the fatigue loading of uncracked specimens. Some specimens were also tested with a precracked corner crack to eliminate the effect of Q on the retardation factor, m:

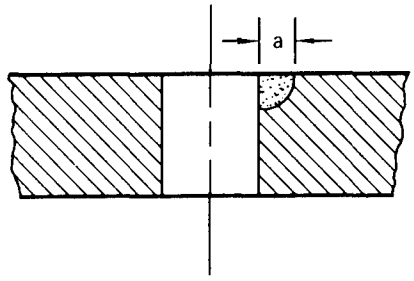

PRECRACKED SPECIMEN

As a result of the predictions of crack growth from over 100 element specimen and full scale test holes in 7075-T651 aluminum, it was noticed that the value of m was larger for those specimens with a relatively high maximum spectrum stress, f_{max}, or with a low value of the flaw shape parameter, Q. Noting that stress intensity, K_I, is similarly related to stress and flaw shape in that it is proportional to stress and inversely proportional to $\sqrt{Q}$, m was plotted versus $f_{max}/\sqrt{Q}$ (Figure 26). The correlation between m and $f_{max}/\sqrt{Q}$ exists for specimens and for full scale aircraft, as well as for several different spectra including block loading and flight by flight loading.

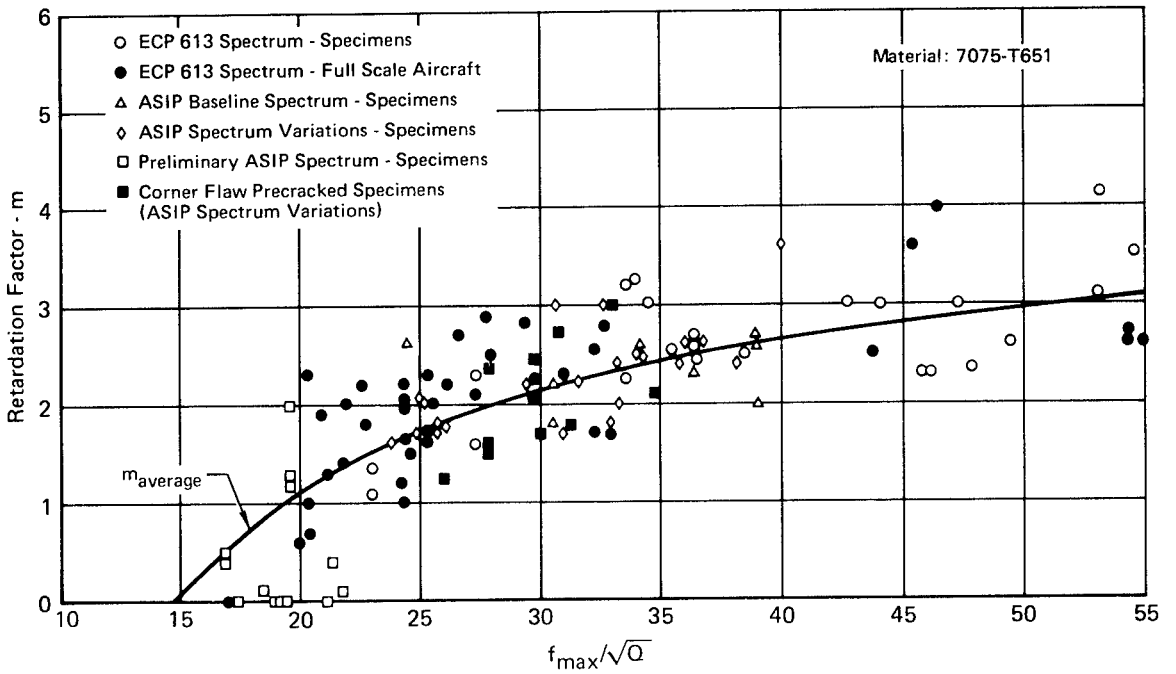

FIGURE 26 AVERAGE RETARDATION FACTOR, m FOR PREDICTION OF CRACK GROWTH IN FLEET AIRCRAFT

An average m curve was determined for the scatter band of data based on a least squares fit analysis. Data from full scale test aircraft, element specimens, and from the precracked corner flaw specimens with the controlled Q values are all located about the average line. It is expected that the loading spectrum could have an effect on the magnitude of m. However, after studying the correlation between test data and predictions for a variety of flight-by-flight spectra, it was noticed that the spectrum did not have a significant impact on m. Based on the above observations, it was decided that the average m values could be used to predict average crack growth rates for F-4C/D and F-4E(S) fleet aircraft.

The other data trend was that Q decreased with an increase in the maximum stress in the fatigue spectrum, shown in Figure 27. For low stress levels the shape of the crack initiating at a fastener hole tends to be a 2 to 1 surface flaw (Q = 2.4), while at high stress levels the crack shape tends to be a long shallow surface crack or through thickness crack (Q = 1.0). It was noticed that cracks tend to initiate at only one point for low stress levels, whereas at high stress levels there were multiple origins in the bore of the hole from which cracks quickly grew together to form a through thickness crack.

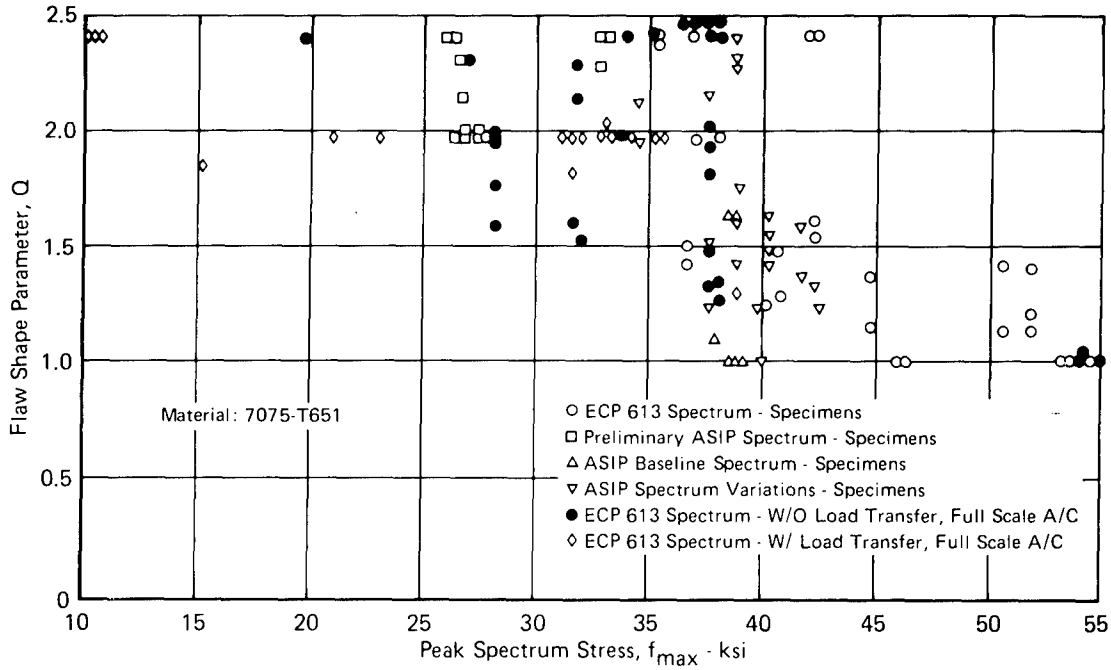

FIGURE 27 EFFECT OF f_{MAX} ON FLAW SHAPE PARAMETER, Q

2.1.4.5 Effects of Load Transfer on $f_{max}/\sqrt{Q}$ - In the determination of $f_{max}/\sqrt{Q}$ for load transfer, the effective $f_{max}/\sqrt{Q}$ is equal to the $f_{max,thru}/\sqrt{Q}$ multiplied by the ratio of the total stress intensity to the stress intensity for the through stress as indicated in Figure 20.

$$\left(\frac{f_{max}}{\sqrt{Q}}\right)_{eff} = \frac{f_{max,\ thru}}{\sqrt{Q}} \left[\frac{K_I(Total)}{K_I(Thru)}\right]_{\frac{a}{r} = 0.1} \qquad (9)$$

The ratio of the stress intensities is chosen to be taken at a/r = 0.1 for several reasons, the most important of which are listed below.

1. The ratio should be taken near the hole since that is where the greatest effect of bearing stress and stress concentration occur.
2. The ratio tends to level off at a/r > 0.1.
3. The major portion of a crack growth curve occurs at small crack lengths.
4. The data points fall well within the scatter band in Figure 26.

2.1.4.6 Crack Growth Predictions and Correlation with Test Results - In Section 2.1.4.3, m (retardation) values were used to obtain a "best fit" of the predictions with the actual crack growth curves. In this section, comparisons are made between the predicted crack growth curves using average m values (of Figure 26) and actual crack growth curves based on test results.

Figure 28 presents the crack growth curves of precracked specimens of 7075-T651 plate material tested to five different F-4 flight-by-flight spectra which represent different mission parameter variations. Also indicated are the predicted crack growth curves using the average m retardation values and the analysis techniques described previously. From this example, it is seen that the modified Wheeler model is adequate to predict the effects of mission parameter variations on crack growth.

Comparisons are also provided between full scale test article crack growth curves and predicted curves. Figure 29 indicates the crack growth trace from the F-4 Block 8 test aircraft at the origin of the catastrophic failure on the lower torque box skin at B.L. 100. (This aircraft was tested to a block type spectrum; failure occurred at 2700 spectrum hours.) Also indicated in that figure is a predicted crack growth curve for an average m of 3.05. The adequacy of the model is indicated in this example in the ability to predict the crack growth of a full scale aircraft to a block test spectrum.

In order to determine if the crack growth analysis method could be used for a completely different spectrum applied to a full scale fatigue test article, a prediction of crack growth was made for the pylon hole in the lower wing skin of the F-4E(S) fatigue test article. That test article was loaded to the F-4E(S) fatigue spectrum (flight-by-flight arrangement of loads) for 7600 spectrum hours before a large crack was discovered at the pylon hole. The pylon hole and crack were cut from the skin and the fracture surface was exposed to obtain a fractographic trace. Then, using an average m value from Figure 26, a prediction was made for that part. The results, shown in Figure 30, indicate that there is excellent correlation between the prediction and test data. Thus, it can be assumed that the average m curve in Figure 26 can be used to give reasonable predictions of crack growth in critical parts on full scale aircraft subjected to loading spectra not used in the establishment of the average m curve.

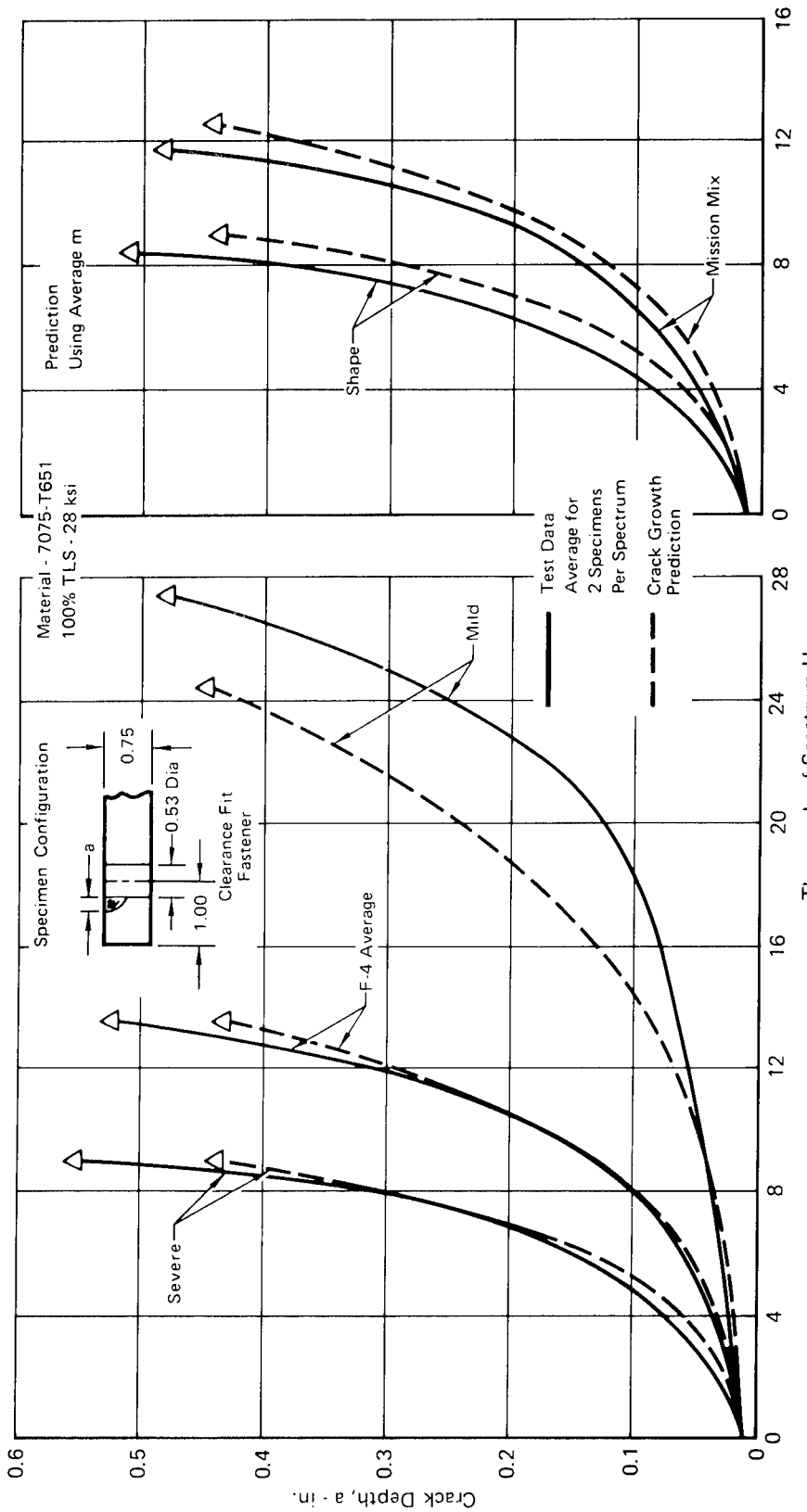

FIGURE 28 CRACK GROWTH PREDICTIONS F-4 PRECRACKED ELEMENT SPECIMENS

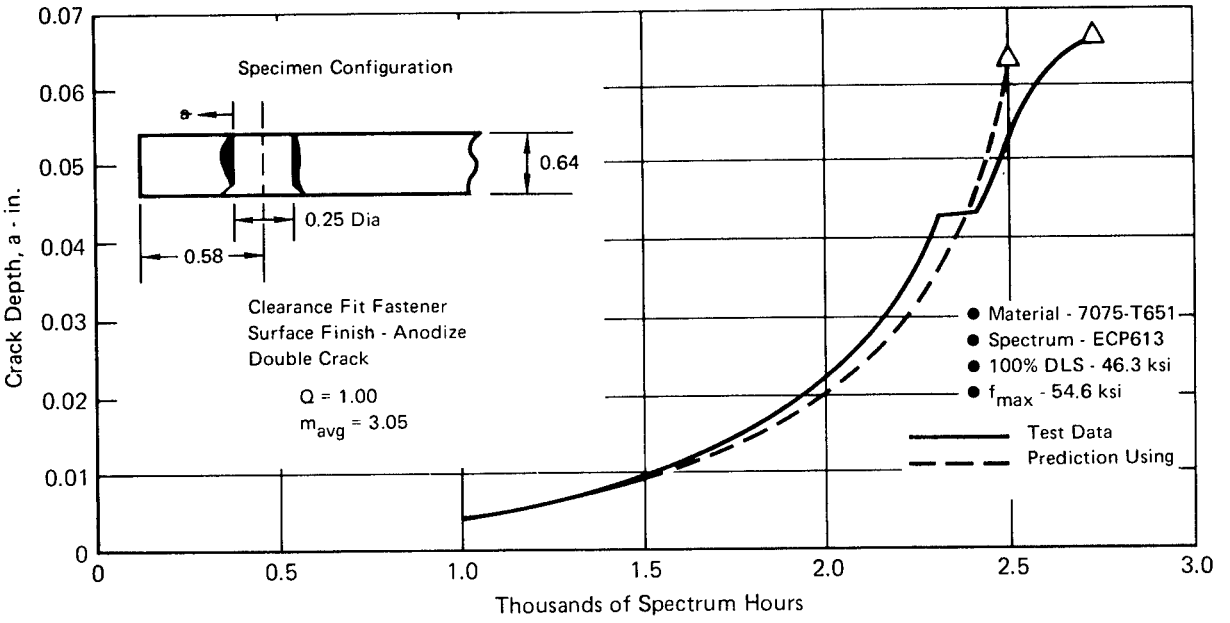

FIGURE 29 CRACK GROWTH PREDICTION
Block 8 - Full Scale Fatigue Test
R/H Wing Failure Hole
Lower Torque Box Skin at Main Spar (BL 100)

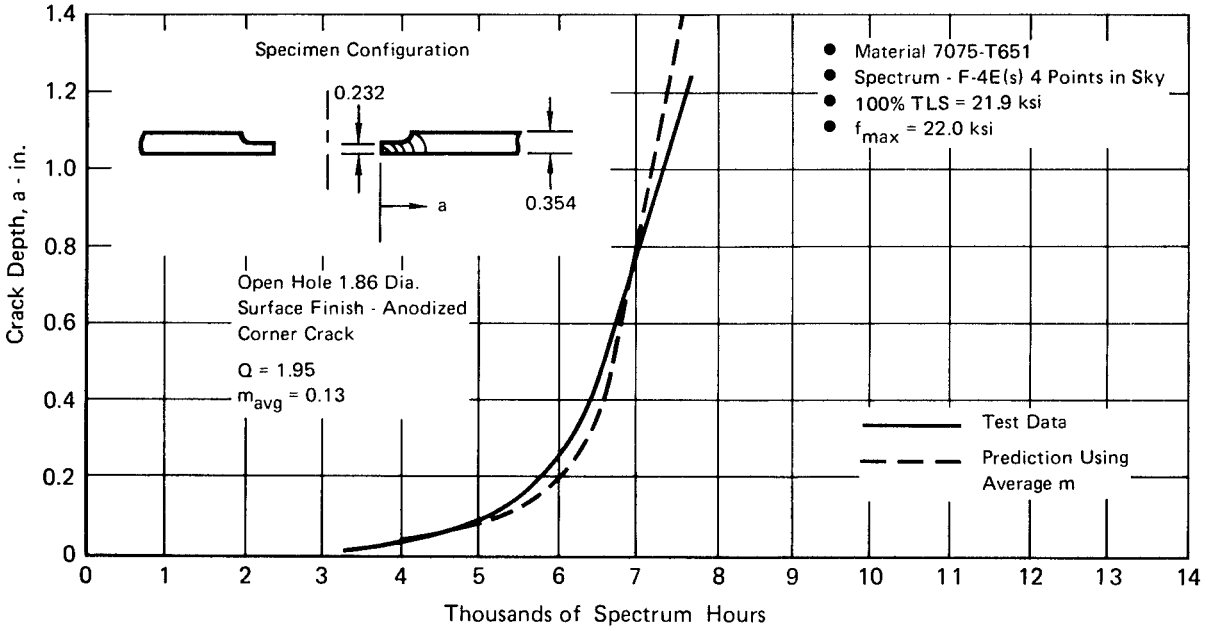

FIGURE 30 CRACK GROWTH PREDICTION
F-4E(S) Full Scale Fatigue Test
Pylon Hole BL 132.50

Crack growth predictions were made at two critical locations on the F-4E(S) aircraft - one wing location and one fuselage location. Several locations were considered. The criteria used in choosing the locations to be used in this study were whether the location: (1) was representative of total wing or fuselage loads, (2) represented typical aircraft design, (3) was most critical, and (4) had high load transfer. The potential wing locations are shown in Figure 31. All these locations experienced cracking in full scale fatigue tests. The choice of the wing location is described in Figure 32. The wing lower skin at the main spar kickpoint was chosen because it best represents total wing loads and is typical of conventional fighter wing design. The following information is given for the wing location:

Wing Baseline Location

Location	Skin @ LRS 70
Max. Baseline Spectrum Stress	32.5 Ksi
Material	7075-T651 Plate
Load Transfer	f_{br} = 21.8 Ksi
Fastener Dia.	0.53 Inch
Material Thickness	0.97 Inch

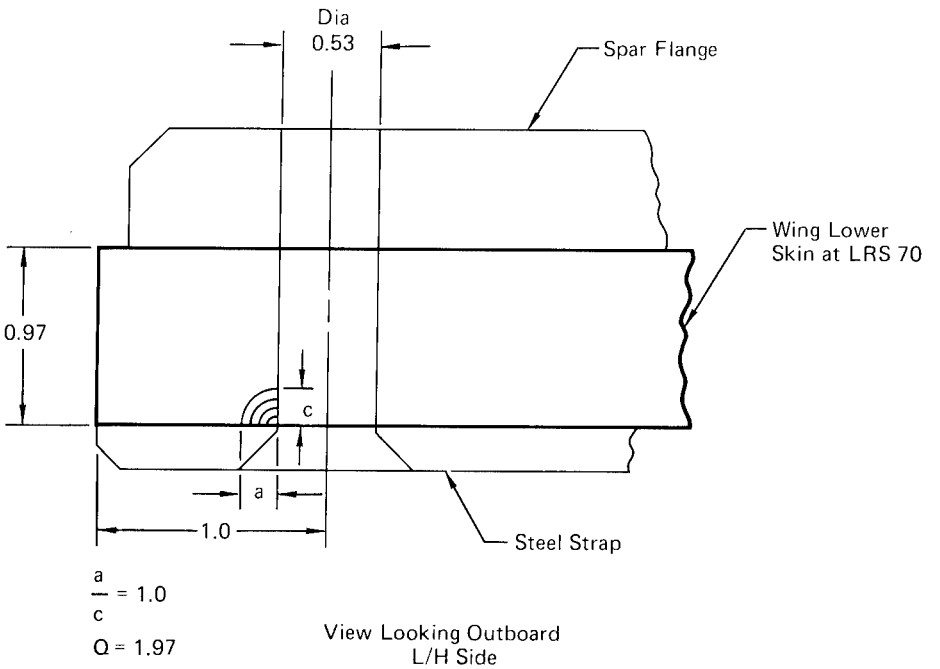

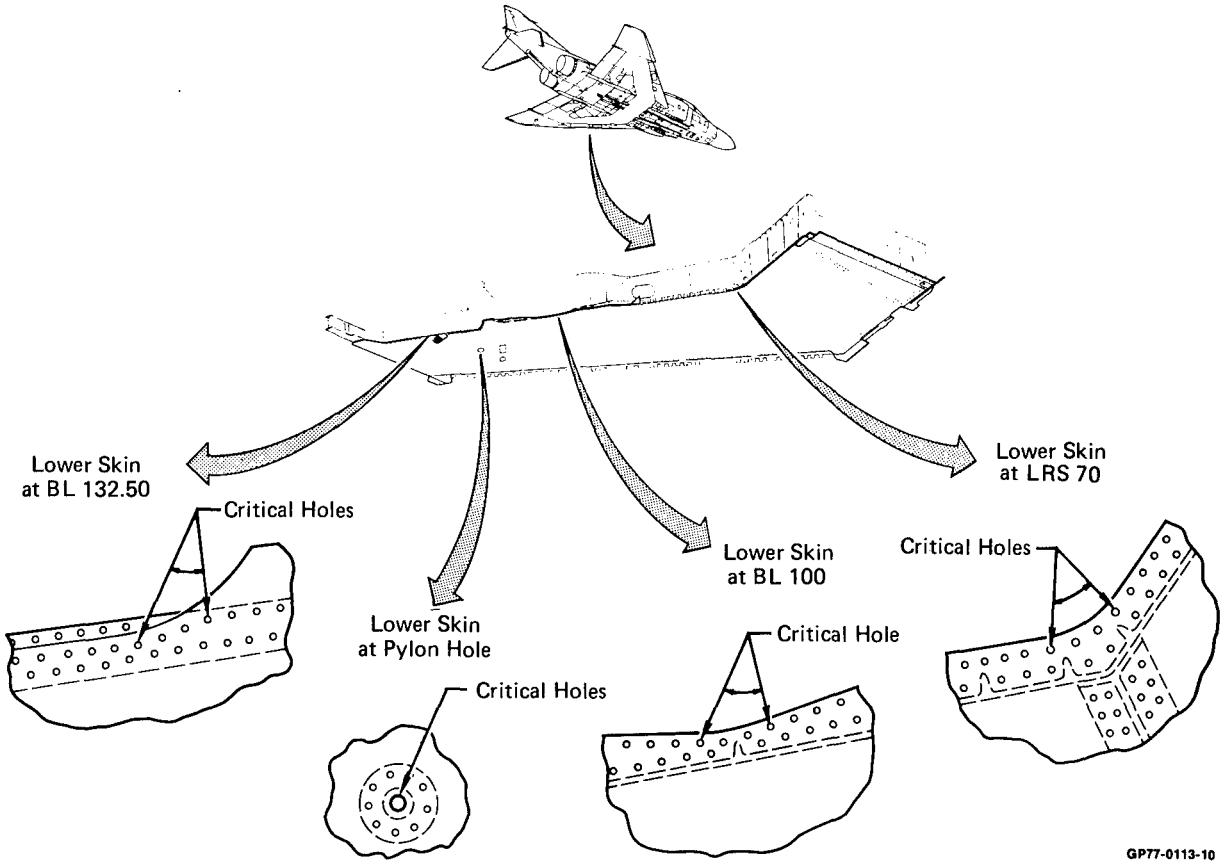

FIGURE 31 POTENTIAL WING LOCATIONS

Location	Best Represents Total Wing Loads	Most Representative of Typical A/C Design	Most Critical	High Load Transfer
LRS 70	√	√		√
BL 100				
BL 132.50		√		√
Pylon Hole			√	

- All Four Locations have Extensive Full Scale and Element Test Data Available
- All Four Locations have had Detailed Strain Surveys
- Flight Measured Loads Available Throughout Wing
- In-Service Inspection Data Available for All Four Locations

Because of Relative Importance of First 2 Criteria
Choose Lower Skin at LRS 70

GP77-0113-6

FIGURE 32 CHOICE OF WING LOCATION

The potential fuselage locations are shown in Figure 33. All these locations experienced cracking in full scale fatigue tests. The choice of the fuselage location is described in Figure 34. Stringer No. 1 at F.S.303 was chosen because it best represents total fuselage loads and is typical of conventional fighter fuselage design. The following information is given for the fuselage location:

Fuselage Baseline Location

Location	Str. No. 1 @ F.S. 303
Max. Baseline Spectrum Stress	26.7 Ksi
Material	7178-T6 Extrusion
Load Transfer	f_{br} = 29.1 Ksi
Fastener Dia.	0.19 Inch
Material Thickness	0.063 Inch

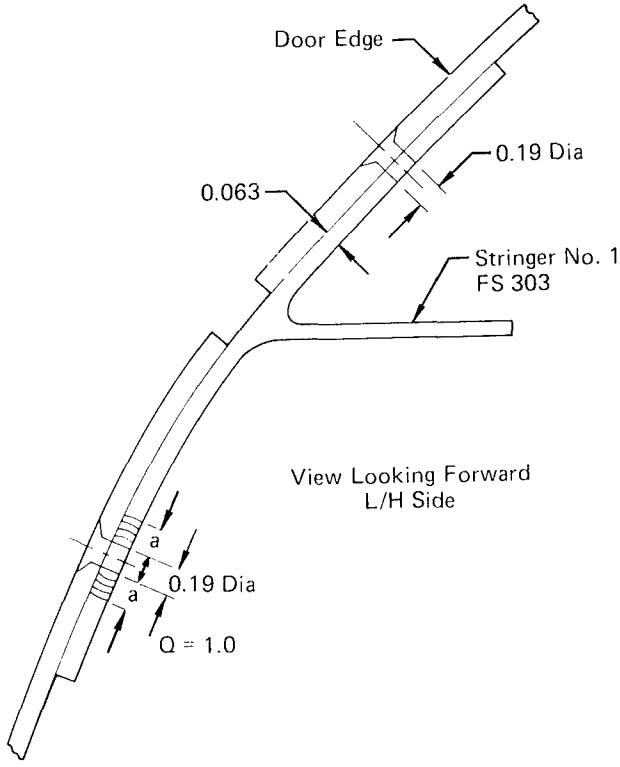

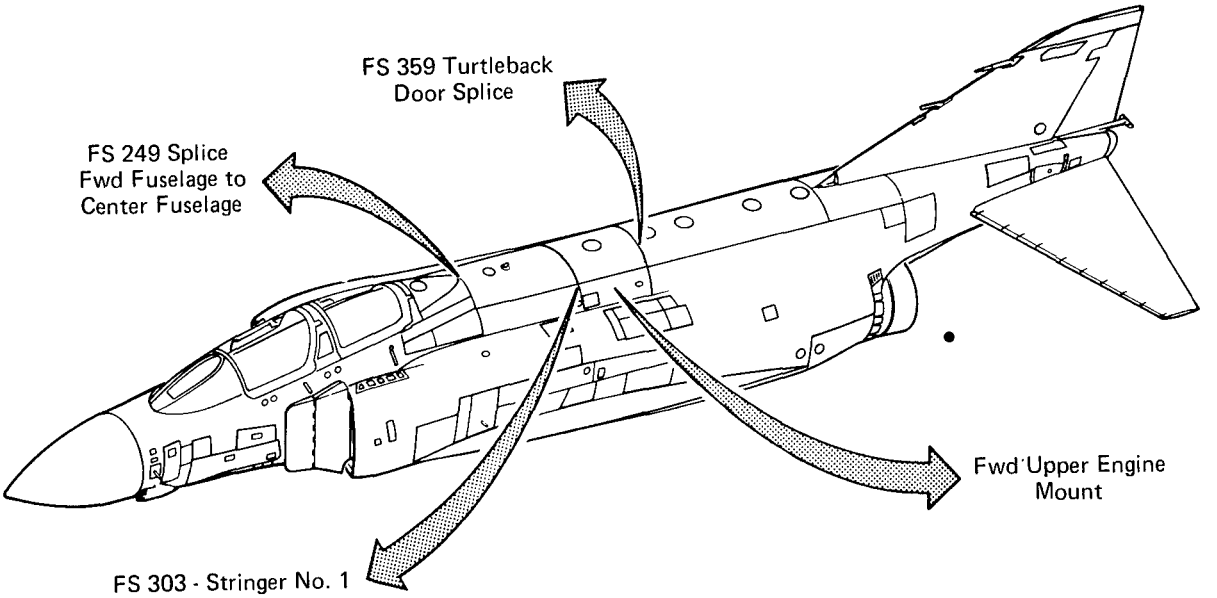

FIGURE 33 POTENTIAL FUSELAGE LOCATIONS

Location	Best Represents Total Fuselage Loads	Most Representative of Typical A/C Design	Most Critical	High Load Transfer
FS 249 Splice	√ (Fwd)			√
FS 303 Str No. 1	√ (Ctr and Aft)	√		
FS 359 Turtle Back Dr				√
Engine Mount			√	

- All 4 Locations have Extensive Full Scale Test Experience
- Element Tests on Str No. 1 and Engine Mount
- Strain Surveys at All 4 Locations
- Flight Measured Loads
- Engine Mt Loads not a Function of Airloads

Because of Relative Importance of First 2 Criteria
Choose Stringer No. 1 at FS 303

FIGURE 34 CHOICE OF FUSELAGE LOCATION

The assumptions used for crack growth predictions are based on studies conducted during the F-4C/D (Reference 10) and F-4E(S) (Reference 2) Damage Tolerance Assessments. The assumptions used in this study are as follows:

- o Initial flaw size (a_i) - 0.01 inch deep
- o Flaw shape parameter (Q) - best estimate of average Q
- o Retardation (m) - average
- o Environment - 1/2 air, 1/2 water

The philosophy used in choosing the above parameters for this study was that the parameters should be realistic, but that taken as a group they should be slightly conservative.

The initial flaw size (a_i) was chosen to be 0.01 inch based on statistical distributions of equivalent initial flaw depths which were developed during the F-4 Damage Tolerance Assessment Programs. An equivalent initial flaw depth is obtained from a fractographic analysis of the fracture surface and an analytical projection of the crack growth curve back to time zero. It was concluded that for the F-4E(S) aircraft, the largest equivalent initial flaw expected to exist in one critical fastener hole per aircraft was 0.0072 inch deep for reamed holes and 0.0095 inch deep for drilled holes (Reference 2).

The flaw shape parameter, Q, was based on the average flaw geometry for each particular area analyzed. The average flaw geometry for each of the F-4E(S) locations was based on a teardown inspection of the F-4E(S) full scale fatigue test article. The flaw geometry for the F-15 locations in paragraph 2.2.3 was based on component tests, and a knowledge of the loading patterns at those locations. In areas where load transfer is appreciable, cracks generally initiate at the corner of the fastener hole (faying surface).

An average value for the retardation parameter, m, was used in the crack growth predictions for this study. The specific value of m which was used for each area is dependent on the material, maximum stress in the spectrum and flaw shape parameter, Q, as explained in Section 2.1.4.4.

The environment was assumed to be a reasonably conservative wet air environment. The da/dN curves which were used were half way between the curves for a distilled water environment and a laboratory air environment.

The results of crack growth predictions for mission parameter variations are shown in Table 1 in terms of a ratio of variation life to baseline life. Explanatory notes appear at the end of the table. Special mission parameter variations are shown in Table 2, and design parameter variations in Table 3.

TABLE 1 MISSION PARAMETER VARIATIONS

Location	Description	Variation/Baseline (1)
LRS 70	Mild Spectrum	1.81
	Severe Spectrum	.67
	Severe A-A	.86
	Severe A-G	.74
	Mild A-A	1.12
	Mild A-G	1.27
	+15% A-A Airspeed	.84
	-15% A-A Airspeed	1.35
	+15% A-G Airspeed	.87
	-15% A-G Airspeed	1.42
	+ 6% A-A Airspeed	.98
	+3000 Lb A-A Gr. Wt. (2)	1.22
	-3000 Lb A-A Gr. Wt. (2)	1.32
	+3000 Lb A-G Gr. Wt. (2)	1.14
	-3000 Lb A-G Gr. Wt. (2)	1.46
	+3000 Lb A-A Gr. Wt. (3)	.91
	+1000 Lb A-A Gr. Wt.	.99
	49% A-A, 26% A-G, 25% N-T	.88
	75% A-A, 25% N-T	.77
	29% A-A, 56% A-G, 15% N-T	.91
	35% A-A, 65% A-G	.77
	75% A-G, 25% N-T	1.18
	+30% A-A Altitude	.93
	-30% A-A Altitude	1.08
	+22% A-A Mission Duration	1.07
	-22% A-A Mission Duration	.91

TABLE 1 MISSION PARAMETER VARIATIONS (Continued)

Location	Description	Variation/Baseline
FS 303	Mild Spectrum	1.62
	Severe Spectrum	.70
	Severe A-A	.86
	+15% A-A Airspeed	.68
	-15% A-A Airspeed	1.43
	-3000 Lb A-A Gr. Wt.	1.38
	+3000 Lb A-G Gr. Wt.	.78
	49% A-A, 26% A-G, 25% N-T	.76
	75% A-A, 25% N-T	.65
	29% A-A, 56% A-G, 15% N-T	.87
	+30% A-A Altitude	.89
	-30% A-A Altitude	1.03

TABLE 2 SPECIAL MISSION PARAMETER VARIATIONS

Location	Description	Variation/Baseline
LRS 70	Simultaneous Variation of:	.89
	+500 Lb A-A Gr. Wt.	
	+500 Lb A-G Gr. Wt.	
	+5% A-A Airspeed	
	+3% A-G Airspeed	
	+10% A-A Altitude	
	30% A-A, 45% A-G, 25% N-T	
	+3000 Lb A-A Gr. Wt. (4)	1.12
	Mildest A/C; Truncated σ Max.	1.32
	Baseline with σ_{Max} = 28.7 Ksi	.69
	Baseline with σ_{Max} = 26.3 Ksi	.46

(1) Life from .010 in. to failure for variation divided by life from .010 in. to failure for baseline.

(2) Mission stresses ratioed by a constant ratio of gross weight.

(3) Same as (2) except spectrum σ_{max} kept same as baseline.

(4) Same as (3) except spectrum σ_{max} is 4% higher than baseline.

5 Baseline life from a = .010 to failure: 10,000 hrs. at LRS 70; 3,700 hrs. at FS 303.

TABLE 3 DESIGN PARAMETER VARIATIONS

Location	Description	Variation/Baseline
LRS 70	K_T: Neat Fit, S.C., Inf. Plate	2.20
	K_T: Clearance Fit, S.C., Inf. Plate	2.17
	DLS = .8 x Baseline ⚠1	1.63
	DLS = .8 x Baseline	1.55
	DLS = 1.2 x Baseline	.55
	DLS = 1.2 x Baseline ⚠1	.64
	- One Fastener Size (3/8 In.)	1.23
	+ One Fastener Size (5/8 In.)	.86
	f_{br} = Baseline f_{br} + Δf_{br} (Δf_{br} = .25 DLS)	.92
	f_{br} = Baseline f_{br} - Δf_{br} (Δf_{br} = .25 DLS)	1.06
	K_T: Clearance Fit, S.C., 2D	.87
FS 303	K_T: Neat Fit, D.C., Inf. Plate	1.90
	K_T: Clearance Fit, D.C., Inf. Plate	1.81
	DLS = .8 x Baseline	1.54
	DLS = .8 x Baseline ⚠2	1.45
	DLS = 1.2 x Baseline	.62
	DLS = 1.2 x Baseline ⚠2	.72
	+ One Fastener Size (1/4 In.)	.78
	- One Fastener Size (5/32 In.)	1.14
	K_T: Clearance Fit, D.C., 2D	.90
	f_{br} = Baseline f_{br} + Δf_{br} (Δf_{br} = .25 DLS)	.92
	f_{br} = Baseline f_{br} - Δf_{br} (Δf_{br} = .25 DLS)	1.08

⚠1 4340 Steel

⚠2 Ti 6Al-4V

S.C. = Single Crack

D.C. = Double Crack

2D = 2 Diameters from ℄ hole to edge of part

2.1.4.7 Effects of Aircraft Usage Sequencing - The effect of mission assignments on fleet aircraft must be understood not only to be able to plan inspections, repairs, and retirement, but to effectively plan aircraft rotation.

During the study three mission sequencing combinations were studied:

1. F-4 Baseline → FMS Severe → FMS Mild → FMS Severe
2. F-4 Mild → F-4 Severe
3. F-4 Baseline → T-Bird Diamond → T-Bird Solo
   T-Bird Diamond → F-4 Baseline

FMS (Foreign Military Sales) spectra in this study are representative of severe and mild usage by a foreign nation using the F-4 aircraft. T-Bird usage is based on load factor exceedance data compiled during the time period that the Air Force demonstration team used the F-4E aircraft. The term diamond is derived from the fact that four of the aircraft maneuvered in a tight diamond formation. The diamond usage was equivalent to F-4C/D severe usage. The solo aircraft performed maneuvers generally independent from the diamond formation. Solo usage was the most severe of all known USAF F-4 usage. Figure 35 shows a load factor exceedance comparison of FMS, T-Bird and F-4E(S) usage.

The generalized Willenborg model (Reference 11) was used for the load sequencing conditions. Results were compared to those obtained from the Wheeler model as modified by MCAIR. The stress sequencing used for the Willenborg analysis was accomplished by the same method as described in Paragraph 2.1.3.

The first spectrum run is the case where an F-4E flies 2000 hours of USAF baseline usage and then is sold to a foreign country that flies more severely than USAF. The aircraft then flies a sequence of FMS severe, FMS mild, FMS severe, etc. in 2000 hour segments until failure. This sequence was first run with the normal placement of loads using the Willenborg model. The .010 to failure life was 11,620 hours. The sequence was then run with the peak load at the end of each FMS severe segment. For this run the .010 to failure life was reduced to 11,540 hours due to the peak load retarding the crack growth of fewer severe loads and more mild loads. Additional variations were run and are summarized in Table 4.

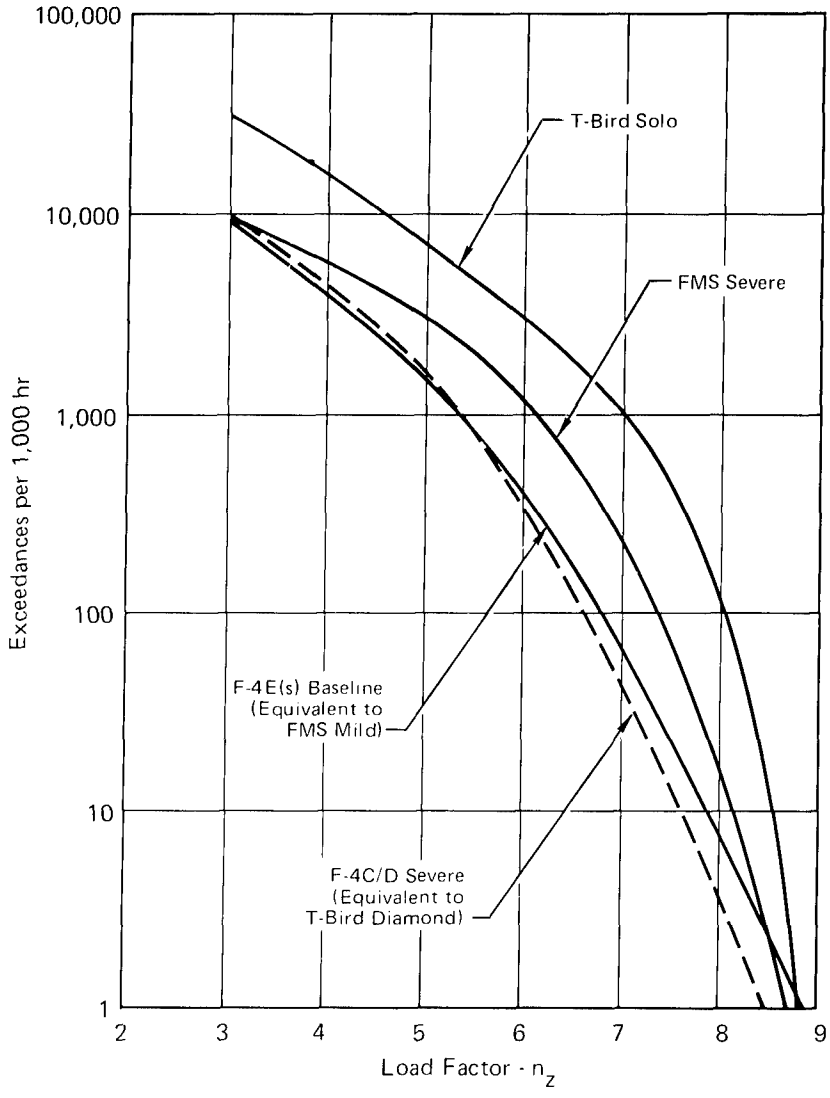

FIGURE 35 F-4 LOAD FACTOR EXCEEDANCE COMPARISON

TABLE 4 SEQUENCE 1 - F-4E BASELINE → FMS SEVERE → FMS MILD

RUN NO.	DESCRIPTION	.010 TO FAILURE LIFE (HOURS)
1	Normal Placement of Peak Loads (1)	11,620 (13,000)
2	Peak Load at End of FMS Severe	11,540
3	Normal Placement of Peak Loads (1000 Hour Segments)	12,040
4	Without History From Preceding Segment (2)	11,620
5	Peak Load Deleted From FMS Severe	11,440

(1) All Runs Made Up of 2000 Hour Segments Unless Otherwise Noted

(2) Delete Plastic Zone at End of Each Segment

( ) Life Using Modified Wheeler Model

The second spectrum run is the case where a USAF F-4E(S) aircraft flies a sequence of F-4E(S) mild, F-4E(S) severe, F-4E(S) mild, etc. in 2000 hour segments until failure. A crack growth curve is shown in Figure 36 and the results for each variation are summarized in Table 5.

The third spectrum run is the case where an F-4E flies 2000 hours of F-4E baseline usage and then becomes a USAF T-Bird. It then flies a sequence of 1000 hours diamond, 1000 hours solo, 1000 hours of diamond and goes back to the using command to fly F-4E baseline usage until failure. The results of each variation are summarized in Table 6.

Crack growth curves for each of the above cases of aircraft usage sequencing are shown in Appendix A.

2.1.4.8 Conclusions - The following conclusions are drawn with regard to the crack growth predictions for F-4E(S) Mission Parameter Variations:

- o The initial mission parameter variations ($\pm$ 15% in airspeed, $\pm$ 3000 lb in gross weight, etc.) were useful in bounding the problem, but variations in airspeed on the order of $\pm$ 5% and in gross weight of $\pm$ 1000 lb are believed to be more realistic.
- o The parameters that should be evaluated and/or accounted for in the development of a tracking program for a conventional fighter such as the F-4 are:
  - Load factor exceedance
  - Airspeed
  - Gross weight
  - Mission mix
  - Altitude

2.2 Multi-Mission Fighter - Variant From Baseline

The F-15 was selected as a variant from the F-4E(S) baseline because it is a convenient example of a fighter aircraft with a more sophisticated control system than the more conventional F-4 (the F-15 has differential tail augmented roll).

2.2.1 Mission Parameter Variations - Crack growth for baseline spectra was evaluated at two locations on the F-15 aircraft - one wing location and one stabilator location. Mission parameter variations were evaluated at the wing location and consisted of three mission mix variations (Figure 37).

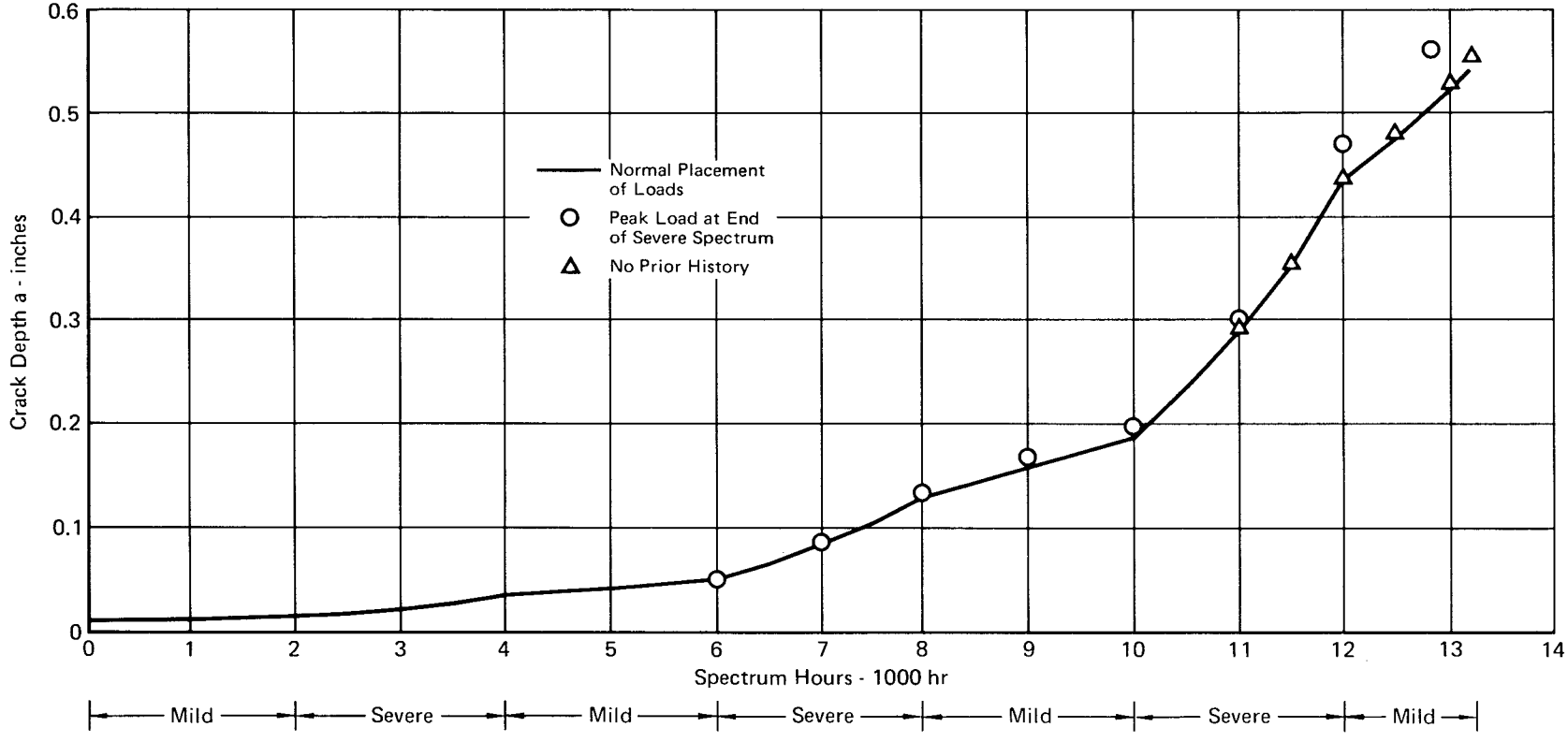

FIGURE 36 AIRCRAFT USAGE SEQUENCING - F-4E(S) MILD, F-4E(S) SEVERE, ETC.

TABLE 5 SEQUENCE 2 - F-4E(S) MILD → F-4E(S) SEVERE → F-4E(S) MILD

RUN NO.	DESCRIPTION	.010 TO FAILURE LIFE (HOURS)
1	Normal Placement of Peak Loads (1)	13,220 (14,200)
2	Peak Load at End of Segment	12,850
3	Without History From Preceding Segment (2)	13,220

(1) All Runs Made Up of 2000 Hour Segments

(2) Delete Plastic Zone at End of Each Segment

( ) Life Using Modified Wheeler Model

TABLE 6 SEQUENCE 3 - F-4E BASELINE → T-BIRD DIAMOND → T-BIRD SOLO → T-BIRD DIAMOND → F-4E BASELINE

RUN NO.	DESCRIPTION	.010 TO FAILURE LIFE (HOURS)
1	Normal Placement of Peak Loads (1)	21,400
2	Peak Load at End of Diamond and Solo Segments	20,400
3	Without History From Preceding Segment (2)	20,400

(1) Runs Are Made of 1000 Hour Segments Except for Final F-4 Baseline Segment

(2) Delete Plastic Zone From Preceding Segment

Mix		Air-to-Air	Air-to-Ground	Non-Tactical
Baseline	(1)	47.5%	32.5%	20%
Variation 1	(2)	32.5%	47.5%	20%
Variation 2	(3)	80%	0%	20%
Variation 3	(4)	0%	80%	20%

(1) Reference 9 - F-15 Service Life Analysis Report

(2) Transpose air-to-air and air-to-ground

(3) Replace air-to-ground with air-to-air

(4) Replace air-to-air with air-to-ground

FIGURE 37 MISSION MIX VARIATIONS

2.2.2 Development of Stress Spectra - The baseline spectrum from the F-15 Service Life Analysis Report (Ref. 9) is the reference spectrum from which variations are defined and evaluated.

The spectrum used for crack growth predictions utilizing the modified Wheeler prediction method is a so-called block spectrum composed of three mission types: air-to-air, air-to-ground, and non-tactical. An example for an individual mission type is shown in Figure 38.

Mission Mix - The three variations were obtained by the same method used for the F-4E(S) block spectra, i.e., ratioing the counts by the mission mix percentages.

For the case of the mix of 80% air-to-ground and 20% non-tactical, a modification was made to the F-15 baseline air-to-ground stress spectrum. The baseline stress spectrum used for fatigue life evaluation of the F-15 was primarily an air-to-air spectrum. The air-to-ground stress spectrum had little or no retardation, therefore, crack growth predictions for mission mix variation 3 (Figure 37) resulted in what is believed to be an unrealistically low fracture life. It was suspected that the maximum spectrum stress for the F-15 air-to-ground design curve was low. A comparison was made of exceedances per 1000 hours vs % DLS for the F-15 and F-4E(S) (Figure 39). This comparison shows that the F-15 design curve has a different shape than the usage curve for the F-4E(S), and that the maximum

	MINIMUM % TLL											
MAX % TLL	.394	.356	.319	.282	.125	.050	.030	-.050	-.131	-.199	-.283	-.380
.374					3168		526		3	3	1	1
.473					2641		472	365	358			
.568				952	737			46	204	1	1	
.659			490		526		211			3		
.766		102			211	54	10	35	21	1		
.882	3				6	4		40	1	3		1
1.017								7	1			
1.162								1				

Air-to-Air Block of Baseline Spectrum

FIGURE 38 F-15 SERVICE LIFE SPECTRUM AIR-TO-AIR OCCURRENCES PER 475 HOURS

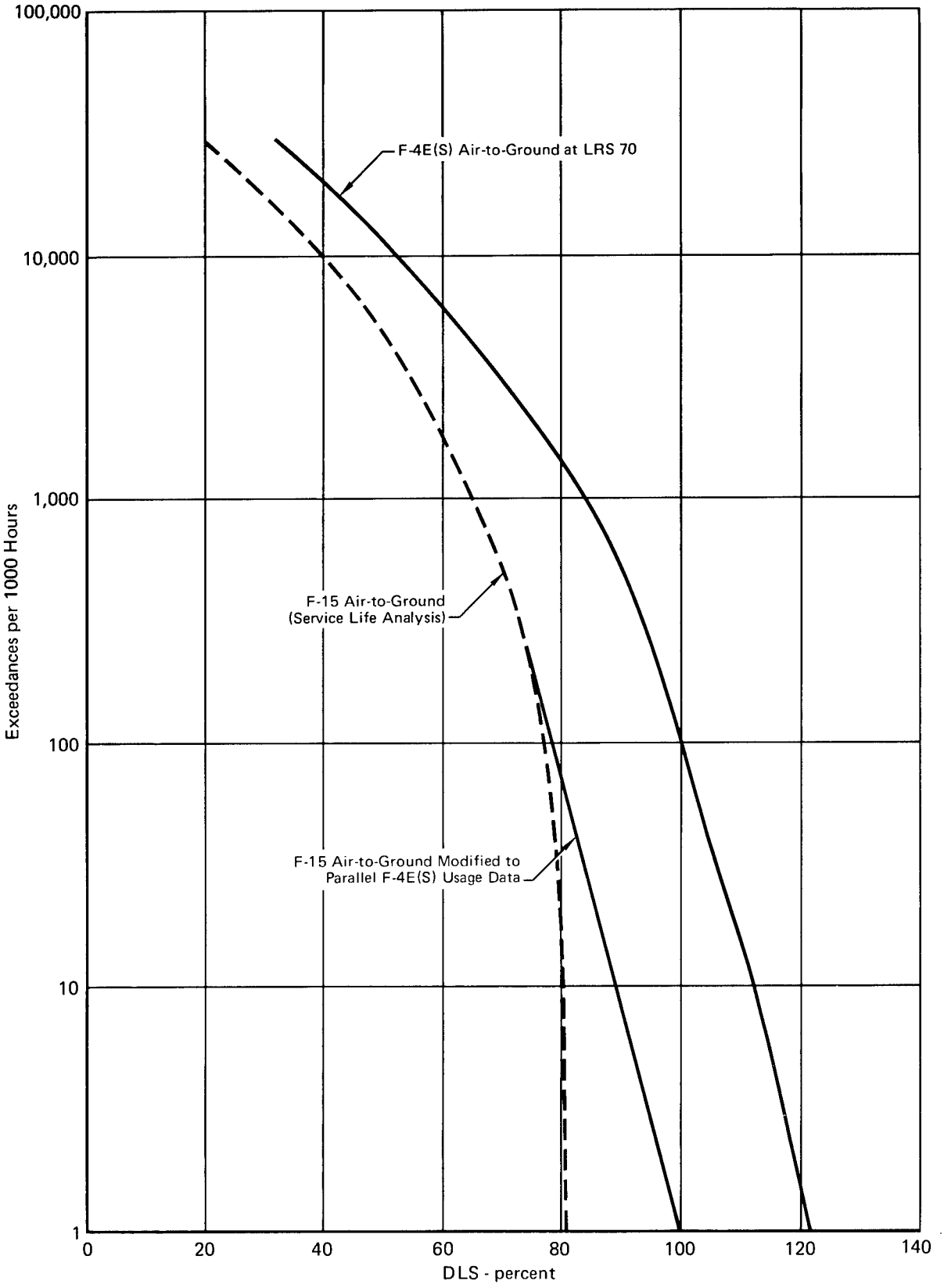

FIGURE 39 F-15 MODIFIED AIR-TO-GROUND PERCENT DLS SPECTRUM

spectrum stress for the F-15 appears low. Since a large amount of F-4 VGH data by mission has been accumulated from which the shape of the air-to-ground stress spectrum can be determined, it was assumed reasonable to let the F-15 air-to-ground stress spectrum approximately parallel that of the F-4E(S), for purposes of this study. The modified F-15 air-to-ground spectrum is shown in Figure 40.

The absence of high stress levels in the baseline air-to-ground spectrum has little effect on F-15 life when used with the baseline mission mix of 47.5% air-to-air, 32.5% air-to-ground, 20% non-tactical. The .010 to failure fracture life for the F-15 spectrum with the modified air-to-ground spectrum is only 1% less than for the unmodified F-15 baseline spectrum.

2.2.3 Crack Growth Predictions - The modified Wheeler crack growth prediction method was chosen for the evaluation of mission parameter variations.

Crack growth predictions were made at two critical locations on the F-15 aircraft - one wing location and one horizontal tail location. The fuel vent line hole in the main spar web was chosen as the wing location and is shown in Figure 41.

Figure 42 shows the stabilator spindle to cover plate splice which was chosen as the stabilator location.

	MINIMUM % TLL					
MAX % TLL	.070	.030	0	-.050	-.131	-.199
.250					6	4
.374	2485					
.473	1065					2
.568	508	267				
.659	137			90	138	
.766			2	115		
.882	13	2	extrapolated counts			
1.017	1					

FIGURE 40 F-15 SERVICE LIFE SPECTRUM AIR-TO-GROUND OCCURRENCES PER 325 HOURS

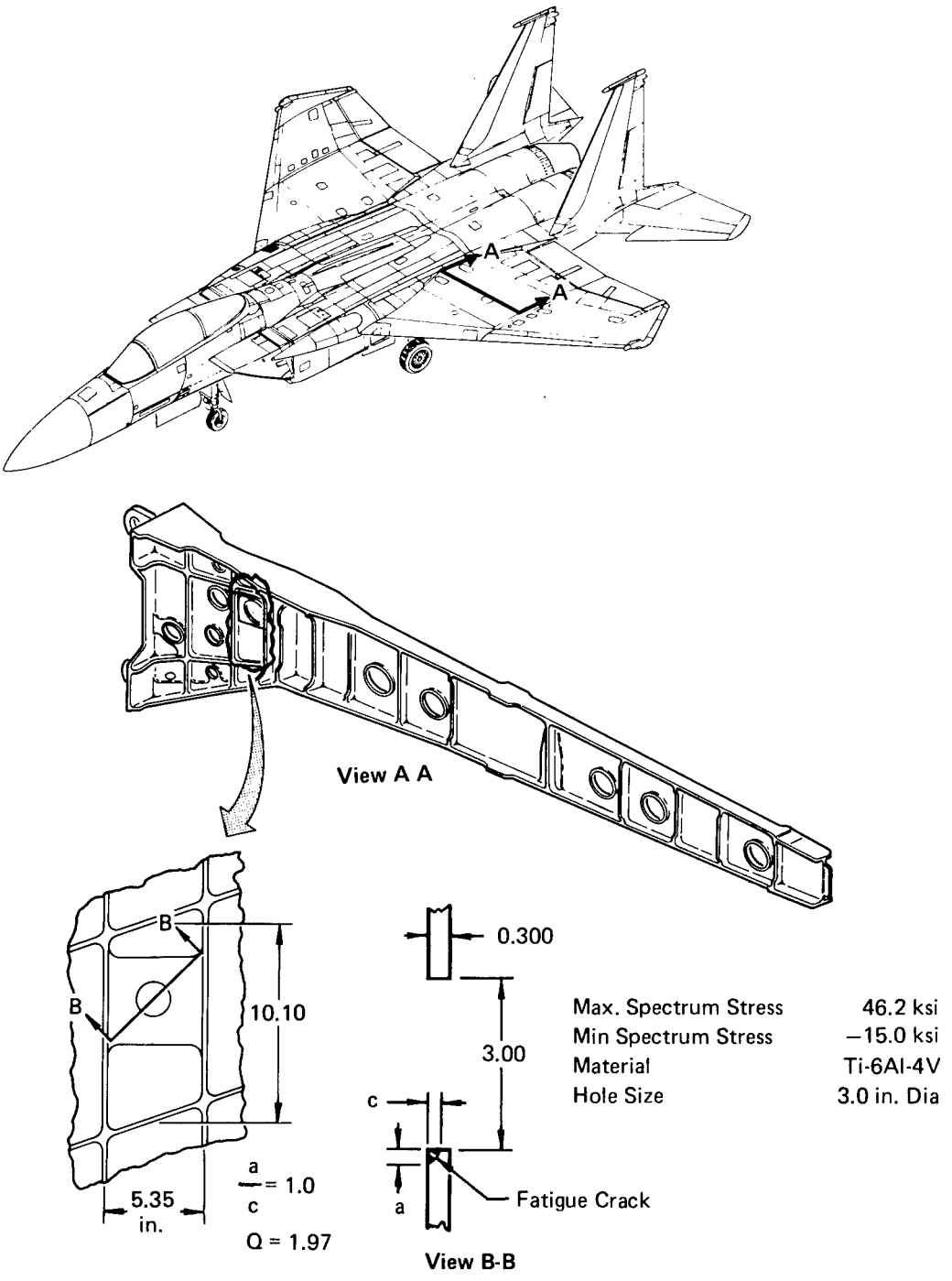

FIGURE 41 WING BASELINE LOCATION - MAIN SPAR WEB FUEL VENT LINE HOLE

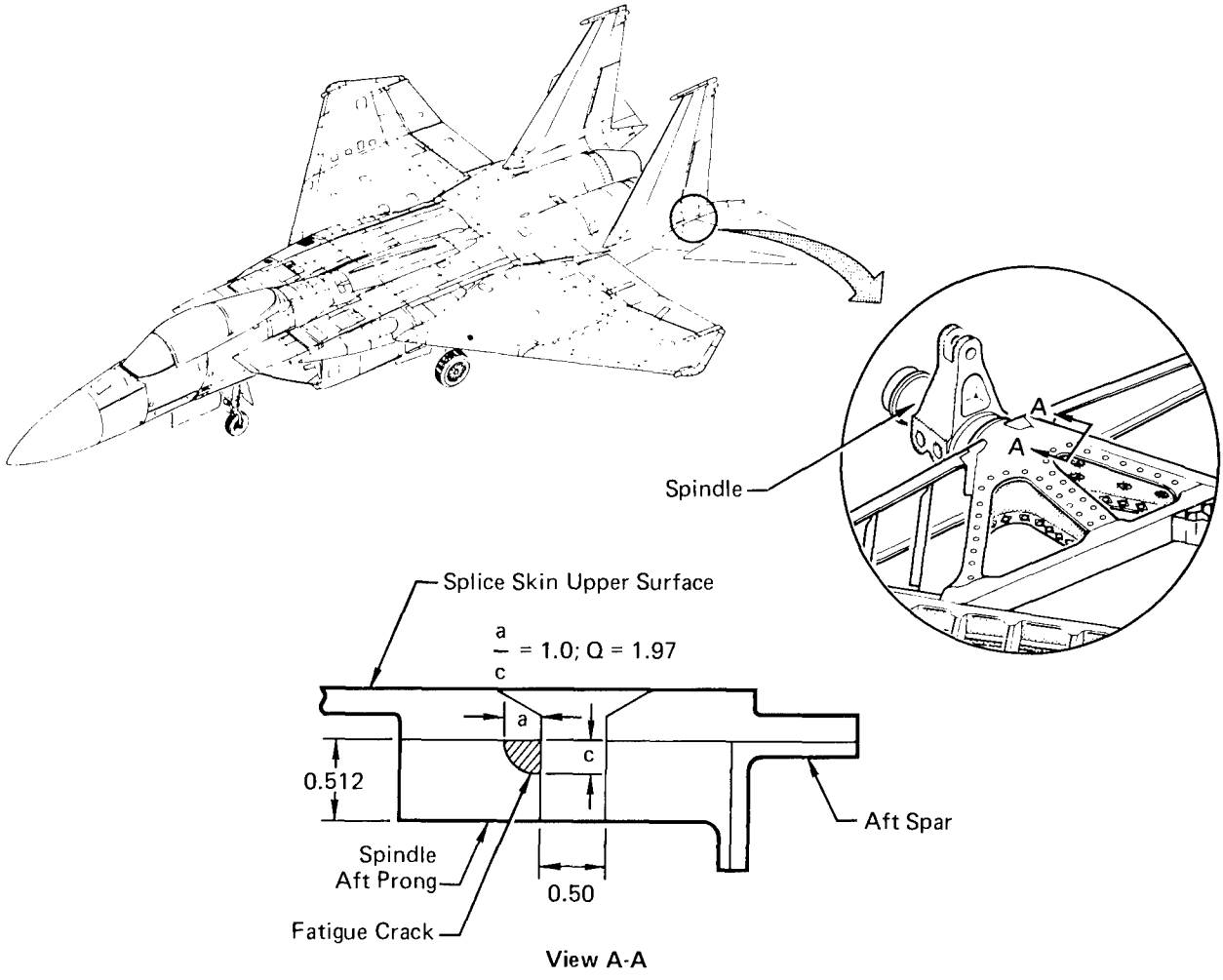

Max Spectrum Stress	50.7 ksi
Min Spectrum Stress	−29.8 ksi
Bearing Stress	29.7 ksi
Material	Ti 6Al-4V
Fastener Size	0.50 in. Dia

FIGURE 42 STABILATOR BASELINE LOCATION-SPINDLE AFT PRONG AT THE STABILATOR SPINDLE TO COVER SPLICE

The results of crack growth predictions for mission parameter variations are shown in Table 7 in terms of a ratio of .010 to failure variation life to .010 to failure baseline life.

TABLE 7 MISSION PARAMETER VARIATIONS

LOCATION	DESCRIPTION	VARIATION/BASELINE
Main Spar Web- Fuel Vent Line Hole	Baseline Spectrum 47.5% A-A, 32.5% A-G, 20% N-T	1.0
	32.5% A-A, 47.5% A-G, 20% N-T	1.13
	80% A-A, 20% N-T	.85
	80% A-G, 20% N-T	.66

A crack growth comparison of the F-15 wing and stabilator locations is shown in Figure 43. As can be seen in Figure 43, the shape of the two crack growth curves are different. A cusp in the curve for the wing location occurs

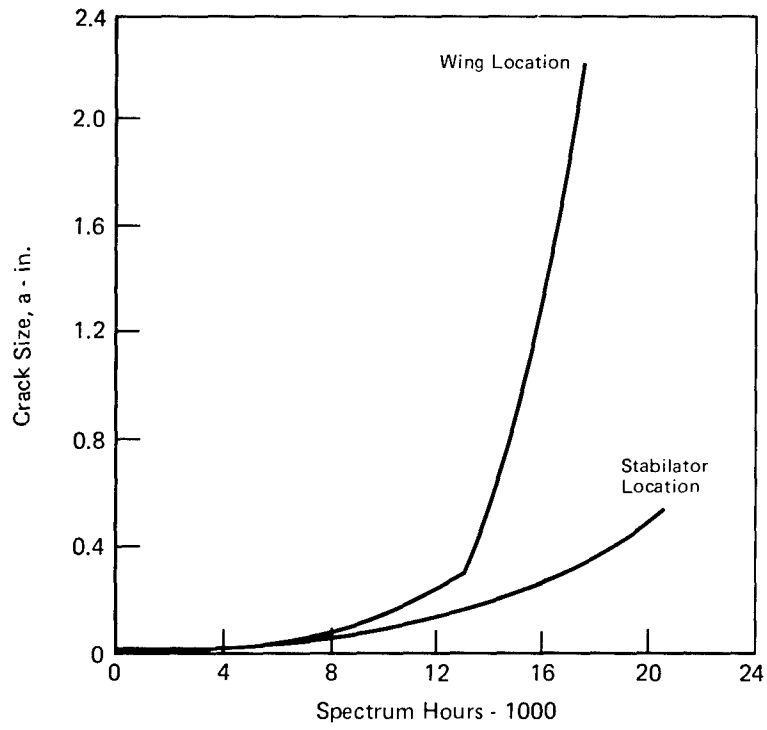

FIGURE 43 F-15 VARIANT FROM BASELINE F-4E(S) WING AND STABILATOR LOCATIONS

when the crack transitions from a corner crack to a through thickness crack, and the critical crack length is large because of the relatively low maximum spectrum stress. The crack growth curve for the stabilator spindle has no transition from a corner crack to a through thickness crack since the crack reaches a critical crack length at the time that it propagates through the thickness.

The loads acting on the F-15 horizontal stabilator are dependent not only on n_z, but on several other parameters as well. Some of the more important parameters are airspeed, altitude, angle of attack, stabilator position, roll rate, roll acceleration, c.g. position, geometric configuration, pitch rate and pitch acceleration. To illustrate the significance of the flight parameters on the stabilator, the stress level at the upper cover plate splice was calculated for six conditions. Those stress levels are summarized in Table 8. The effect of n_z is shown by the comparison of conditions 1 and 2, and of conditions 3 and 4. The effect of airspeed is indicated when conditions 1 and 3, and 2 and 4 are compared. Notice that airspeed has a very significant effect on stress level. In general, stress levels for supersonic maneuvers are greater than those for subsonic maneuvers. The typical effect of roll rate and roll acceleration on stress level can be seen by comparing conditions 5 and 6. Not only does the unsymmetrical maneuver cause stress levels that are 3 or 4 times greater than the symmetrical maneuver, but the load has a sign change between the left and right hand stabilators. Thus, not only should other flight parameters in addition to n_z be monitored in the tracking program, but the left and right hand stabilators should be tracked separately. For the F-15 aircraft, this is accomplished through the use of a signal data recorder system which monitors 22 flight parameters sequentially, as explained in Paragraph 3.2.4. The flight parameters are converted to stresses at fatigue critical locations by the operational fatigue loads computer program.

TABLE 8 STRESS LEVEL AT THE F-15 STABILATOR SPINDLE TO UPPER COVER PLATE SPLICE

CONDITION	STRESS ∿ LEFT STABILATOR (KSI)	STRESS ∿ RIGHT STABILATOR (KSI)
1. Symmetrical Pull-Up Mach 0.9, 20000 Ft., n_z = 1g	0.2	0.2
2. Symmetrical Pull-Up Mach 0.9, 20000 Ft., n_z = 7g	7.8	7.8
3. Symmetrical Pull-Up Mach 1.2, 20000 Ft., n_z = 1g	-8.3	-8.3
4. Symmetrical Pull-Up Mach 1.2, 20000 Ft., n_z = 7g	35.4	35.4
5. Rolling Pull-Out Mach 0.9, 20000 Ft., n_z = 5.86g Roll Rate = 144.6 Deg/Sec Roll Acceleration = -1.76 Rad/Sec^2	-22.0	30.6
6. Symmetrical Pull-Up Mach 0.9, 20000 Ft., n_z = 5.86g	7.1	7.1

Conclusions - The following conclusions are drawn regarding the crack growth predictions for the F-15 variant as compared to the F-4:

- For the F-4 program, N_Z is tracked using a counting accelerometer in each fleet aircraft. To supplement this N_Z data, VGH recorders in 10% of the aircraft furnish data on velocity, altitude, and gross weight, as well as N_Z. The VGH data is used in the development of stress spectra that can be used for periodically updating the tail tracking program.
- For the F-15 more flight parameters must be monitored on the more recent generation of fighters that use more sophisticated control systems such as differential tail augmented roll, variable sweep wings, and canards. Additional parameters that need to be monitored for stabilator loads on the F-15 are:

  Stabilator Position

  Roll Rate

  C.G. Position

  Roll Acceleration

  Pitch Rate

3. DEVELOPMENT OF GENERALIZED PROCEDURES

Generalized procedures have been developed to track crack growth for fighter class aircraft. Two types of fighters were investigated: the F-4E(S) (baseline) type which is relatively insensitive to unsymmetrical loads, and the F-15 (variant from baseline) which is sensitive to unsymmetrical loads and consequently requires a significantly different tracking program. Crack growth predictions from Section 2.0 showing the effects of various mission usage parameters were utilized in developing the generalized tracking procedures. Advantages and disadvantages of various recording systems have been investigated.

Purpose of Tracking Crack Growth

The following is a list of some of the purposes for tracking crack growth:

- When to inspect
- When to repair
- When and where to rotate aircraft
- When to retire an aircraft

Economic limits are associated with the time to repair or modify an aircraft, while safety limits are associated with the useful life of the aircraft. Inspection intervals may be tied to either an economic limit or a safety limit, with NDI capabilities a possible constraint in either case. Rotation of aircraft to different usage bases can help to prolong aircraft life.

In the F-4C/D and F-4E(S) Damage Tolerance Assessment Programs (References 10 and 2) an economic repair limit was defined as the opportune time for retrofit incorporation. The following assumptions were made:

- Any individual hole can have initial flaw size - a_i = 0.01 inch
- Flaw shape parameter Q - Best estimate of average Q
- Environment - Air
- Retardation - Average

The economic repair limit was defined for fastener holes as the time to grow from 0.01 inch to 0.03 inch (radial clean up for one fastener diameter oversize, Figure 44). The average Q value for a particular location was based on the known flaw shapes of cracks existing at that location on the full scale fatigue test article.

The safety limit was defined as the life beyond which a failure potential is believed to exist if no inspection and/or repair is accomplished. The

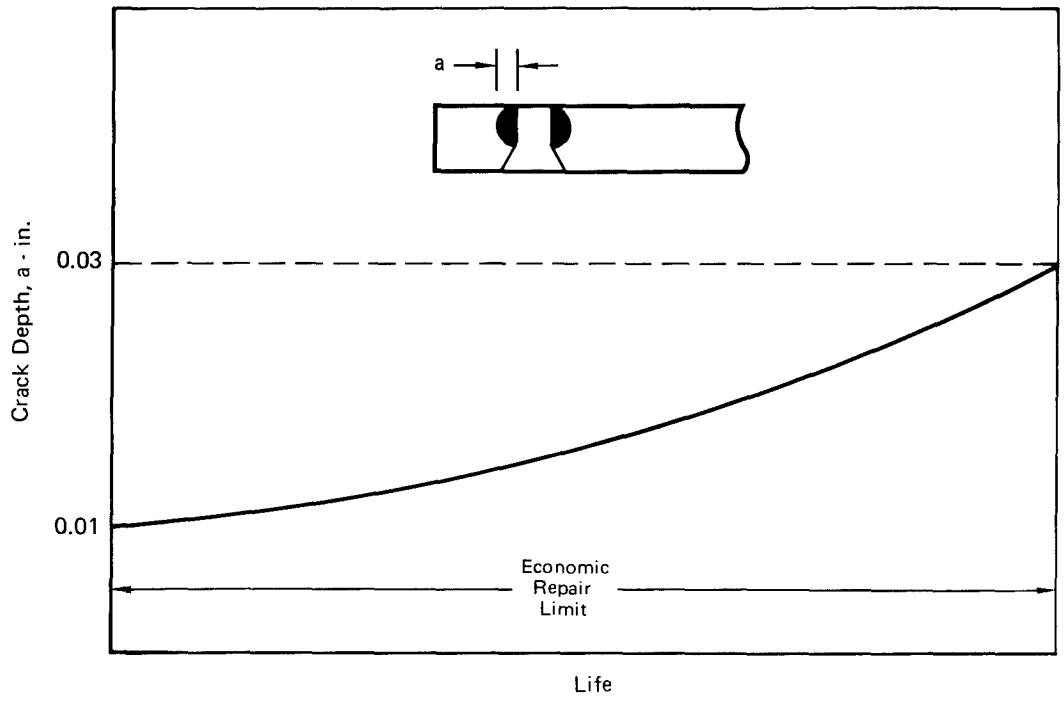

FIGURE 44 ECONOMIC REPAIR LIMIT

following assumptions were made:

- Any individual hole can have a_i = 0.03 inch
- Severe flaw shape
- Severe environment (1/2 air, 1/2 water)
- Retardation is average

The safety limit was defined as the life from a 0.03 inch crack to failure (Figure 45). The da/dN curve for severe environment was taken half-way between the da/dN curves for a laboratory air environment and a distilled water environment for a given material.

Fleet Management

Wide usage variations exist between individual fighter aircraft, therefore, an individual aircraft data acquisition system is required. Two general types were studied: the F-4 type which is relatively insensitive to unsymmetrical loads and a second type (represented by the F-15) which has more complex internal load interaction that is sensitive to unsymmetrical loads. With the F-4, tracking can be keyed to one location, and normalized crack growth will

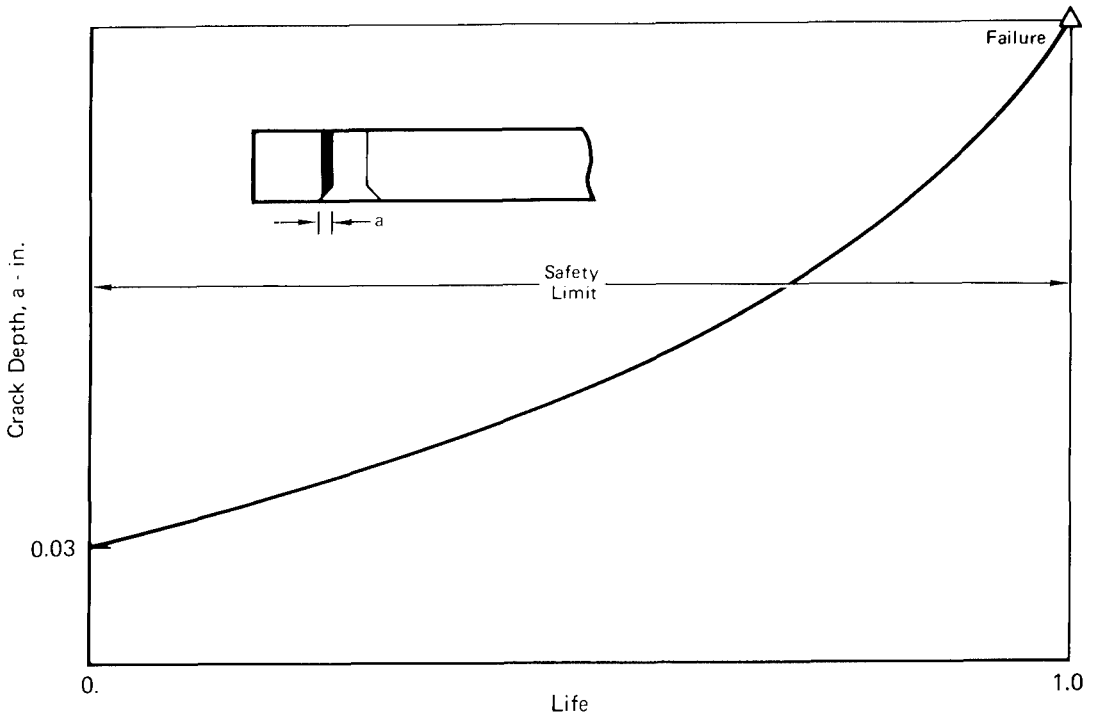

FIGURE 45 SAFETY LIMIT

allow assessment of other locations. For the second type, one set of parameters is required for the wing, another set of parameters is required for the tail, and combinations of wing and tail parameters are required for certain portions of the fuselage. Therefore, more sophisticated tracking procedures and recorders are required.

3.1 Parametric Analysis for Tracking Crack Growth

Analytical methods for tracking crack growth at all critical locations are based on results of parametric studies. Each method must be keyed to the aircraft classification and the types of aircraft within a class as well as the data gathering requirements for fleet tracking. Alternate methods for tracking crack growth are available. A few of the possible approaches are discussed in the following paragraphs.

One approach is to monitor the crack growth at one or more critical locations. Counting accelerometer and VGH data are used to determine the aircraft spectrum. A damage index (D.I.) and S-N system is used to determine the crack growth at monitored locations. The spectra developed from the counting accelerometer and VGH data are used to perform element and full scale fatigue tests. The test data is used to determine crack growth at the monitored locations and to develop S-N data based on crack growth from the element test results. The amount of crack growth at other critical locations is evaluated by damage index

limits which relate to the monitored locations. An explanation of damage index limits is given in paragraph 3.1.2. This method can be used for damage evaluation on fighter aircraft such as the F-4 and F-15, as well as other aircraft types. This approach is supported by the work performed on the F-4C/D and F-4E(S) Fatigue and Damage Tolerance Assessment Programs, References 10 and 2, respectively.

A second approach is to monitor the cycle-by-cycle crack growth at multiple locations through the use of a signal data recorder (SDR). The SDR continuously records several significant flight parameters as a function of time. The tape is input into a computer program to determine the cycle-by-cycle stresses at several locations on the aircraft. With this kind of data, a cycle-by-cycle crack growth analysis could be performed.

Another approach is to monitor the crack growth at one critical location through a damage index and normalized crack growth curve system. Normalized crack growth curves are established for all critical locations by a crack growth analysis at each location. These curves point out trends that can be used in conjunction with damage index limits to determine the damage at all critical locations. This method can be used for those cases where only the flight hours and landings are recorded. This method differs from the first approach in the amount of data available, i.e., no measured data (counting accelerometer, VGH, etc.) is available from individual aircraft - only flight hours and landings. Due to the lack of data, this approach is essentially analytical.

Normalized crack growth curves, damage index limits and S-N data development are described in the following paragraphs.

3.1.1 Normalized Crack Growth Curves - A normalized crack growth curve is obtained by replotting the portion of the analytical crack growth curve for the economic or safety limit as shown in Figures 46 and 47, respectively.

When normalized crack growth curves for all critical locations are superimposed, an envelope is established for a given aircraft configuration and the baseline spectrum. Trends established by the normalized crack growth envelopes on the F-4C/D Damage Tolerance Assessment Program for the economic and safety operational limits at forty-two critical locations indicate that normalized crack growth curves can be valuable when used in a tracking program.

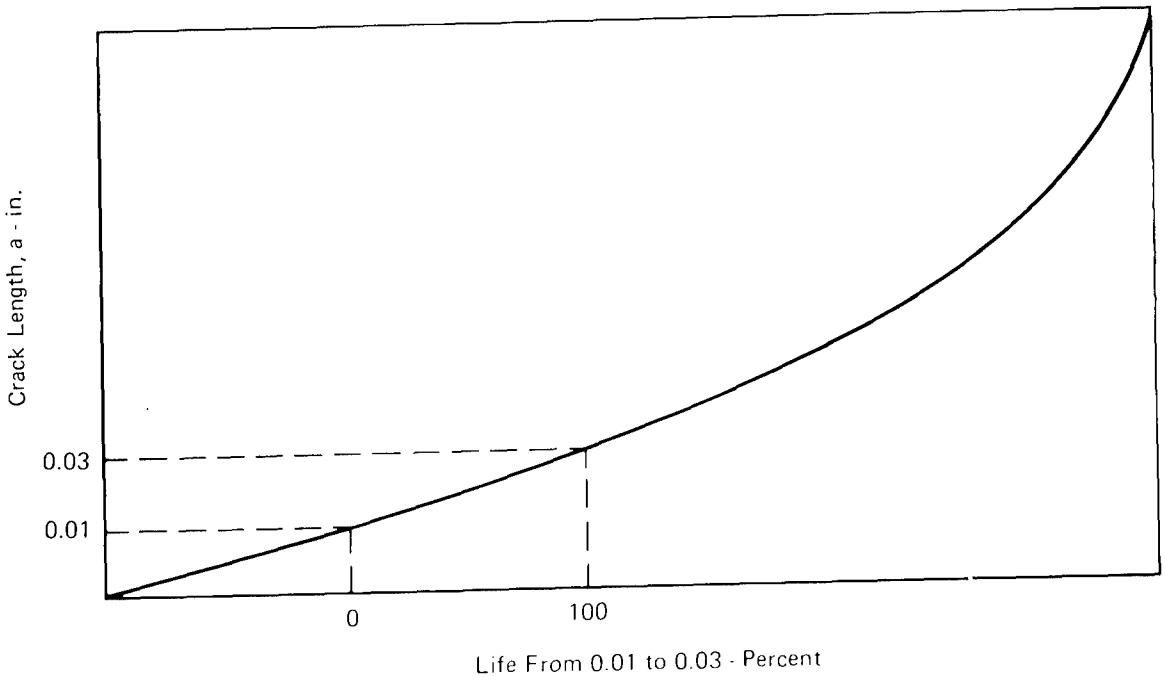

FIGURE 46 ECONOMIC REPAIR LIMIT

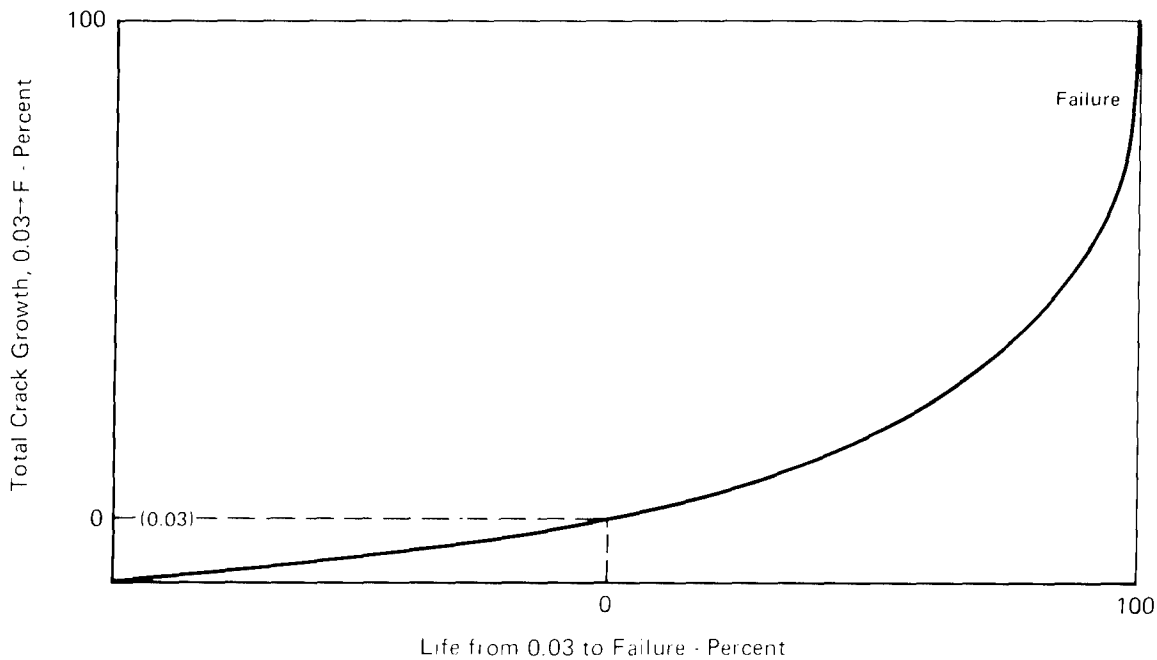

FIGURE 47 SAFETY LIMIT

Figure 48 represents the F-4C/D normalized crack growth envelope for the economic limit at all critical locations as well as some curves for individual locations. As can be seen, very little scatter is evident. The fastest normalized growth rate is for the centerline rib which is a high load transfer location. This is understandable since substantial load transfer induces an initially rapid crack growth rate for a crack propagating from a fastener hole when compared to areas with low load transfer. The slowest normalized crack growth rate is for a crack growing from a hole in the skin at the side brace actuator (SBA) rib which has no load transfer. It is of interest also to note that the crack growth curve for the lower torque box skin at BL 44, which represents the average normalized crack growth rate for all locations, is for a crack growing from a hole due to a combination of through stress and load transfer.

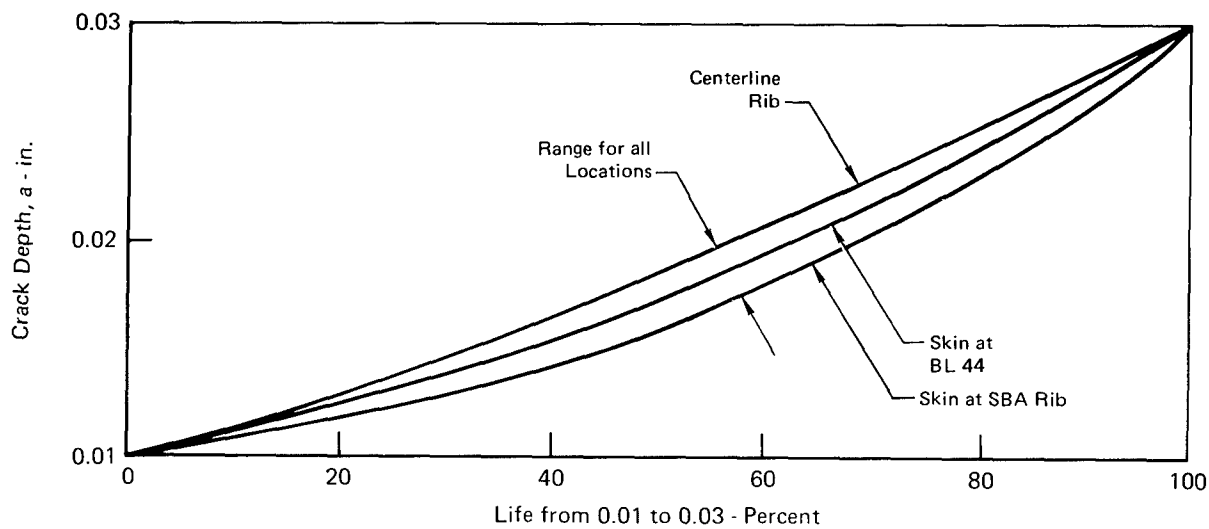

FIGURE 48 COMPARISON OF CRACK GROWTH FROM LOCATION TO LOCATION FOR F-4C/D AIRCRAFT
Economic Repair Limit
ASIP Baseline Spectrum

It is significant that if one location was used to monitor the economic limit for all other locations, very little error would be induced at the other locations.

As an example, assume that the skin at BL44 is used as the monitoring location. Also assume that a particular airplane in the fleet has flown the equivalent of 3000 baseline hours. What size crack would presently exist at the centerline rib if it were assumed that a 0.01 inch flaw existed initially at that location? For the centerline rib, the predicted economic repair limit is 7300 hours. Thus the percentage of the economic repair limit expended is:

$$\% \text{ Life from 0.01 to 0.03 at Location A} = \frac{\text{Hours of Baseline Usage on Aircraft}}{\text{Economic Repair Limit at Location A}} \times 100 \qquad (10)$$

$$= \frac{3000 \text{ hr.}}{7300 \text{ hr.}} \times 100$$

$$= 41\% \text{ for the Centerline Rib.}$$

If the normalized crack growth curve in Figure 48 for the skin at BL 44 is used to monitor other locations, the predicted crack depth at 41% of the centerline rib economic repair limit would be 0.016 inch. In reality, using the centerline rib curve, the crack depth would be 0.017 inch. Thus, only a small error exists.

Similarly, Figure 49 represents the F-4C/D normalized crack growth for the safety limit at all critical locations. Minimal scatter is evident for the safety limit envelope. The percentage of the safety limit expended is:

$$\% \text{ Life from 0.03 to Failure at Location A} = \frac{\text{Hours of Baseline Usage on Aircraft}}{\text{Safety Limit at Location A}} \qquad (11)$$

The percentage of the crack size expended between 0.03 inch and failure is:

$$\% \text{ Crack Depth} = \frac{a - 0.03}{a_{cr} - 0.03} \times 100 \qquad (12)$$

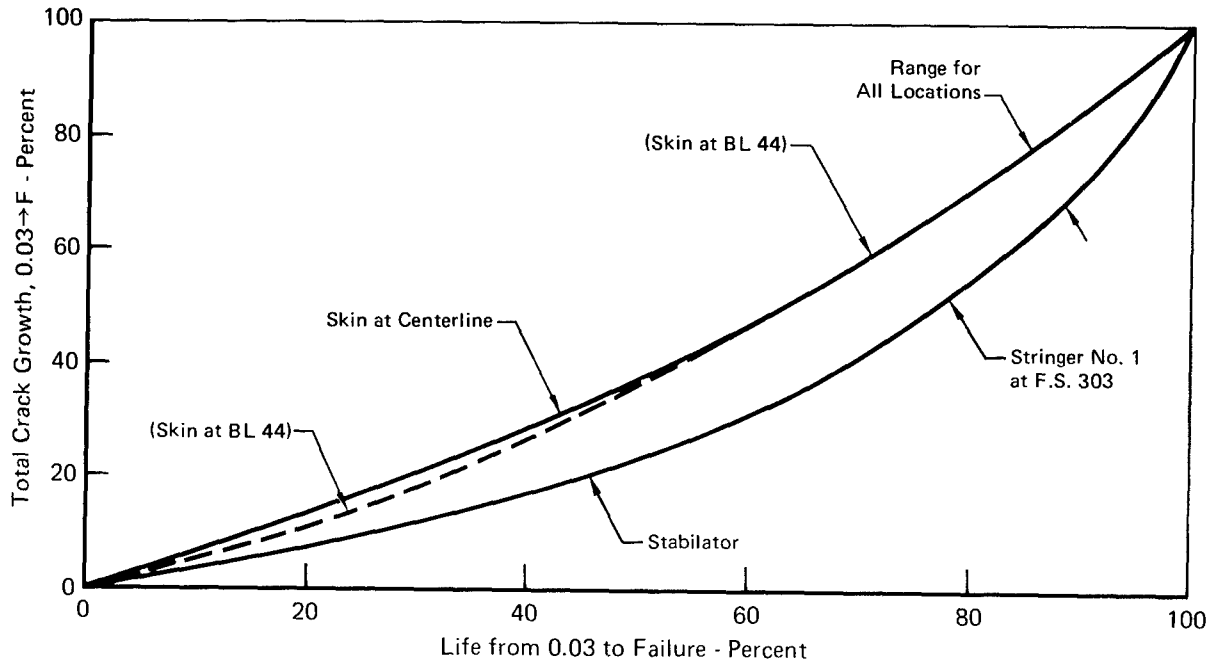

FIGURE 49 COMPARISON OF CRACK GROWTH FROM LOCATION TO LOCATION FOR F-4C/D AIRCRAFT
Safety Limit
ASIP Baseline Spectrum

where "a" is the crack depth at a particular point in time and a_{cr} is the critical crack depth for a particular location on the aircraft. Solving equation (12) for the crack depth, a, gives:

$$a = \left(\frac{\%\ \text{crack depth}}{100}\right)(a_{cr} - 0.03) + 0.03 \qquad (13)$$

As an example, assume that the skin at BL44 is used as the monitoring location, and that a particular airplane in the fleet has flown the equivalent of 10,000 baseline hours. Determine the crack size for stringer #1 at F.S. 303 assuming that an initial flaw 0.03 inch in depth existed at that location. The safety limit for stringer #1 at F.S. 303 is 13,000 hours, and the critical crack depth is 0.15 inch. From equation (11), the percentage of the safety limit expended is:

$$\%\ \text{Life from 0.03 to Failure at Location A} = \frac{10{,}000\ \text{hr.}}{13{,}000\ \text{hr.}} \times 100$$

$$= 77\%$$

Using the curve for the skin at BL44 in Figure 49 the percent crack depth expended between 0.03 inch and failure is 66%. Thus, using equation (13), the predicted crack depth at stringer #1 at F.S. 303 is:

$$a = .66\ (0.15 - 0.03) + 0.03$$

$$= 0.109 \text{ inch}$$

If the stringer #1 curve had been used instead of the curve for the monitored location, the percent crack depth would have been 49%, and the crack depth would have been:

$$a = .49\ (0.15 - 0.03) + 0.03$$

$$= 0.089 \text{ inch}$$

Therefore, by using the curve for the monitored location, skin at BL44, a slightly conservative estimate of the crack depth is obtained.

Normalized crack growth curves can be used to determine the approximate size of crack existing at a particular location for a given number of flight hours. This is an aid in establishing what type of non-destructive inspection technique should be used to detect the crack.

The objective of the economic repair limit is to project the opportune time for economic repair for the average aircraft. The skin at BL 44 represents average growth characteristics (Figure 48). The objective of the safety limit is to protect the flight safety of the aircraft. As it approaches fracture, BL 44 has expended the largest percentage of the critical crack length, therefore, the safety at all locations is protected (Figure 49).

It should be recognized that errors are induced only when a portion of the operational limit has been expended. No theoretical error exists at the operational limit itself (100%). Thus monitoring at one critical location, and scaling by operational limits, will provide an accurate assessment of damage at other locations.

3.1.2 Damage Index Limits - Conversion of the operational limits into damage index limits (D.I. limits) is required in order to account for individual aircraft usage rates. The economic or inspection limit for the baseline spectrum crack growth at the critical location to be monitored is given a damage index limit equal to 1.0.

As an example, the economic limit for the monitored location is "X" hours of baseline spectrum (D.I. limit = 1.0). When a given aircraft is flown to the

baseline spectrum for X hours, the damage index (D.I.) of the airplane is equal to 1.0. A second aircraft that is flown at a usage rate that is more severe than the baseline will attain the same damage in a proportionately lower number of hours. Therefore, its damage index is also equal to 1.0, i.e., it has accrued the equivalent of X baseline hours.

The damage index limits for all other critical locations are equal to their baseline operational limits divided by X hours. Therefore, the assumption is: When the equivalent of X hours has been expended at the monitoring location, the equivalent of these same X hours has been expended at all other critical locations. Since the operational limit at the monitoring location is X, then 100% of the limit has been expended. If the operational limit at another location (Y) is 2X hours, then 50% of the limit has been expended.

The linear relationship between damage at the monitoring location and damage at another location is only valid if the fatigue spectra at the two locations are both based on n_z or on some other flight parameter. If, on the other hand, the loading spectrum at one location is based on n_z and the loading spectrum at another location is based on roll acceleration, then crack growth damage cannot be ratioed from one location to the other. For the F-4, the spectra for the critical locations on the fuselage and wing are all based on n_z. Therefore ratioing the damage from the monitoring location to another location based on the damage index limits of the two locations is valid. The percent of the operational limit expended at a particular location is obtained from the following equation:

$$\%\ \text{Operational Limit Expended at Location A} = \frac{\text{Damage Index of Airplane}}{\text{Damage Index Limit of Location A}} \qquad (14)$$

Note the difference between "damage index" and "damage index limit". The term "damage index" is the measure of the damage expended on a given airplane in the fleet, and is calculated from S-N data as explained in paragraph 3.1.3. The "damage index" increases for a given airplane as flight hours are accumulated. The numerical value of a "damage index limit" is a constant, and is associated with either the economic repair limit, the first inspection interval, or the safety limit for a specific critical location on the aircraft.

The damage index system is not based on the normalized crack growth curves discussed in paragraph 3.1.1. The percentage of crack growth life expended at a critical location is obtained in the damage index system by equation (14). The damage index limit corresponds to the operational limit at 100% of the life from 0.01 to 0.03 inch, or from 0.03 inch to failure (Figures 48 and 49). Thus the

shape of the crack growth curve between 0% and 100% of the life has no effect on the damage index limit. What is important in the damage index system is that the loading spectra at the various critical locations should all be based on the same flight parameters as is used in determining the spectrum at the monitored location.

This method of applying damage index limits to determine the proportion of life expended at other critical locations was developed during the F-4C/D Damage Tolerance Assessment Program. The economic limit for BL 44 was chosen for monitoring purposes (D.I. limit = 1.0) since the wing lower skin at BL 44 (main spar kickpoint) was the most critical area requiring fastener removal and subsequent rework.

The damage index limits presented herein (Figure 50) as an example are for a few of the more well known critical locations on the F-4E(S) retrofit aircraft and are equal to the baseline operational limits divided by 3900 hours (F-4C/D BL 44 economic limit).

3.1.3 S-N Data Development - The use of an S-N curve to convert counting accelerometer data to a damage index for individual aircraft in a fleet has been investigated. S-N curves currently available for most materials are developed for constant amplitude loading conditions and represent total fatigue life. They are presented in the form of stress vs. number of cycles to failure. When this S-N data is used in simple damage computations (i.e., Miner's rule), the resulting fatigue life predictions can be significantly in error. The effect of residual stresses during the "crack initiation" and the effect of

ITEM	ECONOMIC REPAIR ④	FIRST INSPECTION ①	SAFETY
Skin at BL 44	.69	1.15	2.31
Skin at Pylon Hole	2.12	.73	1.46
Skin at 29% Stiffener	N/A	1.68	3.36
Wingfold Rib	③	1.00	2.00
FS 303 Bulkhead	N/A	.55	1.10

① First inspection is 1/2 the safety limit

2 For MCAIR Ser. No. 1-755

③ Replace rib before safety limit

④ From slat kit installation - assumed at 2250 hours

FIGURE 50 DAMAGE INDEX LIMITS BASELINE F-4E(S) AIRCRAFT

retardation during the "crack propagation" phase are not accounted for in the fatigue life calculations. S-N curves have been developed which convert recorded data to a damage index (D.I.) which in turn can be put in terms of accumulated crack growth. The S-N curves account for the effects of retardation due to spectrum loading and were derived through the use of scanning electron microscope (SEM) fractographic traces and through the use of analytical crack growth curves. Each method is discussed in the following paragraphs.

3.1.3.1 Development of S-N Data from Fractographic Traces - For critical areas on the aircraft where crack growth specimens are available from full scale test programs or element test programs, SEM traces are obtained at representative locations on the fracture surface. Individual striations of crack growth are measured for each load level in order to determine the relative percentages of crack growth caused by each load level. The percent of crack growth for each load level in the spectrum is then plotted on a bar graph as shown in Figure 51. A cumulative histogram of percent crack growth vs. test limit load (TLL) is then plotted (Figure 52). Figure 53 shows a curve of cumulative percent crack growth vs. % TLL based on Figure 52.

- From relationship of stress to load factor (Figure 54) read exceedances at 3, 4, 5, 6, 7, and 8G from the load factor exceedance curve (Figure 55).
- Enter BL 44 stress spectrum curve (Figure 56)with above exceedance values and read a stress for each exceedance.
- Calculate f_{max} to be applied to midpoint load level (3.5, 4.5, 5.5G, etc.) by averaging stresses from adjacent levels (Table 9).
- From curve of cumulative percent crack growth vs. % TLL (Figure 53) the % crack growth for each stress level is obtained by reading the curve at adjacent levels (3, 4, 5, 6, 7, and 8G) and applying the delta (Δ) crack growth at the midpoint level (Table 9).

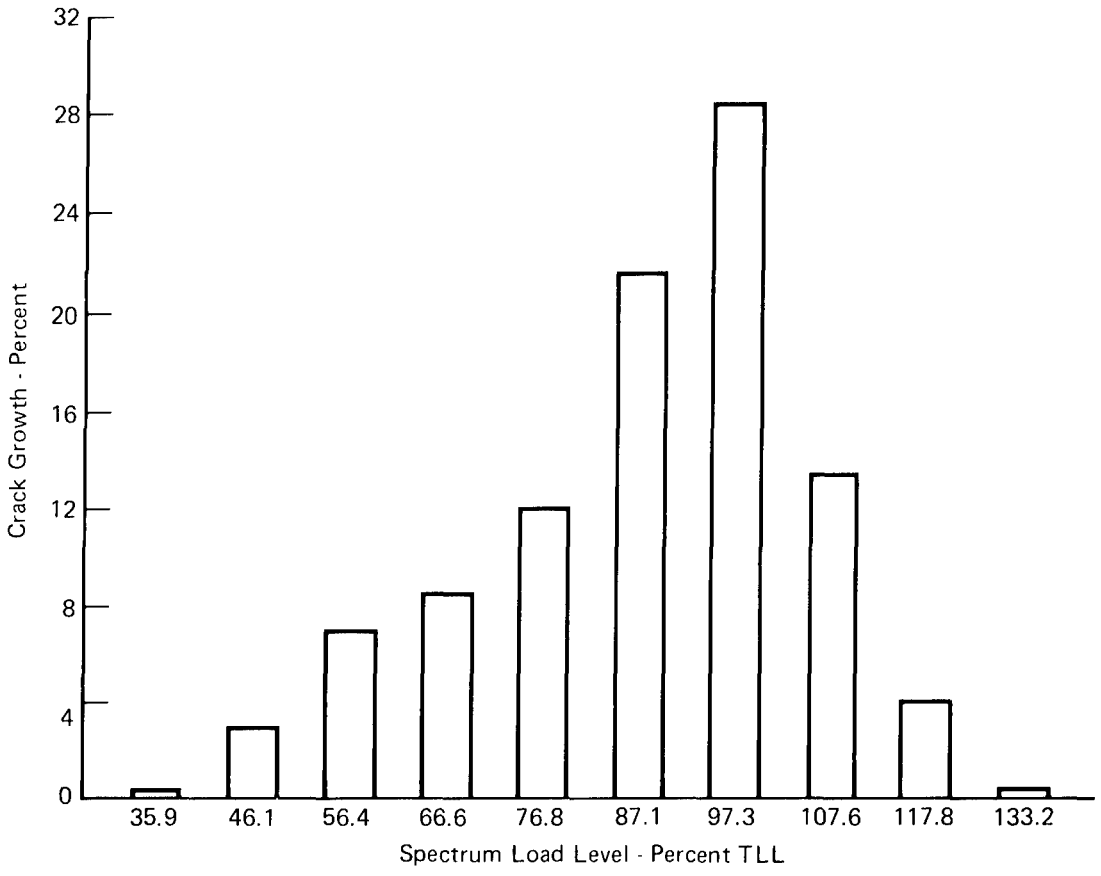

FIGURE 51 PERCENT CRACK GROWTH vs LOAD LEVEL BASELINE SPECTRUM

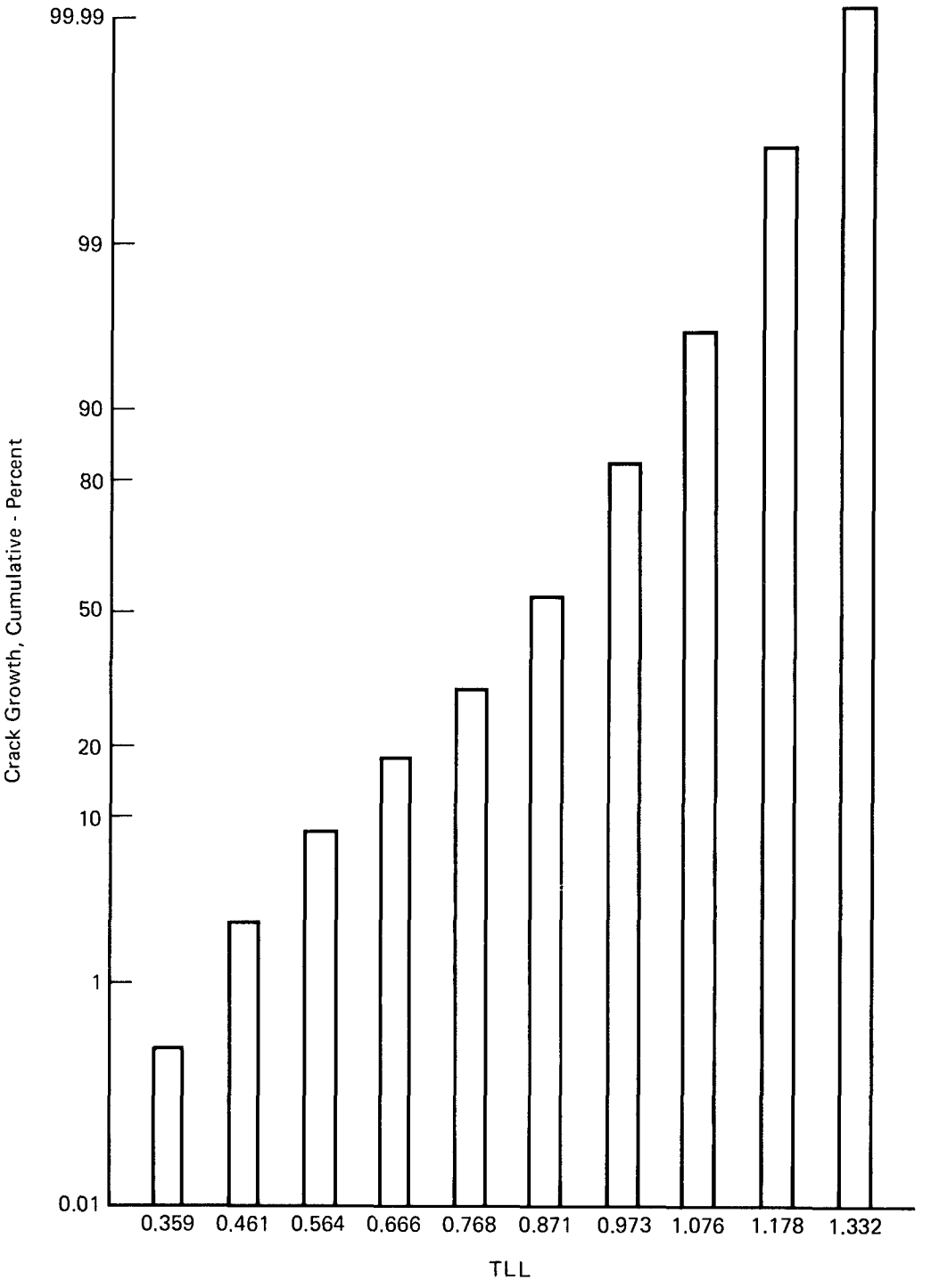

FIGURE 52 CUMULATIVE CRACK GROWTH vs TEST LIMIT LOAD (TLL) BASELINE SPECTRUM

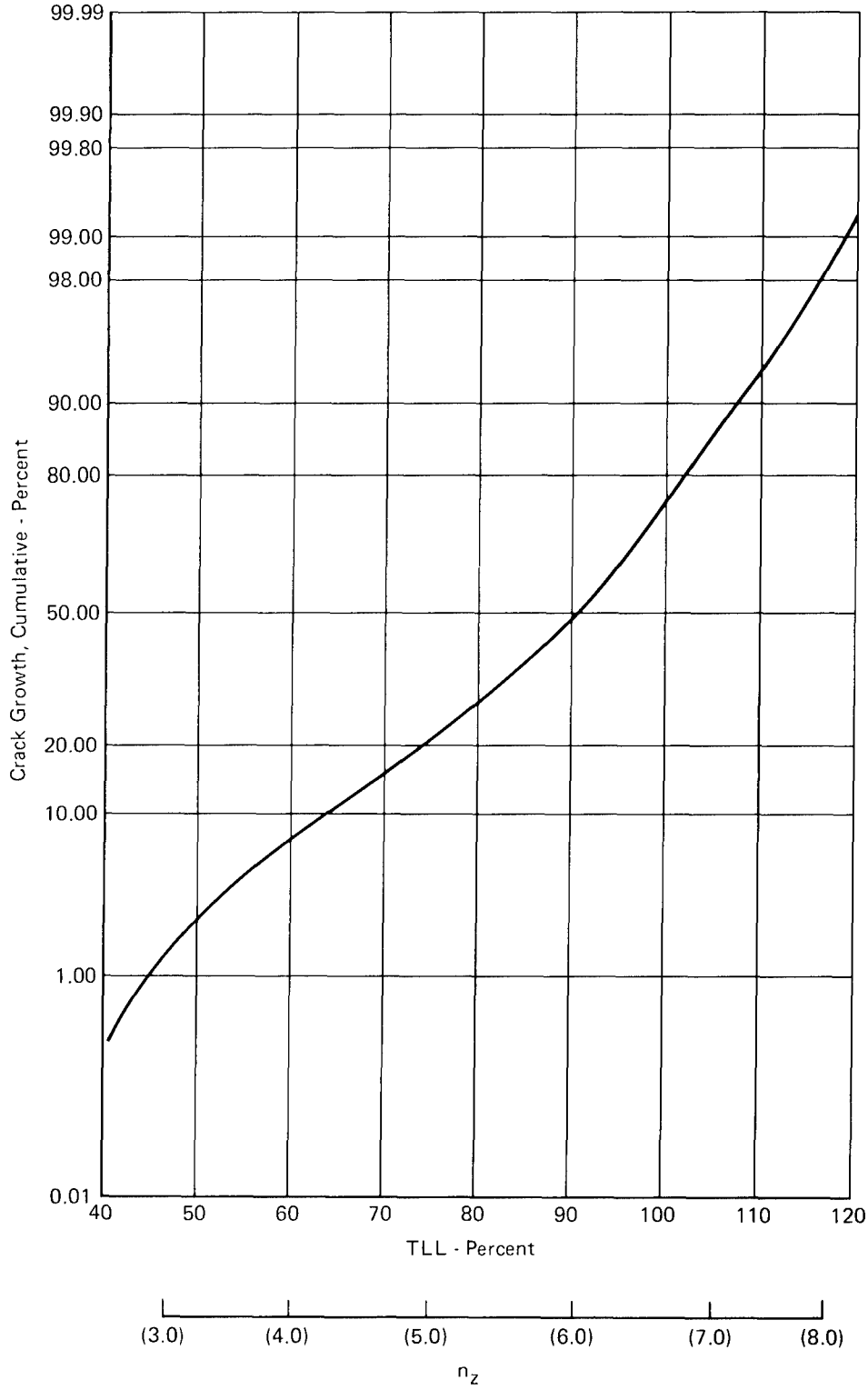

FIGURE 53 CUMULATIVE CRACK GROWTH vs PERCENT TEST LIMIT LOAD (PERCENT TLL) BASELINE SPECTRUM

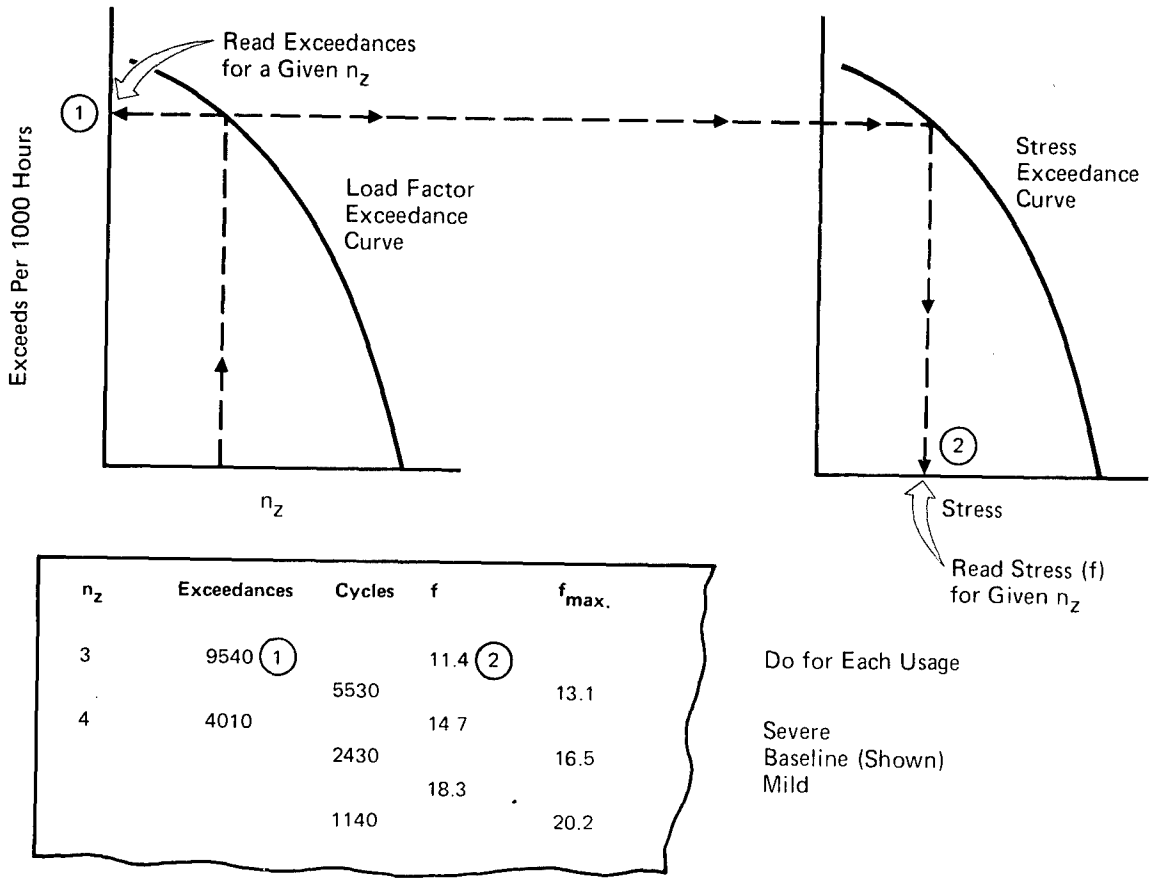

FIGURE 54 RELATIONSHIP OF STRESS AND LOAD FACTOR

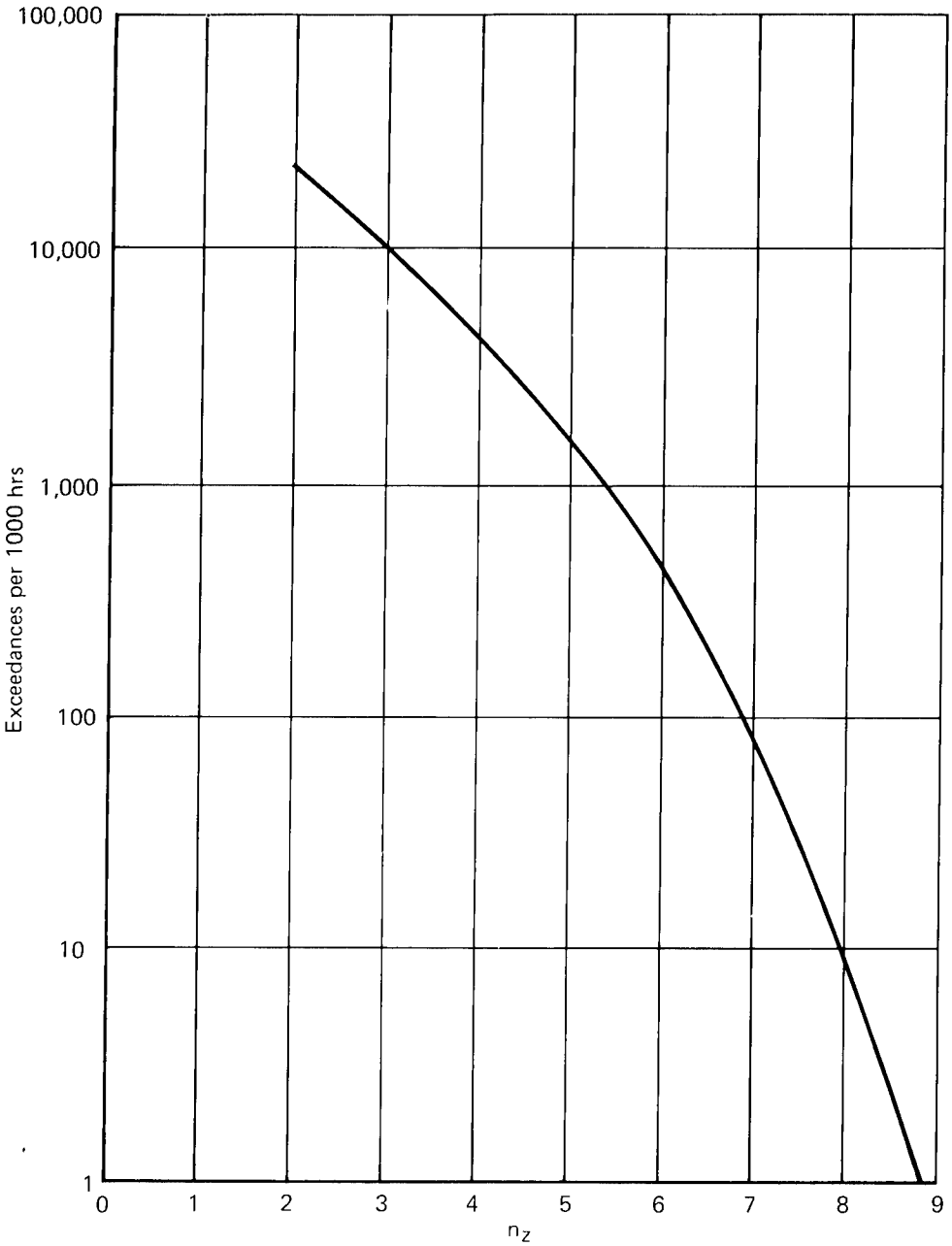

FIGURE 55 BASELINE LOAD FACTOR EXCEEDANCES

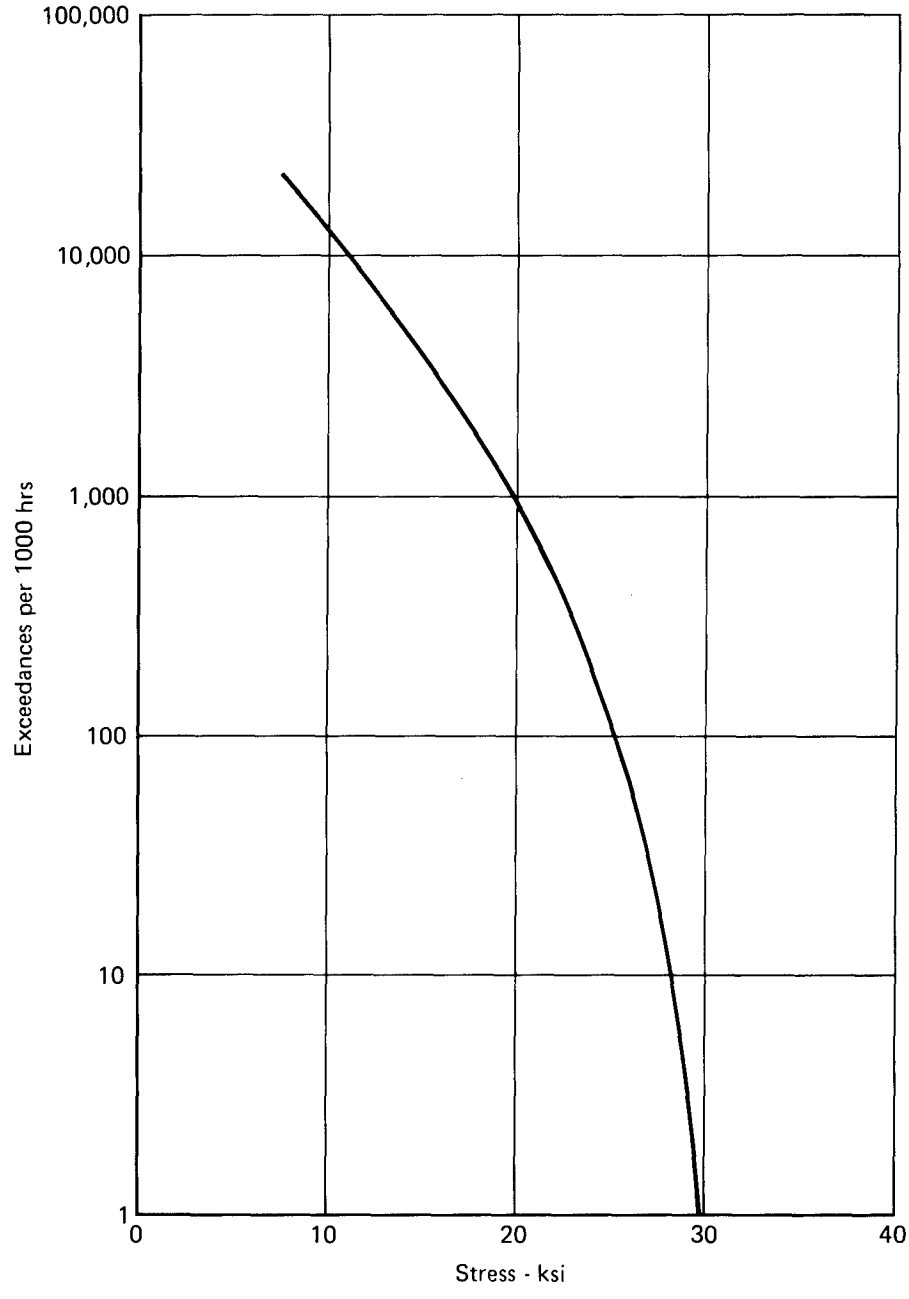

FIGURE 56 BL 44 STRESS SPECTRUM BASELINE

TABLE 9 CALCULATION OF N - BASELINE SPECTRUM

n_z	n_z mid point	f (ksi)	f_{max} (ksi)	Cycles	Crack Growth (1) (%)	ΔD.I. (2)	N (3)
3.0		11.4					
	3.5		13.1	5,530	7.5	0.0192	288,000
4.0		14.7					
	4.5		16.5	2,430	13.5	0.0344	71,000
5.0		18.3					
	5.5		20.2	1,140	28.0	0.0716	16,000
6.0		22.1					
	6.5		23.9	377	37.0	0.0947	3,980
7.0		25.7					
	7.5		27.1	55	12.1	0.0310	1,780
8.0		28.5					
	8.5		29.8	8	1.9	0.0049	1,630
						0.2558	

GP77-0113-25

(1) See figure 53

(2) ΔD.I. Percent crack growth x D.I.

(3) N - Cycles/ΔD.I.

D.I. 1000/3,900 0.256 per 1000 hrs

° Calculate damage index per 1000 hours:

$$\text{D.I. per 1000 hours} = \frac{1000}{\text{Operational Limit}}$$

° Calculate delta D.I. for each load level (Table 9).

Delta D.I. = Percent crack growth x D.I.

° From load factor exceedance curve (Figure 55), calculate cycles for each n_z load level (Table 9)

° N for each load level is

$$N = \frac{\text{Number of cycles at load level}}{\text{Delta D.I.}} \qquad \text{(Table 9)}$$

° Repeat above procedure for each usage: Severe, baseline, and mild. The S-N curves for F-4E(S) usage are shown in Figure 57.

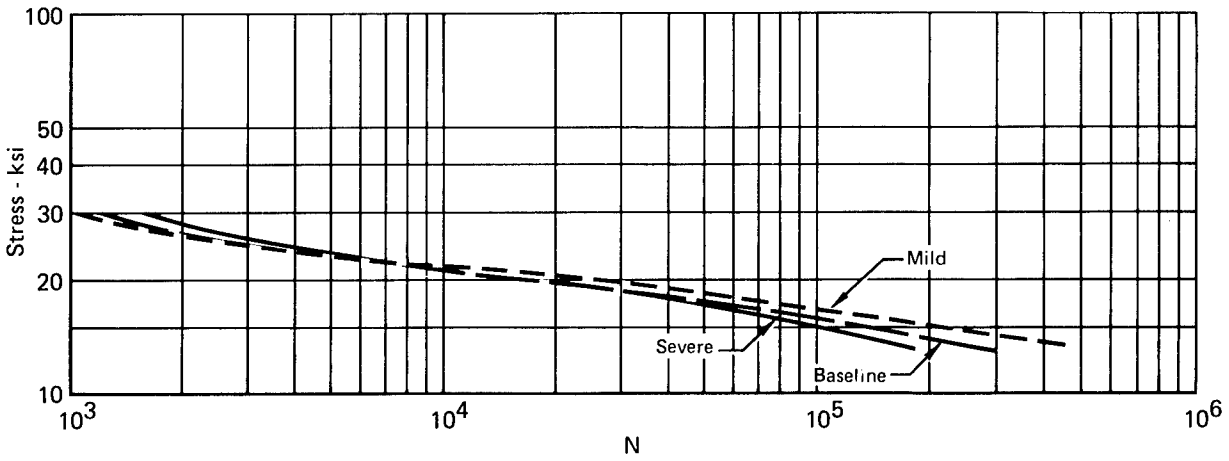

FIGURE 57 S-N CURVES USED IN TRACKING PROGRAM

For fleet tracking purposes, the severe, baseline, or mild S-N data are used to calculate the damage index of an individual aircraft depending upon which usage spectrum best describes the actual usage of the aircraft for the particular time period, usually monthly. Load factor exceedances are read from the counting accelerometer, and the number of occurrences, n, at each n_z mid-point (3.5G, 4.5G, 5.5G, etc.) is determined. Exceedance ranges (bands) were developed at the 5G load factor level to establish the usage category to which a given aircraft would be assigned (for D.I. calculations for that month). The bands at 5G are as follows:

Usage	5G Exceedances per 1000 Hours (Threshold Levels)
Severe	> 2200
Baseline	1100 < Baseline < 2200
Mild	< 1100

The damage index (D.I.) for that aircraft is then simply the sum of n/N.

3.1.3.2 Development of S-N Data from Crack Growth Analysis - For critical areas where crack growth specimens are not available, a crack growth analysis is used instead of fractographic traces. For any 1000 hour segment of the analytical crack growth curve, the percent crack growth for each load level can be tabulated. From this data the percent crack growth vs % load level can be determined. From this point, the same procedure that was used to develop S-N data from fractographic traces can be used to obtain an S-N curve.

3.1.4 Parametric Analysis - F-4E(S) Baseline Aircraft - The data compiled from the variation studies of Section 2.1 form the base for the normalized crack growth study of this section. Normalized crack growth envelopes have been developed for the wing (LRS 70) and for the fuselage (FS 303).

A normalized crack growth study was then made for all mission and design parameter variations for the chosen locations.

3.1.4.1 Crack Growth Trends For Mission and Design Parameters - Crack growth trends for mission parameter variations at the LRS 70 wing location and the FS 303 fuselage location are shown in Figure 58. If one location (LRS 70) is monitored very little error is induced at FS 303. For example, 14% of total .010 inch to failure crack growth at LRS 70 is attained at 30% of the total spectrum hours to failure, while 10% of total .010 inch to failure crack growth at FS 303 is attained at 30% of the total spectrum hours to failure - an incremental error of only 4%.

Crack growth trends for design parameter variations at LRS 70 are shown in Figure 59. For this range of design parameter variations it is apparent that there is not much variance from the baseline. As an example, 16% of total .010 inch to failure crack growth is attained at 30% spectrum hours for the upper bound, and 10% of total .010 inch to failure crack growth is attained at 30% spectrum hours for the lower bound - only $\pm$ 3% variance from baseline. FS 303 crack growth trends are shown in Figure 60.

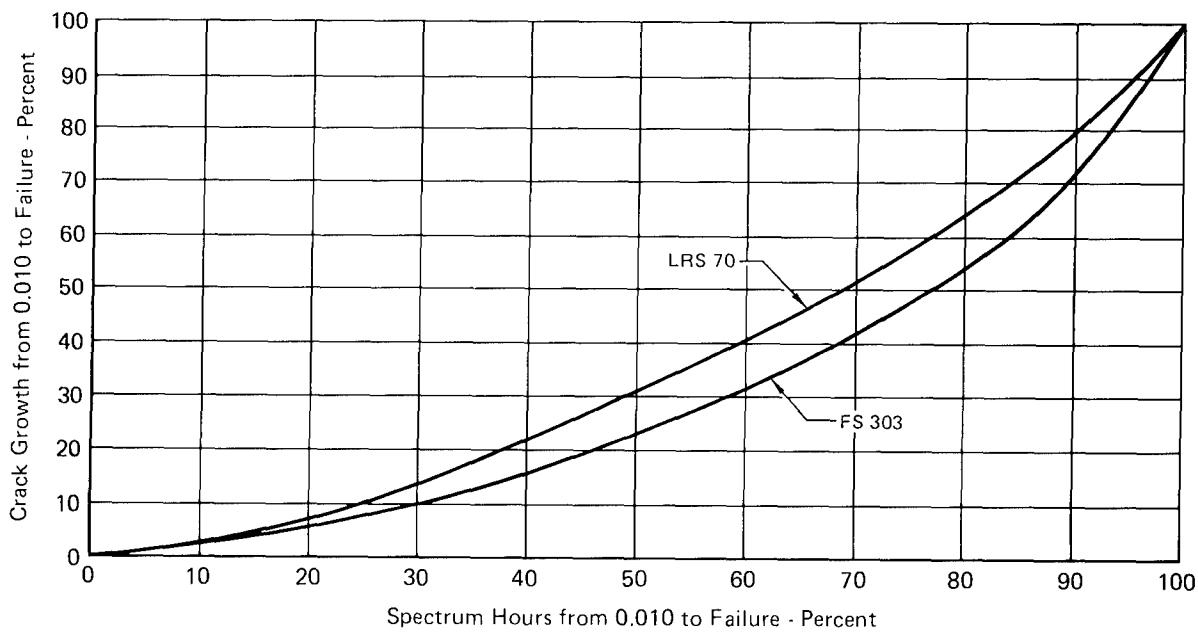

FIGURE 58 F-4E(S) MISSION PARAMETER CRACK GROWTH TRENDS

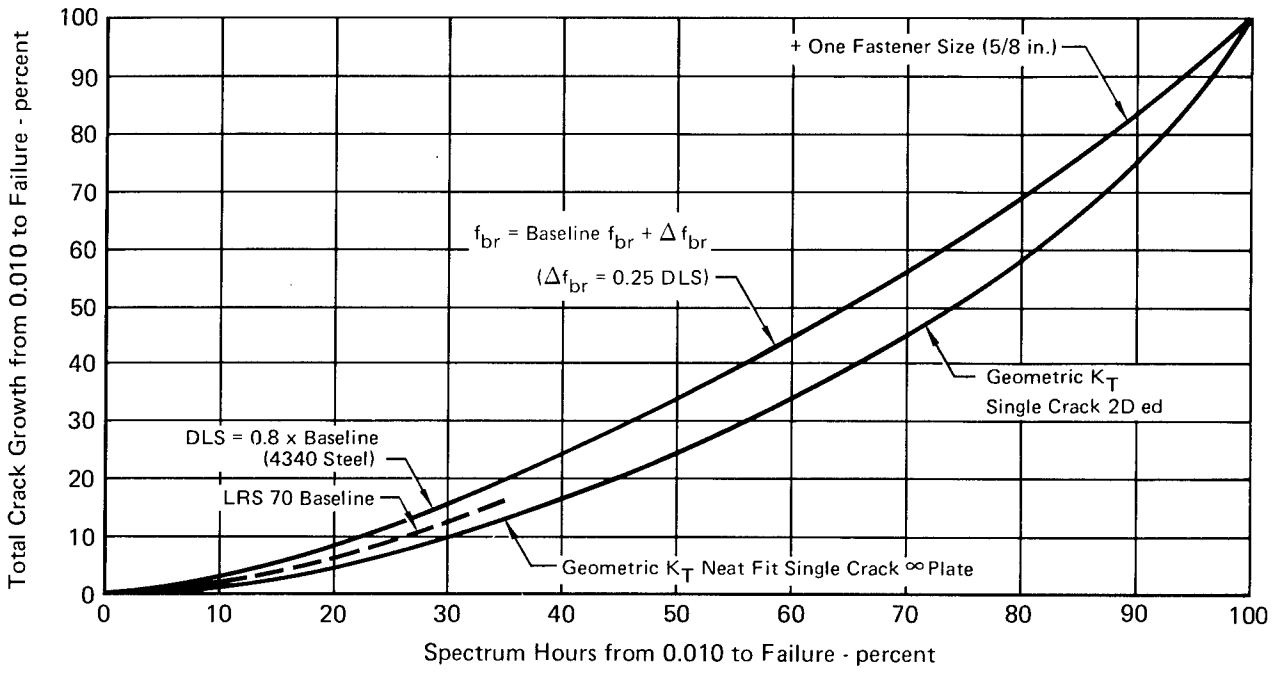

FIGURE 59 F-4E(S) DESIGN PARAMETER CRACK GROWTH TRENDS LRS 70

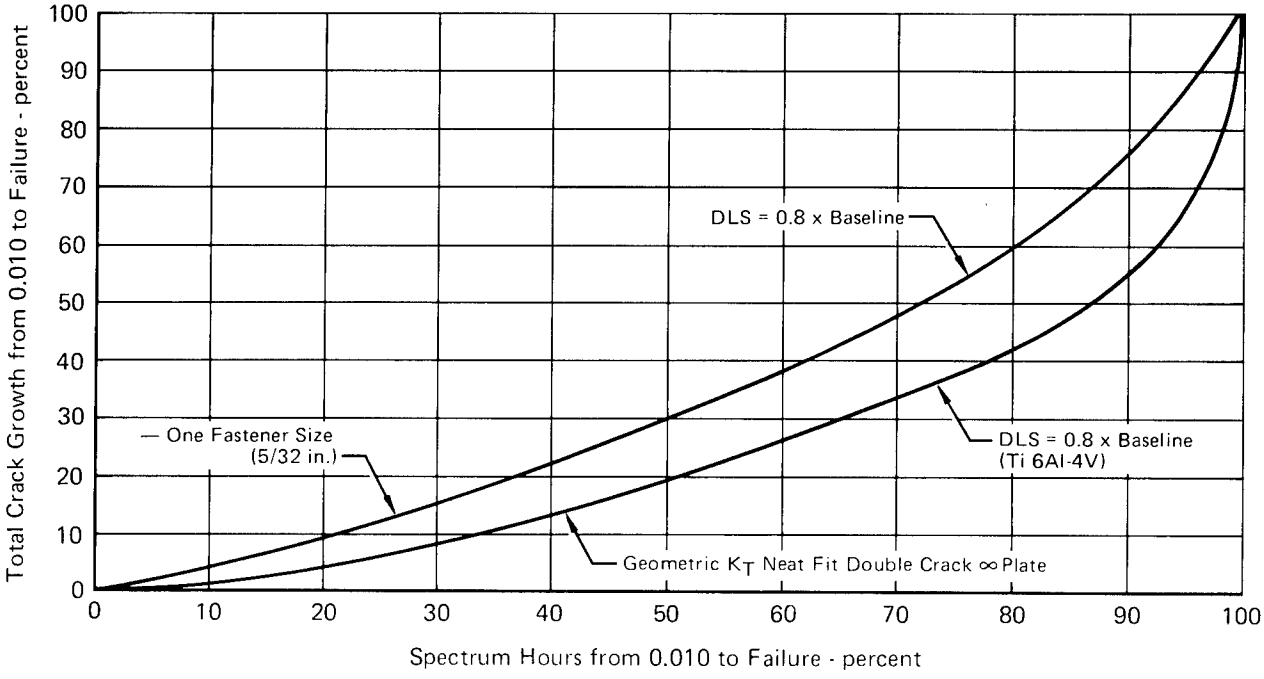

FIGURE 60 F-4E(S) DESIGN PARAMETER CRACK GROWTH TRENDS FS 303

3.1.4.2 Accuracy of Parametric Analysis Methods - The accuracy of using the monitored location(s) to predict the crack depth at other critical locations can be determined from the placement of the normalized crack growth curves for the other locations relative to the normalized crack growth curves for the monitored location(s). Examples were given in paragraphs 3.1.1 and 3.1.4.1.

The accuracy of the S-N data developed from the fractographic trace method and from the crack growth analysis method was evaluated. Starting with the raw data from a counting accelerometer on an individual aircraft (F-4E Slat, Serial No. 711072), the damage index of the monitored location for this aircraft was calculated using the S-N approach. Then, using the same counting accelerometer data, a stress exceedance curve and associated spectrum was developed, and a crack growth curve predicted at the LRS 70 monitored location. The percentage of crack growth life expended is compared to the damage index to determine the accuracy of the S-N approach. The D.I. calculation using S-N data from the F-4E(S) tracking program is shown in Table 10.

TABLE 10 D.I. CALCULATION FOR F-4E(S) SERIAL NO. 711072 USING S-N DATA

n_z	n_z mid point	Total Exceedances	Exceedances per 1000 HR	Occurrences per 1000 HR	N (3)	ΔD.I.
3		6,274	13,500			
	3.5			8,300	290,000	0.0286
4		2,417	5,200			
	4.5			3,300	71,000	0.0465
5		882	1,900 (3)			
	5.5			1,324	16,000	0.0828
6		268	576			
	6.5			461	4,000	0.1153
7		–	115 (2)			
	7.5			103	1,800	0.0572
8		–	11.5 (2)			
	8.5			12	1,200	0.0100
				D.I. Per 1,000 Hr		0.3404

1. Total Flight Hr = 465

(2) Estimated

(3) 5 G Exceedances per 1000 Hr = 1,900 < 2,200, Therefore Use Baseline N Values

Since D.I. is directly proportional to life, the following relationship applies:

$$\frac{\text{Prediction D.I. per 1000 hours}}{\text{Baseline D.I. per 1000 hours}} = \frac{\text{Baseline Life}}{\text{Prediction Life}}$$

The modified Wheeler crack growth prediction for this individual aircraft spectrum is 7700 hours. The corresponding D.I. based on this crack growth prediction is:

$$\frac{\text{LRS 70 Baseline Life}}{\text{LRS 70 Life for Serial No. 711072}} \text{ X Baseline D.I. per 1000 hours}$$

$$\frac{10000}{7700} \text{ X } .256 = .332$$

This is only an error of 2% when compared with .3404 per 1000 hours as derived in Table 10.

In addition tc the damage index versus crack growth comparison performed for F-4E(S) Serial Number 711072, damage indices were calculated for several mission parameter variations in order to compare them with damage indices based on modified Wheeler crack growth predictions. For D.I. based on crack growth predictions:

- Baseline D.I. = .256 per 1000 hours (Ref 2 and Table 9)
- From the evaluation of crack growth for mission parameter variations in this study,
- The ratio of variation/baseline =

  $$\frac{\text{Predicted Life for .010 to Failure for Variation}}{\text{Predicted Life for .010 to Failure for Baseline}}$$

- Variation D.I. per 1000 hours = $\frac{\text{Baseline Life}}{\text{Variation Life}}$ x .256 per 1000 hours

For D.I. calculated using S-N data:

- Develop n_z exceedance curve for load factor variations
- Use baseline n_z exceedance curve for all other mission parameter variations
- Develop composite stress spectrum
- Number of cycles from n_z exceedance curve
- Stress spectrum for stress at various n_z levels
- Use appropriate S-N (severe, baseline, or mild) for calculating D.I.

The following is an example calculation for the D.I. of a mission parameter variation using S-N data:

- o 3000 pound lighter air-to-air gross weight
- o Ratio air-to-air stress spectrum by gross weight
- o Plot composite stress spectrum
- o Use baseline n_z exceedance
- o Baseline S-N (Ref 2 and Figure 57)
- o LRS 70 wing lower skin and stringer No. 1 at FS 303

The D.I. comparison at LRS 70 for the above mission parameter variation is shown in Table 11. For another location on the airplane such as FS 303:

- o Ratio LRS 70 D.I. by fracture life to get D.I. at the other location
- o .010 to failure fracture life

  LRS 70: 10,000 hours

  FS 303: 3,700 hours

- o Baseline D.I. FS 303 = $\frac{10000}{3700}$ X BASELINE D.I. @ LRS 70

  = $\frac{10000}{3700}$ X .256 = .692 PER 1000 HOURS

TABLE 11 D.I. AT LRS 70 FOR 3,000 LB LIGHTER GROSS WEIGHT - AIR-TO-AIR

n_z	Exceeds per 1000 HR		Cycles	f (KSI)	f_{max}	N	D.I.
3	9540			11.2			
		3.5	5530		12.8	3.5×10^5	0.01580
4	4010			14.4			
		4.5	2430		16.2	8.4×10^4	0.02892
5	1580			17.9			
		5.5	1140		19.8	2.0×10^4	0.05700
6	440			21.6			
		6.5	377		23.3	5.2×10^3	0.07250
7	63			24.9			
		7.5	55		26.1	2.4×10^3	0.02291
8	8			27.2			
		8.5	8		28.1	1.6×10^3	0.00500
				29.0			
					Σ Per 1000 Hr		0.20213

Modified wheeler crack growth prediction for this variation is a fracture life = 1.32 x baseline

D.I. per 1000 hours = $\frac{0.256}{1.32}$ = 0.194 (4% less than 0.2021 above)

The D.I. comparison at FS 303 for the above mission parameter variation is shown in Table 12. A summary of comparisons for 11 mission parameter variations is shown in Table 13.

TABLE 12 D.I. AT FS 303 FOR 3,000 LB LIGHTER GROSS WEIGHT - AIR-TO-AIR

- Since D.I. is Directly Proportional to Life,

$$\frac{\text{D.I. at FS 303}}{\text{D.I. at LRS 70}} = \frac{\text{LRS 70 LIFE}}{\text{FS 303 LIFE}}$$

- D.I. per 1000 hours at FS 303 = $\frac{10{,}000}{3{,}700} \times 0.2021 = 0.5470$ (S-N)
- Modified Wheeler Crack Growth Prediction for this Variation is a Fracture Life = 1.38 x Baseline
- D.I. per 1000 hours = $\frac{0.692}{1.38} = 0.5010$ (from Crack Growth Prediction)
- S-N D.I. is 9% Greater than Crack Growth D.I.

TABLE 13 D.I. COMPARISON FOR SEVERAL MISSION PARAMETER VARIATIONS

Location	Variation	Variation/ Baseline (1)	Crack Growth D.I. (2)	S-N D.I. (2)	Percent Difference
LRS 70	75% Air-Ground, 25% N-T	1.18	0.2170	0.2166	~0
↓	Severe Air-Ground	0.74	0.3460	0.3493	+1
FS 303	3000 lb Lighter Air-Ground	1.27	0.5450	0.5380	–1.2
LRS 70	15% Slower Air-Ground	1.42	0.1802	0.1760	–2.5
FS 303	15% Slower Air-Air	1.43	0.4840	0.4960	+2.5
LRS 70	35% Air-Air, 65% Air-Ground	0.77	0.3320	0.3217	–3
↓	Severe Air-Air	0.86	0.2970	0.2884	–3
	15% Slower Air-Air	1.35	0.1896	0.1835	–3
	3000 lb Lighter Air-Air	1.32	0.1940	0.2021	+4
FS 303	3000 lb Lighter Air-Air	1.38	0.5010	0.5470	+9
LRS 70	3000 lb Lighter Air-Ground	1.46	0.1753	0.1992	+12

(1) Variation Life ÷ Baseline Life (2) D.I. per 1000 hours

3.1.4.3 Conclusions

- o Due to the small difference between crack growth D.I. and S-N D.I. for FS 303, it is concluded that for a conventional fighter such as the F-4E(S) an adequate job can be done by monitoring one location and scaling by operational limits to obtain the damage at other locations.
- o It is also concluded from the normalized crack growth curves of page 79 that there is no appreciable difference from baseline for the reasonably conservative F-4E(S) design parameter variations chosen for this study.

3.2 Recorded Data Requirements

In order to establish the effects of change in aircraft usage parameters on the crack growth rate, the usage must be defined in terms of the flight loads data available from existing data acquisition systems. The type of usage data available depends on the type(s) of data acquisition systems on the aircraft in question. Several systems have been evaluated.

Figure 61 addresses a system which uses counting accelerometers as the prime data source. For this system, data from other sources are integrated with the counter data in the service monitoring program to develop stress spectra for fleet application, from which crack growth predictions on each fleet aircraft are made. This is the type of system used on the F-4. Figure 62 outlines the tracking procedures to be used for a data acquisition system which uses strain exceedance counters as the main source of data. A variant of this system is shown in Figure 63, the main data source in this case being sequential strain history instead of strain exceedances. The following paragraphs describe the systems considered in the evaluation.

3.2.1 Operational Data - Pilot logs, pilot interviews, field service reports, and user usage forecasts are examples of sources of operational data. In addition, operational data can be defined through the use of the flight loads recorders as outlined in the following sections. The data gathered is valuable in establishing trends, interpreting questionable recorded data, defining special usages, and forecasting. For instance, when pilot logs are available, the recorded flight loads data can be better defined with respect to various usage parameters.

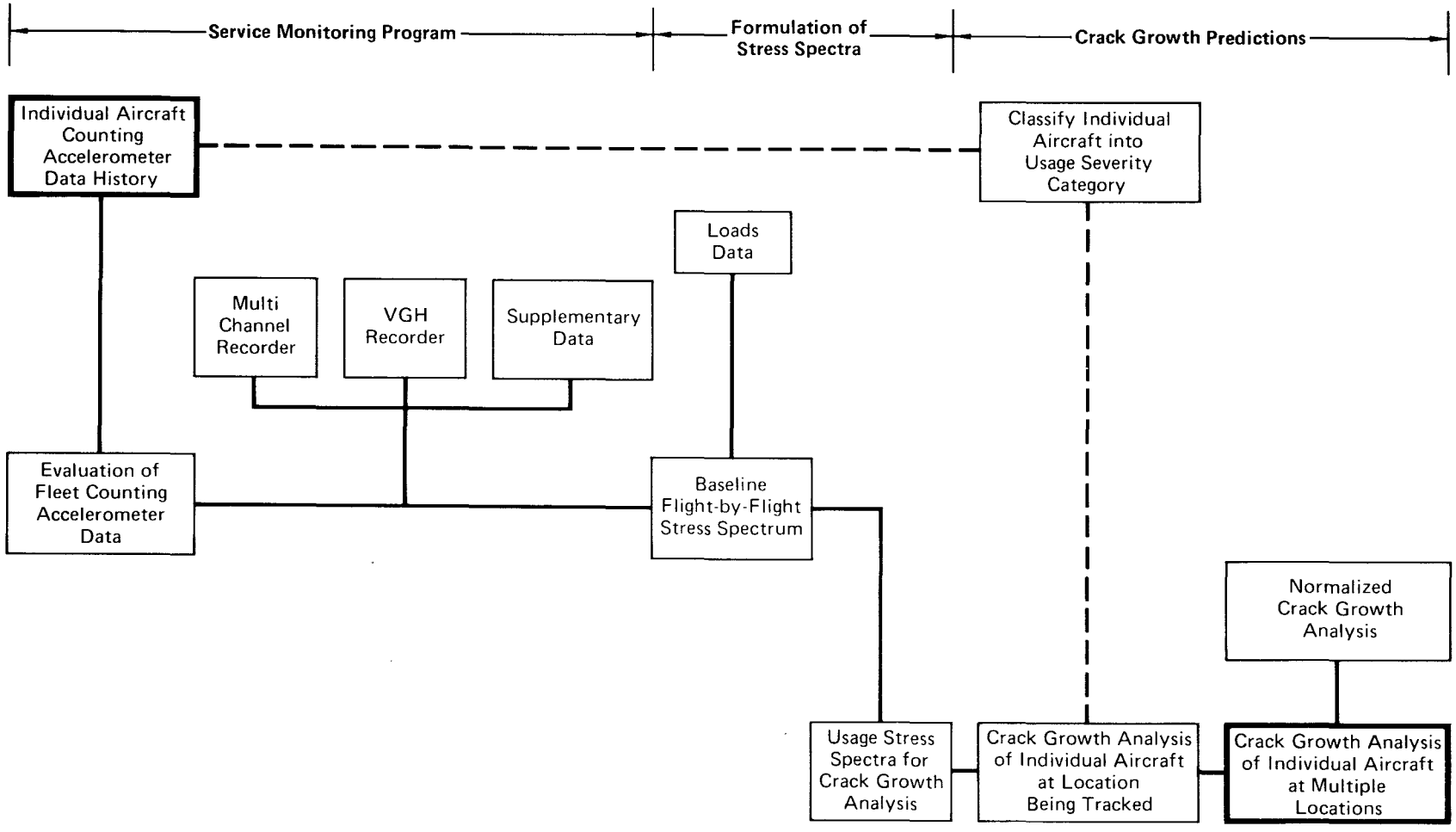

FIGURE 51 TRACKING CRACK GROWTH IN INDIVIDUAL FLEET AIRCRAFT
Using Counting Accelerometer Data

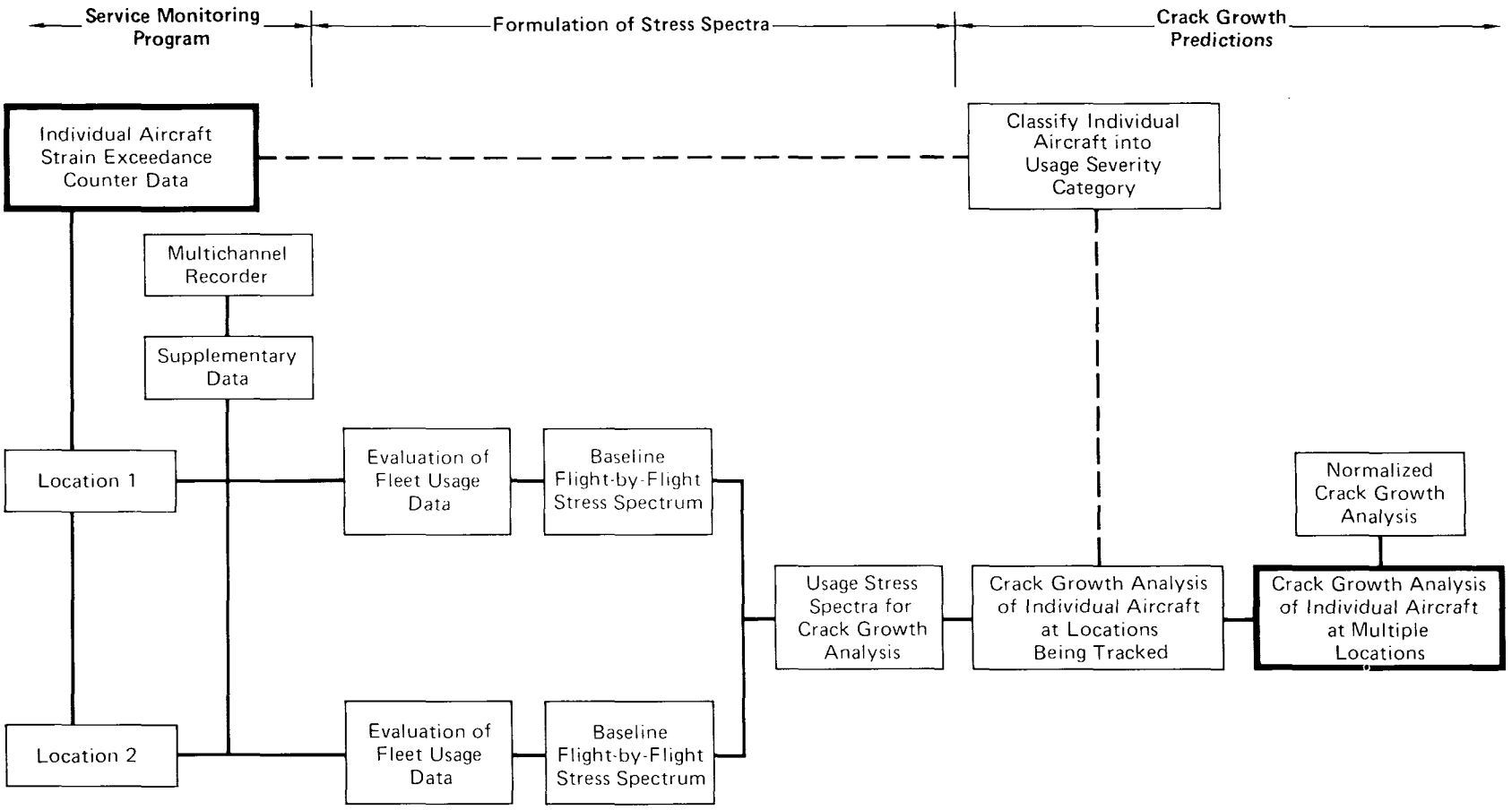

FIGURE 62 TRACKING CRACK GROWTH IN INDIVIDUAL FLEET AIRCRAFT
Using Electrical Equipment
That Records Strain Exceedances

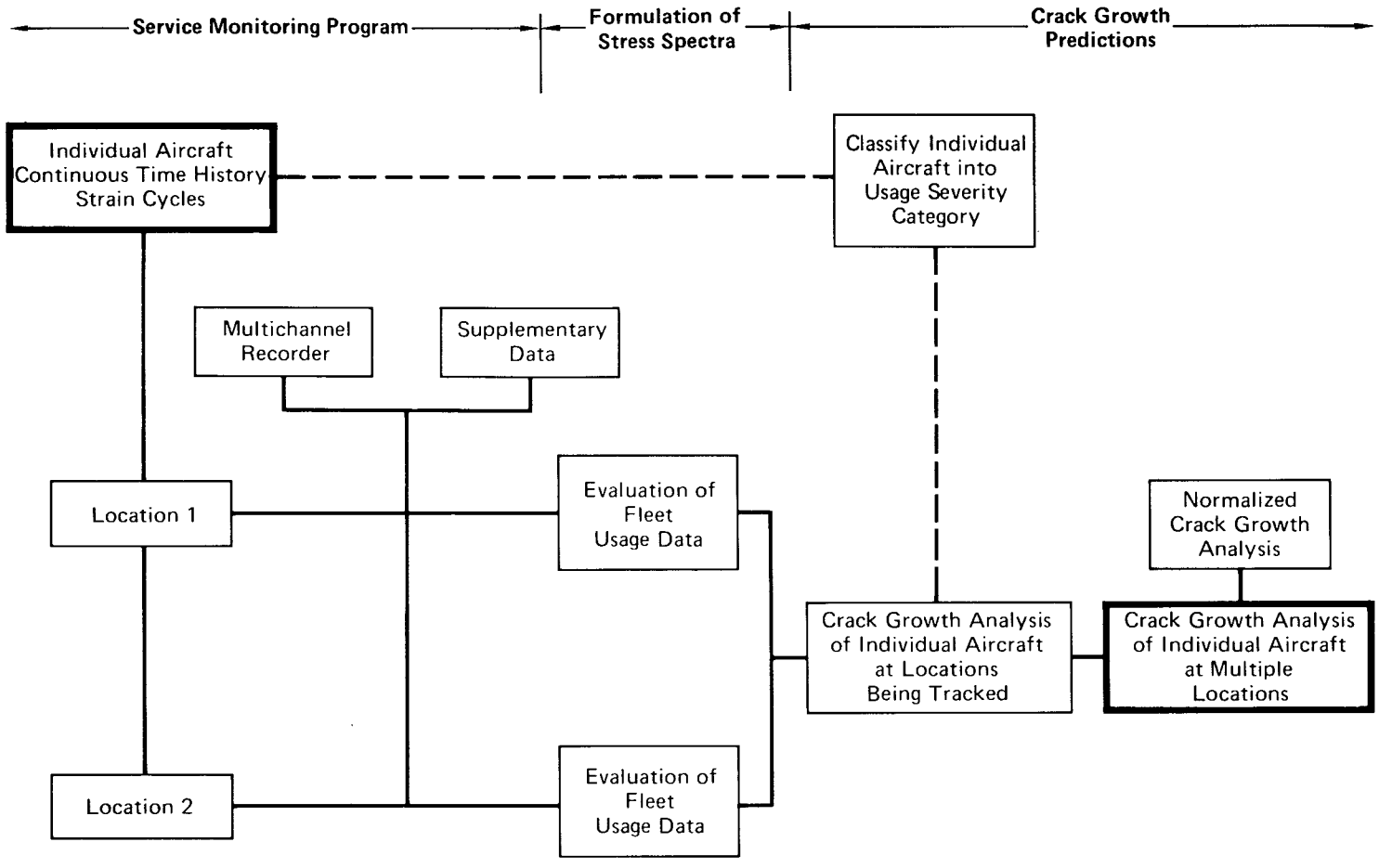

FIGURE 63 TRACKING CRACK GROWTH IN INDIVIDUAL FLEET AIRCRAFT
Using Mechanical/Electrical Equipment
That Records Continuous Strain

3.2.2 Counting Accelerometers - The counting accelerometer is a compact, simple, inexpensive device which measures and records normal load factors (n_z) experienced by an aircraft. The data obtained may be used as a basis for (a) calculating the life expended on an individual aircraft, (b) estimating life remaining on an individual aircraft, and (c) monitoring overall fleet load factor usage. The counting accelerometer consists of (1) a counting indicator with the capability of recording pre-set load factor levels, and (2) a load sensitive transducer. The transducer senses normal load factors (n_z) that the aircraft experiences and transmits electrical signals to the counting indicator which records load factor exceedances. Successive peaks are counted only if separated by a specified minimum level of load factor. Extraneous accelerations, such as might be introduced by shock or vibrations, are excluded from sensing. Only maneuver accelerations of the aircraft are recorded on the F-4.

The advantages of using counting accelerometers are: (1) their low cost makes it feasible to install them on all aircraft in the fleet, (2) it is easy to detect changes in service usage, and (3) aircraft accumulating unusually severe usage can be isolated for special monitoring.

There are several disadvantages to the counting accelerometer. The counter does not supply data which indicates the airspeed, altitude, gross weight, mission mix, or unsymmetrical maneuvering. The transducer that records n_z is located near the aircraft C.G., therefore, transfer functions to other locations on the aircraft are required after a flying regime has been assumed or established from operational data. The human error involved in reading the counter, transferring the exceedances to paper, and reporting induces some minor errors which complicate the data reduction process.

One counting accelerometer per aircraft is required, however there have been applications in which two or more counting devices are packaged in a common container and designed so that one counter is operative for one range of wing sweep positions while another counter is operative for a different range of sweep positions.

The counting accelerometer was designed to measure only vertical accelerations. The load levels to be recorded can be selected so as to be applicable to the range in which the aircraft is expected to be responsive, without regard to other airplane characteristics.

3.2.3 VGH Recorders - A typical VGH recorder system includes a computer-recorder, a hermetically sealed tape magazine, and a servo-accelerometer which is mounted near the aircraft C.G. Two pressure transducers within the computer-recorder sense static and differential pressure from the aircraft pitot-static system. The computer converts the differential and static pressure to the corresponding pre-set intervals of indicated airspeed and pressure altitude before recording them.

The computer-recorder continuously monitors the vertical acceleration and detects and tallies acceleration peaks in counters with pre-set acceleration levels.

Elapsed time (from a ten-minute digital clock) and the current indicated airspeed and pressure altitude codes are also stored by the computer-recorder. The contents of all acceleration counters, the elapsed time, and the airspeed and altitude interval codes are transferred to the tape whenever any one of the following four events occurs: (1) the airspeed interval changes, (2) the altitude interval changes, (3) an acceleration counter reaches capacity, or (4) the ten-minute clock completes its cycle. After each data transfer, the acceleration counters are reset to zero and any new airspeed and altitude interval codes are stored. The clock counter is reset only after it completes the ten-minute cycle.

The VGH recording system has the capability of recording load factor counts at prescribed airspeed and altitude ranges. This allows calculations of stress levels at different locations on the aircraft, providing that adequate equations for internal loads are available in terms of VGH data and gross weight. The potential for human error that is present in the collection of counting accelerometer data is absent in the VGH system due to the use of the magnetic recording tapes.

The disadvantages to the VGH system are, (1) a transfer function to calculate stresses at different locations on the aircraft is required, (2) there is no distinction made between symmetrical and unsymmetrical maneuvers, (3) it does not account for six dimensional accelerations, (4) control surface position is not recorded, and (5) gross weight is known only by using take-off and landing gross weights (from pilot's data sheets) along with fuel burn rates.

Since VGH recorders are normally used as supplementary data sources, one recorder is required on every 5 to 10 aircraft so as to insure a continuous sampling of data at each base.

The recording of airspeed and altitude is the primary application of the VGH recorder. The recording of load factor occurrences near the aircraft C.G. can serve as a check of the accuracy of counting accelerometer data.

3.2.4 Multi-Channel Recorders - The multi-channel recorder registers various mission parameters associated with maneuvers being performed. The system is generally digital and records flight parameters at sampling rates ranging from 1 to 30 times per second.

The multi-channel recorder that was installed in a limited number of F-4 aircraft records 8 different parameters. Complete time histories of 3 axis linear accelerations, 3 axis angular rates, speed, and altitude are provided. Each of these parameters is recorded 30 times per second.

The F-15 signal data recorder (SDR) records 22 flight parameters on a cassette tape from 1 to 30 times per second as indicated in Figure 64. One out of 5 fleet aircraft contains a SDR installed as shown in Figure 65. The cassette, which records 25 hours of data, is input into the computerized data reduction program.

The multi-channel recording system has substantially greater capability than the VGH system. The additional capability allows for better definition of the mission parameters in terms of airspeed, altitude, 6 dimensional accelerations, angle of attack, flight control system, and control positions. Another important capability of the multi-channel recorder is the ability to record the loading on the aircraft in a sequence. It also affords the possibility of recording strains directly at a selected location or locations.

The disadvantages of the system are (1) a transfer function is necessary in order to calculate stress levels for the critical locations on the aircraft, (2) the expense of the system makes it unfeasible to equip all aircraft with multi-channel recorders, which therefore calls for judgements based on counter data for the aircraft that do not have recorders.

The design of the multi-channel system accounts for basic flight parameters, therefore, only one recorder is required on a given aircraft.

3.2.5 Strain Exceedance Recorders - There are two basic system types which can provide strain exceedance data. The electrical type makes use of a bonded electrical strain gage as a transducer coupled to a signal conditioner which delineates strain levels and amplitudes into peaks. The electro-mechanical type has a transducer which converts a mechanical displacement (over gage length) into an electrical signal that is similarly conditioned for peak counting. In both of these systems a counter similar to that used in the counting accelerometer system is used, which provides window readouts of exceedances at the desired strain levels.

Signal Source	Aircraft Parameter	Units of Measure	Sampling per Second
Central Computer	Date	–	–
	Mission Number	–	–
	Aircraft Serial Number	–	–
	Squadron	–	–
	Weapon Identification	–	–
	Altitude	Feet	1
	Velocity	Knots	1
	Angle of Attack	Degrees	10
	Weapon Count	Item/Station	1
	Vertical Velocity	Feet/Second	5
	Gunfire	Rounds	1
Counting Accelerometer	Vertical Acceleration	g	30
Automatic Flight Control System	Stabilator Deflection - Right	Degree	10
	Stabilator Deflection - Left	Degree	10
	Control Augmentation System (3 Axis)	On-Off	1
Fuel Gaging System	Fuel Quantity	Percent Total Fuel Remaining	1
Aircraft Sensors	Aileron Deflection - Right*	Degree	30
	Aileron Deflection - Left	Degree	30
	Rudder Deflection*	Degree	10
	Speed Brake	In-Out	1
	Wheels	Up-Down	1
Signal Data Recorder	Roll Rate	Hertz	30
	Pitch Rate	Hertz	15
	Yaw Rate	Hertz	10
	Roll Acceleration	Rad/Second^2	30
	Lateral Acceleration	g	5
	Longitudinal Acceleration	g	5
	Time	Seconds	1
		Total	239

*Transducers recording these parameters were added to the aircraft specifically for the SDR.

FIGURE 64 FLIGHT PARAMETERS CONTINUOUSLY RECORDED ON SIGNAL DATA RECORDER CASSETTES

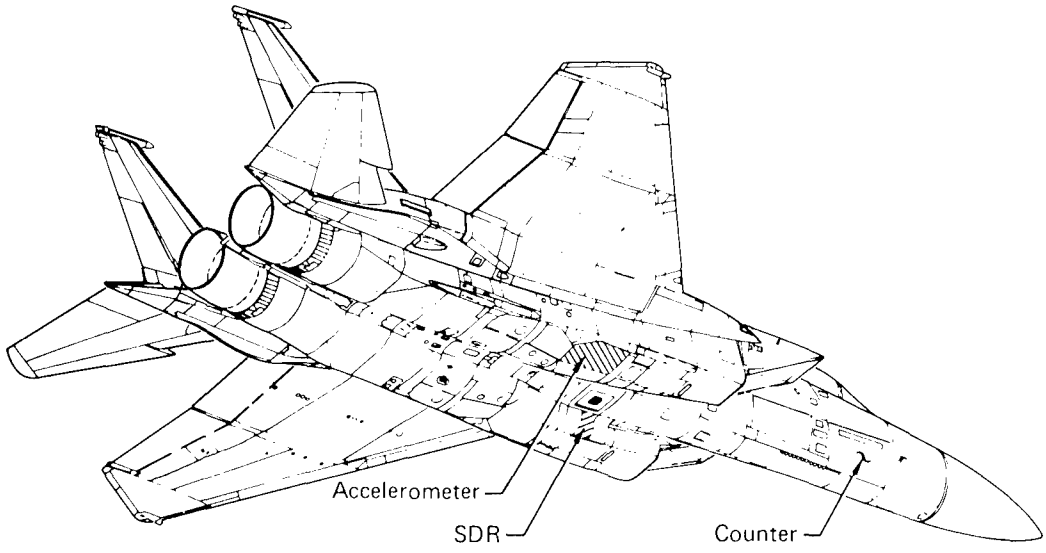

FIGURE 65 LOCATIONS OF COUNTING ACCELEROMETER AND SIGNAL DATA RECORDER ON F-15

The strain exceedance recorder has all the advantages of the counting accelerometer, i.e., low cost, efficient fleet monitoring, and ready monitoring of individual aircraft. An added advantage is that a knowledge of flight parameters (airspeed, altitude, gross, and load factor) is not required, since strain and thereby stress exceedances are known directly for the locations monitored. The applicability of this system is insensitive to variations in aircraft classes.

Only one location on an aircraft can be monitored with one of these systems, making it necessary to provide additional units to monitor other critical locations on the airplane, or develop accurate transfer functions, or both.

A minor disadvantage shared with the counting accelerometer is the error introduced by the human element in the reading of the counter. In addition, this system does not provide information that would be suitable for up-dating structural design criteria (such as load factor exceedance data), however, this could be remedied by using a relatively small number of VGH recorders or multichannel recorders.

Since this type of system is applicable directly to only one location on the aircraft, it may be necessary to utilize more than one system per airplane. A spin-off of multiple locations might be a better accounting for unsymmetrical maneuvers.

This system, with one or more units per aircraft, is suitable for any type of airplane; however, limiting installations to one or two per airplane could hamper effective monitoring of control devices such as canards, variable geometry wings, critical tail surfaces, etc.

3.2.6 Strain Cycle Sequential Recorder - There are three basic types of systems that can provide strain cycle sequential data. The electrical type makes use of a bonded electrical strain gage as a transducer, while the electro-mechanical type has a transducer that converts a mechanical displacement over a gage length to an electrical signal. These transducers could be identical to those used in the strain exceedance recorder system. For each system the signal is recorded and stored on board. The data is then read periodically by ground equipment. The mechanical type (scratch gage) records displacement over the gage length as an inscription on a metallic record, either disc or tape. The record is removed from the airplane periodically and read visually with special equipment to consign the data to a computer record.

This system enjoys all the advantages of the strain exceedance recorder system. The added advantage is that the effect of load sequence on life can be evaluated. Further, this data can be developed into strain exceedance data. The low cost of these instruments make it feasible to monitor several locations at once, thereby enhancing the suitability of this system for monitoring several critical locations.

As in the case of the strain exceedance recorder, load factor exceedance data for future design cannot be developed using strain sequential recorders.

The number of recorders required per airplane is largely determined by the number of critical locations on the airplane. This could be modified by using other data systems to establish transfer functions.

The applicability of this system is similar to that of the strain exceedance recorder system with respect to airplane characteristics.

4. IMPLEMENTATION OF TRACKING PROGRAM

Since the existence of an individual aircraft tracking program is essential to a well managed fleet in the interest of economy and flight safety, it follows that it must be fully implemented and maintained.

4.1 Logistics

For each new aircraft program, well defined plans must be made for procurement of necessary recording/counting equipment. This must also include plans for procurement and installation of any required interface equipment at appropriate bases. Recording/counting equipment must be properly maintained. Report forms that must be manually completed are frequently a source of substantial difficulty. Illegible forms contribute to data reduction errors and added costs.

4.2 Potential Technical Difficulties

Each combination of recording/counting equipment to be considered for use in a viable tail tracking program has unique difficulties consistent with the degree of complexity of the system in question. An attempt was made here to rate the possible systems relative to the approach used on the F-4 individual aircraft tracking program. The systems are listed in Table 14 in the approximate order of increasing complexity/cost.

4.3 Considerations in Defining a Tracking System

As can be seen in Table 14 there is a large difference in relative complexity/cost between the simplest systems and the most sophisticated systems. Table 14 was based on the following assumptions:

- 1000 aircraft fleet
- 300 flight hours per year per aircraft (25 flight hours/ month/aircraft)
- 15 years of tracking
- $3000 per year automation costs for counting accelerometer tracking program
- 2800 man hours per year engineering support for counting accelerometer program
- .25 man hours per aircraft per month to read counting accelerometer

  Cost of reading counting accelerometer =

  Man hours per A/C per flight hour x hourly rate x fleet flight hours per year x no. of years of tracking =

  .01 x hourly rate x 1000 x 300 x 15 = 45000 x hourly rate
- Assume engineering support for cycle-by-cycle recorders is 25% higher than that for counting accelerometer in order to account for squadron level ground equipment and associated manpower

- o Mechanical strain recorder: .04 man hours per flight hour for data reading; $.50 per flight hour for cartridge replacement; $11000 per year automation costs
- o Hardware costs (not including installation)

  Counting accelerometer, $1000; VGH recorder, $25000; Multi-channel recorder, $50,000; strain recorder, $2500; Sequential strain counter, $4700; mechanical strain recorder, $800

TABLE 14 POTENTIAL MONITORING SYSTEMS

Description of System	Relative Cost
One Counting Accelerometer Per Aircraft	.60
One Strain Exceedance Counter Per Aircraft	.85
One Counting Accelerometer Per Aircraft + One VGH Recorder In Every Tenth Aircraft	1.0 (F-4)
One Sequential Strain Counter Per Aircraft	1.1
One Mechanical Strain Recorder (4) Per Aircraft	1.7
One Sequential Strain Counter Per Aircraft + 50 Multi-Channel Recorders (Approx. 3 Per Base)	1.8
One Sequential Strain Counter Per Aircraft + One Multi-Channel Recorder In Every Tenth Aircraft	2.2
One Counting Accelerometer Per Aircraft + One Multi-Channel Recorder In Every Fifth Aircraft	2.3

Notes:

1. 1,000 Aircraft Fleet
2. 15 Years of Monitoring
3. Generally, Complexity Increases Directly With Cost

(4) Sequential Strain

Some of the more important considerations in selecting a particular system are:

- o Degree of Sophistication
- o Operating Cost
- o Ease of Maintenance
- o Relative State of the Art of:
  - Crack Detection techniques
  - Initial Quality
  - Individual Aircraft Instrumentation

The success of an individual aircraft tail tracking program depends on the following:

- o Technical Concept Chosen for Monitoring the Fleet
- o Reliability of Instrumentation Used for Individual Aircraft Tracking
- o Reliability of Instrumentation used for Fleet Sampling
- o Degree of Support by the Using Command

5. CONCLUSIONS

The following general conclusions are made with regard to the tracking of crack growth in individual fleet aircraft:

- o Load factor exceedance variations of severe and mild (from baseline) are much more significant than realistic mission parameter variations, and the load factor exceedance variations are accounted for in the individual tail tracking program.
- o More than one critical location should be monitored on the more recent generation of fighters that use more sophisticated control systems such as differential tail augmented roll, variable sweep wings, and canards.
- o For a conventional fighter such as the F-4E(S), an adequate job can be done by monitoring one location and scaling by operational limits to get the damage at other locations.
- o The effects of aircraft usage sequencing using the F-4 aircraft are shown to be negligible (less than 5%) when considering conservative combinations of usage sequence/location of peak load. The life calculated using F-4E(S) ASIP type S/N data is only 10% greater than the life obtained from the Willenborg crack growth model.
- o The Damage Index Method developed during the F-4E(S) Damage Tolerance Assessment results in evaluation of individual aircraft damage equivalent to that determined when using the modified Wheeler crack growth prediction method.
- o Even the most elaborate system for recording fleet and individual aircraft usage data is cost effective when compared with total program costs of a given fleet, therefore, the choice of a monitoring system could depend on the degree of sophistication that is desired.

6. REFERENCES

1. Department of the Air Force Contract No. F33615-75-C-3136, dated 15 September 1975.

2. MCAIR MDC A3390, "Model F-4E Slatted Airplane Fatigue and Damage Tolerance Assessment - Volume I," dated 31 July 1975.

3. Forman, R. G., Kearney, V. E., and Engle, R. M., "Numerical Analysis of Crack Propagation in Cyclic Loaded Structures," Journal of Basic Engineering, Transactions of ASME, September 1967.

4. Bowie, O. L., "Analysis of an Infinite Plate Containing Radial Crack Originating From the Boundary of Internal Circular Hole," Journal of Mathematics and Physics, Vol. 35, 1956.

5. MCAIR MDC A1936, Vol. I, "Interference Fit Fastener Investigation," 5 October 1972.

6. Isida, M., "Stress Intensity Factors For the Tension of an Eccentrically Cracked Strip," Journal of Applied Mechanics, Transactions of ASME, September 1966.

7. Paris, P. C. and Sih, G. C., "Stress Analysis of Cracks," Fracture Toughness Testing and Its Applications, ASTM STP 381, 21 June 1964.

8. Impellizzeri, L. F. and Rich, D. L., "Spectrum Fatigue Crack Growth in Lugs", Fatigue Crack Growth Under Spectrum Loads, ASTM STP 595, 1976 pp 320-336.

9. MCAIR MDC A1456, "F-15 Service Life Analysis", dated 31 December 1975.

10. MCAIR MDC A2883, "F-4 Fatigue and Damage Tolerance Assessment Program - Volume I", dated 28 June 1974.

11. Gallagher, J. P., and Hughes, T. F., "Influence of Yield Strength on Overload Affected Fatigue Crack Growth Behavior in 4340 Steel," AFFDL-TR-74-27, March 1974.

APPENDIX A

This appendix presents (1) the loads used in the development of stress spectra, (2) stress spectra used for mission and design parameter variations, and (3) crack growth curves for all the variations.

1. Loads Used in Stress Spectra Development

The loads used in the development of stress spectra are based on the bending moments from the flight loads survey for the F-4E slatted airplane and are shown in the form of stresses (Ksi) at the LRS 70 wing location (Table A-1) and the F.S. 303 fuselage location (Table A-2). These stress levels were derived during the Reference 2 F-4E(S) damage tolerance assessment. The corresponding occurrences per 1000 hours are shown in Table A-3.

2. Stress Spectra

The baseline F-4E(S) load factor spectra for air-to-air, air-to-ground, and non-tactical mission types as well as composite usage were developed during the Reference 2 ASIP Program using counting accelerometer and VGH data and are shown in Figure A-1.

Load factor spectra for the usage categories of severe, baseline, and mild established during the Reference 2 ASIP Program are shown in Figure A-2.

Stress spectra developed during the Reference 2 ASIP Program for the LRS 70 wing location and for the F.S. 303 fuselage location are shown in Figures A-3 and A-4 respectively for the F-4E(S) baseline. Design limit stress (DLS) at LRS 70 and F.S. 303 is 24.4 Ksi and 18.8 Ksi, respectively.

The block spectra used in making crack growth predictions utilizing the modified Wheeler method are:

Spectrum	Figure No.
LRS 70 F-4E(S) ASIP Baseline	A-5
FS 303 F-4E(S) ASIP Baseline	A-6
LRS 70 F-4E(S) ASIP Severe	A-7
FS 303 F-4E(S) ASIP Severe	A-8
LRS 70 F-4E(S) ASIP Mild	A-9
FS 303 F-4E(S) ASIP Mild	A-10
LRS 70 +15% Air-Air Airspeed	A-11
FS 303 +15% Air-Air Airspeed	A-12
LRS 70 -15% Air-Air Airspeed	A-13
FS 303 -15% Air-Air Airspeed	A-14

Spectrum	Figure No.
LRS 70 +15% Air-Ground Airspeed	A-15
LRS 70 -15% Air-Ground Airspeed	A-16
LRS 70 +3000 Lb Air-Air Gross Weight	A-17
LRS 70 +30% Air-Air Altitude	A-18
LRS 70 -30% Air-Air Altitude	A-19
FS 303 +30% Air-Air Altitude	A-20
FS 303 -30% Air-Air Altitude	A-21
LRS 70 +1000 Lb Air-Air Gross Weight	A-22
LRS 70 Mildest Aircraft - Truncated σ_{max}	A-23
LRS 70 Simultaneous Variation	A-24
LRS 70 Variation of Max. Spectrum Stress - σ_{max} = 28.7 ksi	A-25
LRS 70 Variation of Max. Spectrum Stress - σ_{max} = 26.3 ksi	A-26
LRS 70 +6% Air-Air Airspeed	A-27
LRS 70 FMS Severe	A-28
LRS 70 T-Bird Solo	A-29
LRS 70 Serial No. 711072	A-30

3. Crack Growth Curves

Crack growth curves for mission parameter variations at LRS 70 and FS 303 are shown in Figures A-31 through A-52.

Crack Growth curves for design parameter variations at LRS 70 and FS 303 are shown in Figures A-53 through A-60.

Crack growth curves for aircraft usage sequencing are shown in Figures A-61, A-62, and A-63.

Airspeed	Altitude						
	500	1,500	3,500	7,500	12,500	17,500	25,000
275			11.6	11.6	11.6	12.9	12.5
325			15.6	15.8	16.3	16.0	14.2
375		15.5	15.6	16.0	17.1	17.6	17.7
425		15.9	16.2	17.0	18.7	20.0	21.3
475			17.5	18.8	21.1	22.5	22.1
525			17.3	18.2	19.5	20.4	21.1
587			18.3	18.6	18.8	19.2	20.1
662				17.5	18.3	18.6	

GP77-0840-6

1. Tables exist for positive n_z of 2.0, 2.4, 2.8, 3.4, 4.2, 5.0, 6.0, 7.2, and 8.4.
2. Tables exist for n_z below 1 G of 0.40, 0.0, −0.40, −0.80, −1.4, and −2.2.
3. Tables also exist for air-to-ground, and non-tactical missions.
4. Distribution of occurrences based on VGH data; occurrences based on counter data.
5. Speeds, altitudes, and load factors are midpoints between intervals of VGH data.

TABLE A-1
TYPICAL TABLE OF STRESS
F-4E(S) Air-to-Air Mission 5.0 G LRS 70

Airspeed	Altitude						
	500	1,500	3,500	7,500	12,500	17,500	25,000
275			10.3	10.1	11.1	11.1	10.7
325			13.7	13.9	14.1	13.9	12.6
375		14.0	14.1	14.3	14.9	15.3	15.8
425		14.7	14.9	15.3	16.4	17.6	18.6
475			16.2	17.1	19.0	20.1	19.8
525			16.7	17.6	18.5	19.0	19.7
587			18.2	18.4	18.6	19.0	19.5
662				18.6	18.6	19.0	

GP77-0840-5

1. Tables exist for positive n_z of 2.0, 2.4, 2.8, 3.4, 4.2, 5.0, 6.0, 7.2, and 8.4.
2. Tables exist for n_z below 1 G of 0.40, 0.0, −0.40, −0.80, −1.4, and −2.2.
3. Tables also exist for air-to-ground, and non-tactical missions.
4. Distribution of occurrences based on VGH data; occurrences based on counter data.
5. Speeds, altitudes, and load factors are midpoints between intervals of VGH data.

TABLE A-2
TYPICAL TABLE OF STRESS
F-4E(S) Air-to-Air Mission 5.0 G FS 303

Airspeed	Altitude						
	500	1,500	3,500	7,500	12,500	17,500	25,000
275			25.9	22.5	83.8	87.0	42.0
325			6.4	32.3	119.3	103.2	51.6
375				45.2	145.2	125.8	58.0
425				35.4	148.3	80.6	38.6
475		0.8	4.9	21.7	76.6	92.7	9.6
525				35.4	74.1	6.4	3.2
587			3.2	61.3	16.1	16.1	
662					6.4		

GP77-0840-4

1. Tables exist for positive n_z of 2.0, 2.4, 2.8, 3.4, 4.2, 5.0, 6.0, 7.2, and 8.4.
2. Tables exist for n_z below 1 G of 0.40, 0.0, −0.40, −0.80, −1.4, and −2.2.
3. Tables also exist for air-to-ground, and non-tactical missions.
4. Distribution of occurrences based on VGH data; occurrences based on counter data.
5. Speeds, altitudes, and load factors are midpoints between intervals of VGH data.

TABLE A-3
TYPICAL TABLE OF OCCURRENCES - 1000 HRS
F-4E(S) Air-to-Air Mission 5.0 G

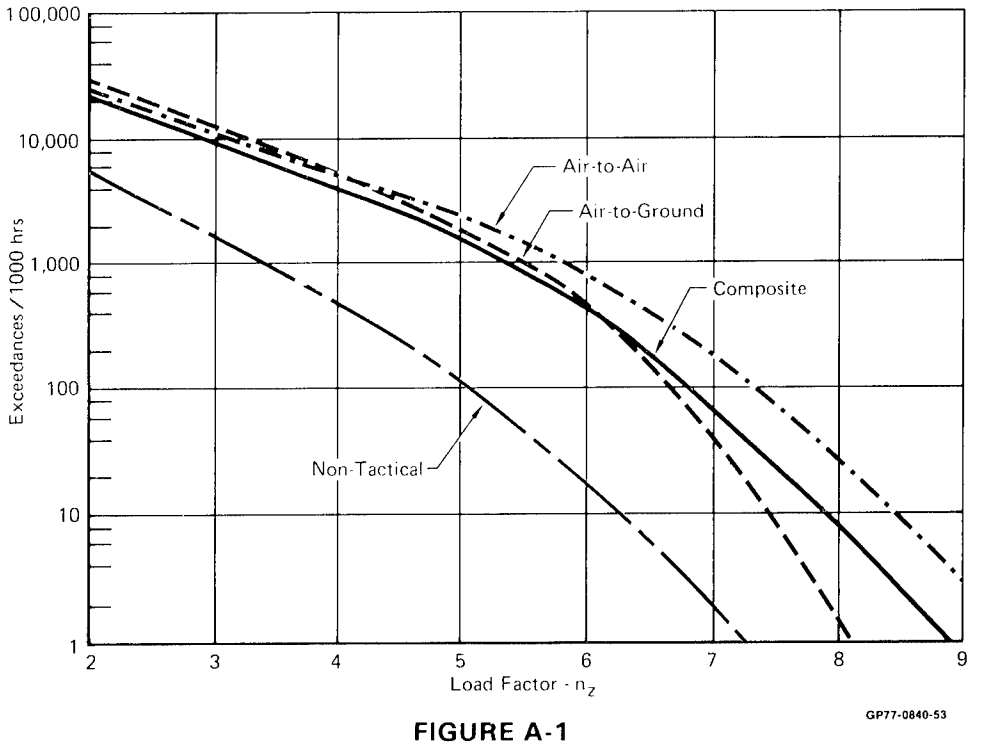

FIGURE A-1
F-4E(S) BASELINE LOAD FACTOR EXCEEDANCE

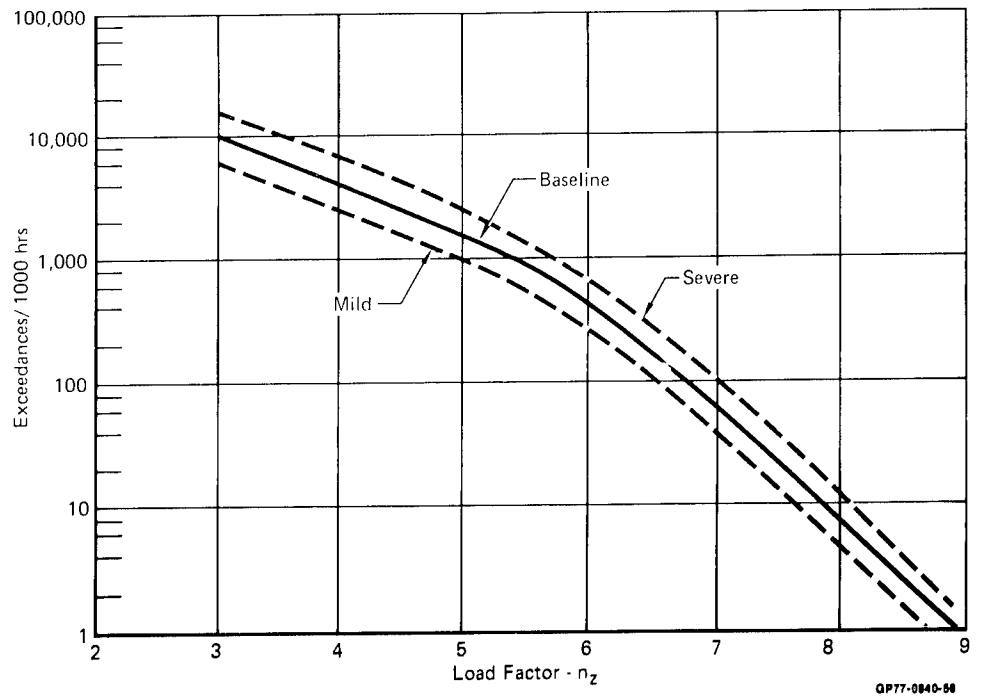

FIGURE A-2
F-4E(S) LOAD FACTOR EXCEEDANCE
Usage Variations

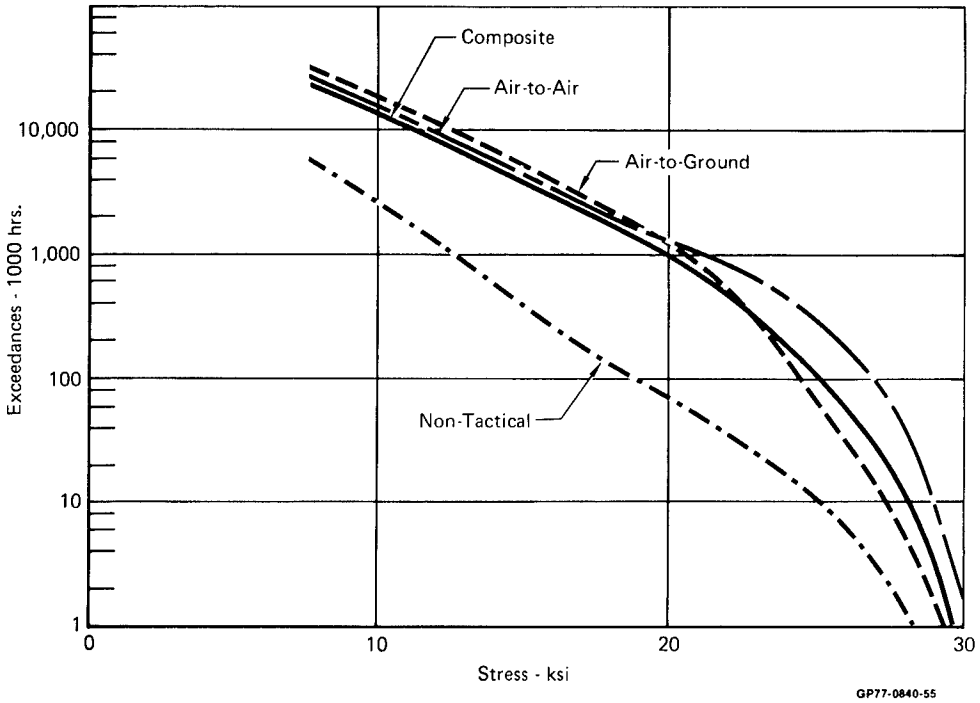

FIGURE A-3
F-4E(S) BASELINE STRESS EXCEEDANCE
LRS 70

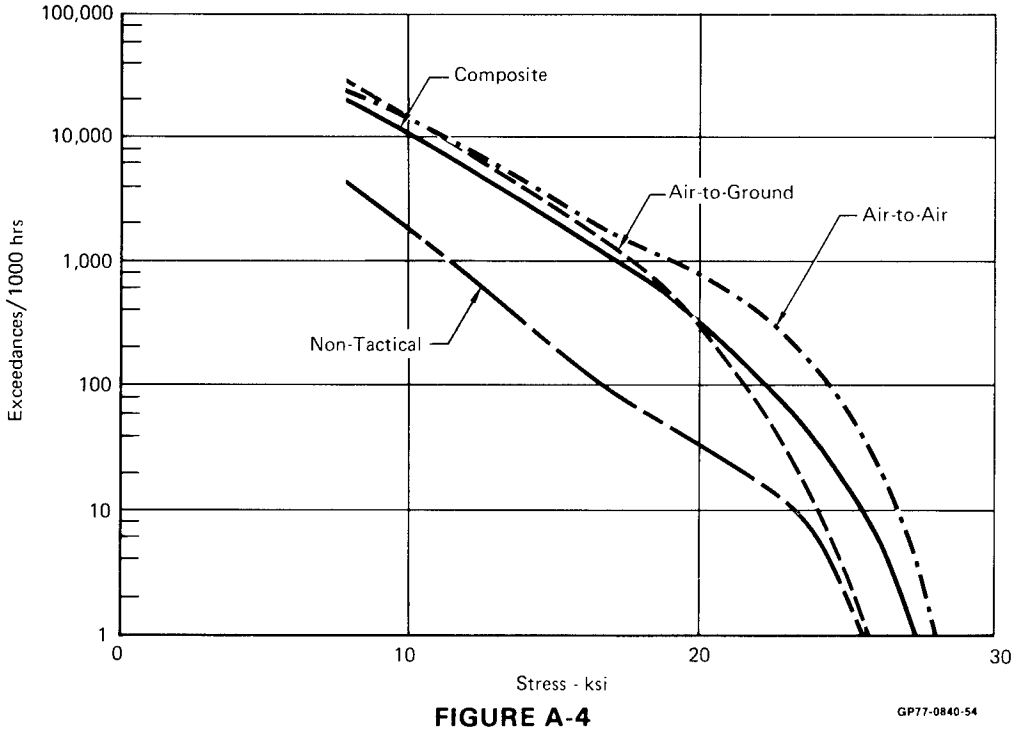

FIGURE A-4
F-4E(S) BASELINE STRESS EXCEEDANCE
FS 303

Max % DLS	Minimum % DLS					
	0.166	0.020	−0.154	−0.051	−0.256	−0.359
0.359	2358	162	74	6	1	1
0.461	1131	413	189	15	3	3
0.564	816	188	86	7	2	1
0.666	415	63	29	3	1	
0.768	215	27	12	1		
0.871	131	18	8	1		
0.973	88	13	6			
1.076	38	13	6			
1.178	16					
1.332	0.3					

100% DLS = 24.4 ksi

GP77-0840-8

FIGURE A-5
LRS 70 F-4E(S) ASIP BASELINE AIR-TO-AIR SPECTRUM
OCCURRENCES PER 260 HRS

Max % DLS	Minimum % DLS			
	0.160	0.020	−0.051	−0.154
0.359	5829	206	55	3
0.461	3261	608	162	9
0.564	2080	195	52	3
0.666	1136	75	20	1
0.768	636	29	8	1
0.871	385	19	5	
0.973	144	9	2	
1.076	17	6	2	
1.178	4			
1.332	0.2			

GP77-0840-9

100% DLS = 24.4 ksi

FIGURE A-5 (Continued)
LRS 70 F-4E(S) ASIP BASELINE AIR-TO-GROUND SPECTRUM
OCCURRENCES PER 490 HRS

Max % DLS	Minimum % DLS				
	0.148	0.020	–0.051	–0.154	–0.256
0.359	747	49	13	1	
0.461	221	143	39	2	1
0.564	110	46	13	1	
0.666	35	17	5		
0.768	12	7	2		
0.871	5	5	1		
0.973	2	2	1		
1.076	1	1			
1.178	1				
–	–				

100% DLS = 24.4 ksi

GP77-0840-10

FIGURE A-5 (Concluded)
LRS 70 F-4E(S) ASIP BASELINE NON-TACTICAL SPECTRUM OCCURRENCES PER 250 HRS

Max % DLS	Minimum % DLS					
	0.223	0.073	0.010	−0.100	−0.209	−0.286
0.405	2358	162	74	6	1	1
0.507	1131	413	189	15	3	3
0.612	816	188	86	7	2	1
0.174	415	63	29	3	1	
0.811	215	27	12	1		
0.917	131	18	8	1		
1.034	88	13	6			
1.148	38	13	6			
1.279	16					
1.415	0.3					

100% DLS = 18.8 ksi

GP77-0840-11

FIGURE A-6
FS 303 F-4E(S) ASIP BASELINE AIR-TO-AIR SPECTRUM
OCCURRENCES PER 260 HRS

Max % DLS	Minimum % DLS			
	0.214	0.092	0.012	−0.087
0.379	5829	206	55	3
0.476	3261	608	162	9
0.578	2080	195	52	3
0.680	1136	75	20	1
0.782	636	29	8	1
0.893	385	19	5	
1.012	144	9	2	
1.131	17	6	2	
1.255	4			
1.383	0.2			

GP77-0840-12

100% DLS = 18.8 ksi

FIGURE A-6 (Continued)
FS 303 F-4E(S) ASIP BASELINE AIR-TO-GROUND SPECTRUM OCCURRENCES PER 490 HRS

Max % DLS	Minimum % DLS				
	0.194	0.090	0.017	–0.102	–0.197
0.381	747	49	13	1	
0.493	221	143	39	2	1
0.602	110	46	13	1	
0.701	35	17	5		
0.799	12	7	2		
0.917	5	5	1		
1.051	2	2	1		
1.170	1	1			
1.279	1				
1.396	–				

100% DLS = 18.8 ksi

GP77-0840-13

FIGURE A-6 (Concluded)
FS 303 F-4E(S) ASIP BASELINE NON-TACTICAL SPECTRUM OCCURRENCES PER 250 HRS

Max % DLS	Minimum % DLS					
	0.166	0.020	−0.051	−0.154	−0.256	−0.359
0.445	2358	162	74	6	1	1
0.535	1131	413	189	15	3	3
0.633	816	188	86	7	2	1
0.732	415	63	29	3	1	
0.826	215	27	12	1		
0.920	131	18	8	1		
1.010	88	13	6			
1.096	38	13	6			
1.184	16					
1.332	0.3					

GP77-0840-14

100% DLS = 24.4 ksi

FIGURE A-7
LRS 70 F-4E(S) ASIP SEVERE AIR-TO-AIR SPECTRUM
OCCURRENCES PER 260 HRS

Max % DLS	Minimum % DLS			
	0.160	0.020	−0.051	−0.154
0.445	5829	206	55	3
0.535	3261	608	162	9
0.633	2080	195	52	3
0.732	1136	75	20	1
0.826	636	29	8	1
0.920	385	19	5	
1.010	144	9	2	
1.096	17	6	2	
1.184	4			
1.332	0.2			

100% DLS = 24.4 ksi

GP77-0840-15

FIGURE A-7 (Continued)
LRS 70 F-4E(S) ASIP SEVERE AIR-TO-GROUND SPECTRUM OCCURRENCES PER 490 HRS

Max % DLS	Minimum % DLS				
	0.148	0.020	−0.051	−0.154	−0.256
0.445	747	49	13	1	
0.535	221	143	39	2	1
0.633	110	46	13	1	
0.732	35	17	5		
0.826	12	7	2		
0.920	5	5	1		
1.010	2	2	1		
1.096	1	1			
1.184	1				
–	–				

100% DLS = 24.4 ksi

GP77-0840-16

FIGURE A-7 (Concluded)
LRS 70 F-4E(S) ASIP SEVERE NON-TACTICAL SPECTRUM OCCURRENCES PER 250 HRS

Max % DLS	Minimum % DLS					
	0.223	0.073	0.010	−0.100	−0.209	−0.286
0.501	2358	162	74	6	1	1
0.589	1131	413	189	15	3	3
0.687	816	188	86	7	2	1
0.785	415	63	29	3	1	
0.873	215	27	12	1		
0.968	131	18	8	1		
1.072	88	13	6			
1.169	38	13	6			
1.286	16					
1.415	0.3					

100% DLS = 18.8 ksi

GP77-0840-17

FIGURE A-8
FS 303 F-4E(S) ASIP SEVERE AIR-TO-AIR SPECTRUM
OCCURRENCES PER 260 HRS

Max % DLS	Minimum % DLS			
	0.214	0.092	0.012	−0.087
0.470	5829	206	55	3
0.552	3261	608	162	9
0.649	2080	195	52	3
0.748	1136	75	20	1
0.841	636	29	8	1
0.944	385	19	5	
1.051	144	9	2	
1.152	17	6	2	
1.262	4			
1.383	0.2			

100% DLS = 18 8 ksi

GP77-0840-18

FIGURE A-8 (Continued)
FS 303 F-4E(S) ASIP SEVERE AIR-TO-GROUND SPECTRUM OCCURRENCES PER 490 HRS

Max % DLS	Minimum % DLS				
	0.194	0.090	0.017	−0.102	−0.197
0.472	747	49	13	1	
0.572	221	143	39	2	1
0.676	110	46	13	1	
0.770	35	17	5		
0.860	12	7	2		
0.968	5	5	1		
1.091	2	2	1		
1.190	1	1			
1.228	1				
–	–				

100% DLS = 18.8 ksi

GP77-0840-19

FIGURE A-8 (Concluded)
FS 303 F-4E(S) ASIP SEVERE NON-TACTICAL SPECTRUM OCCURRENCES PER 250 HRS

Max % DLS	Minimum % DLS					
	0.166	**0.020**	−0.051	−0.154	**−0.256**	**−0.359**
0.277	2358	162	74	6	1	1
0.373	1131	413	189	15	3	3
0.482	816	188	86	7	2	1
0.583	415	63	29	3	1	
0.695	215	27	12	1		
0.809	131	18	8	1		
0.926	88	13	6			
1.041	38	13	6			
1.164	16					
1.332	0.3					

100% DLS = 24.4 ksi

GP77-0840-20

FIGURE A-9
LRS 70 F-4E(S) ASIP MILD AIR-TO-AIR SPECTRUM
OCCURRENCES PER 260 HRS

Max % DLS	Minimum % DLS			
	0.160	0.020	−0.051	−0.154
0.277	5829	206	55	3
0.373	3261	608	162	9
0.482	2080	195	52	3
0.588	1136	75	20	1
0.695	636	29	8	1
0.809	385	19	5	
0.926	144	9	2	
1.041	17	6	2	
1.164	4			
1.332	0.2			

100% DLS = 24.4 ksi

GP77-0840-21

FIGURE A-9 (Continued)
LRS 70 F-4E(S) ASIP MILD AIR-TO-GROUND SPECTRUM
OCCURRENCES PER 490 HRS

Max % DLS	Minimum % DLS				
	0.148	0.020	−0.051	−0.154	−0.256
0.277	747	49	13	1	
0.373	221	143	39	2	1
0.482	110	46	13	1	
0.588	35	17	5		
0.695	12	7	2		
0.809	5	5	1		
0.926	2	2	1		
1.041	1	1			
1.164	1				
–	–				

100% DLS = 24.4 ksi

GP77-0840-22

FIGURE A-9 (Concluded)
LSR 70 F-4E(S) ASIP MILD NON-TACTICAL SPECTRUM
OCCURRENCES PER 250 HRS

Max % DLS	Minimum % DLS					
	0.223	0.073	0.010	−0.100	−0.209	−0.286
0.313	2358	162	74	6	1	1
0.410	1131	413	189	15	3	3
0.523	816	188	86	7	2	1
0.630	415	63	29	3	1	
0.734	215	27	12	1		
0.851	131	18	8	1		
0.985	88	13	6			
1.110	38	13	6			
1.266	16					
1.415	0.3					

100% DLS = 18.8 ksi

GP77-0840-23

FIGURE A-10
FS 303 F-4E(S) ASIP MILD AIR-TO-AIR SPECTRUM
OCCURRENCES PER 260 HRS

Max % DLS	Minimum % DLS			
	0.214	0.092	0.012	−0.087
0.292	5829	206	55	3
0.385	3261	608	162	9
0.494	2080	195	52	3
0.600	1136	75	20	1
0.707	636	29	8	1
0.829	385	19	5	
0.964	144	9	2	
1.096	17	6	2	
1.135	4			
1.383	0.2			

100% DLS = 18.8 ksi

GP77-0840-24

FIGURE A-10 (Continued)
FS 303 F-4E(S) ASIP MILD AIR-TO-GROUND SPECTRUM
OCCURRENCES PER 490 HRS

Max % DLS	Minimum % DLS				
	0.194	0.090	0.017	−0.102	−0.197
0.294	747	49	13	1	
0.399	221	143	39	2	1
0.515	110	46	13	1	
0.619	35	17	5		
0.723	12	7	2		
0.852	5	5	1		
1.000	2	2	1		
1.132	1	1			
1.265	1				
–	–				

100% DLS = 18.8 ksi

GP77-0840-25

FIGURE A-10 (Concluded)
FS 303 F-4E(S) ASIP MILD NON-TACTICAL SPECTRUM
OCCURRENCES PER 250 HRS

Max % DLS	Minimum % DLS					
	0.166	0.020	−0.051	−0.154	−0.256	−0.359
0.359	2358	162	74	6	1	1
0.494	1131	413	189	15	3	3
0.611	816	188	86	7	2	1
0.725	415	63	29	3	1	
0.835	215	27	12	1		
0.940	131	18	8	1		
1.029	88	13	6			
1.086	38	13	6			
1.180	16					
1.332	0.3					

100% DLS = 24.4 ksi

GP77-0840-28

FIGURE A-11
+15% AIR-TO-AIR AIRSPEED - LRS 70
OCCURRENCES PER 260 HRS

Max % DLS	Minimum % DLS					
	0.223	0.073	0.010	–0.100	–0.209	–0.286
0.405	2358	162	74	6	1	1
0.528	1131	413	189	15	3	3
0.668	816	188	86	7	2	1
0.796	415	63	29	3	1	
0.907	215	27	12	1		
1.020	131	18	8	1		
1.126	88	13	6			
1.204	38	13	6			
1.300	16					
1.415	0.3					

100% DLS = 18.8 ksi

G77-0840-27

FIGURE A-12
+15% AIR-TO-AIR AIRSPEED - FS 303
OCCURRENCES PER 260 HRS

Max % DLS	Minimum % DLS					
	0.166	0.020	−0.051	−0.154	−0.256	−0.359
0.359	2358	162	74	6	1	1
0.449	1131	413	189	15	3	3
0.525	816	188	86	7	2	1
0.599	415	63	29	3	1	
0.673	215	27	12	1		
0.750	131	18	8	1		
0.829	88	13	6			
0.914	38	13	6			
1.002	16					
1.132	0.3					

100% DLS = 24.4 ksi

GP77-0840-28

FIGURE A-13
—15% AIR-TO-AIR AIRSPEED - LRS 70
OCCURRENCES PER 260 HRS

Max % DLS	Minimum % DLS					
	0.223	0.073	0.010	−0.100	−0.209	−0.286
0.405	2358	162	74	6	1	1
0.493	1131	413	189	15	3	3
0.565	816	188	86	7	2	1
0.636	415	63	29	3	1	
0.712	215	27	12	1		
0.797	131	18	8	1		
0.894	88	13	6			
0.986	38	13	6			
1.100	16					
1.217	0.3					

100% DLS = 18.8 ksi

GP77-0840-29

FIGURE A-14
−15% AIR-TO-AIR AIRSPEED - FS 303
OCCURRENCES PER 260 HRS

Max % DLS	Minimum % DLS			
	0.160	0.020	−0.051	−0.154
0.359	5829	206	55	3
0.476	3261	608	162	9
0.597	2080	195	52	3
0.719	1136	75	20	1
0.840	636	29	8	1
0.961	385	19	5	
1.070	144	9	2	
1.170	17	6	2	
1.251	4			
1.332	0.2			

100% DLS = 24.4 ksi

GP77-0840-30

FIGURE A-15
+15% AIR-TO-GROUND AIRSPEED - LRS 70
OCCURRENCES PER 490 HRS

Max % DLS	Minimum % DLS			
	0.160	0.020	−0.051	−0.154
0.359	5829	206	55	3
0.451	3261	608	162	9
0.532	2080	195	52	3
0.612	1136	75	20	1
0.691	636	29	8	1
0.775	385	19	5	
0.860	144	9	2	
0.946	17	6	2	
1.031	4			
1.165	0.2			

100% DLS = 24.4 ksi

GP77-0840-31

FIGURE A-16
—15% AIR-TO-GROUND AIRSPEED - LRS 70
OCCURRENCES PER 490 HRS

Max % DLS	Minimum % DLS					
	0.179	0.021	−0.055	−0.165	−0.276	−0.386
0.386	2358	162	74	6	1	1
0.496	1131	413	189	15	3	3
0.607	816	188	86	7	2	1
0.717	415	63	29	3	1	
0.826	215	27	12	1		
0.937	131	18	8	1		
1.031	88	13	6			
1.126	38	13	6			
1.207	16					
1.332	0.3					

⚠1 Spectrum σ_{max} Kept Same as Baseline
100% DLS = 24.4 ksi

GP77-0840-32

FIGURE A-17
+3000 LB AIR-TO-AIR GW ⚠1 - LRS 70
OCCURRENCES PER 260 HRS

Max % DLS	Minimum % DLS					
	0.166	0.020	−0.051	−0.154	−0.256	−0.359
0.359	2358	162	74	6	1	1
0.477	1131	413	189	15	3	3
0.590	816	188	86	7	2	1
0.697	415	63	29	3	1	
0.799	215	27	12	1		
0.899	131	18	8	1		
0.993	88	13	6			
1.089	38	13	6			
1.183	16					
1.332	0.3					

100% DLS = 24.4 ksi

GP77-0840-33

FIGURE A-18
+30% AIR-TO-AIR ALTITUDE - LRS 70
OCCURRENCES PER 260 HRS

Max % DLS	Minimum % DLS					
	0.166	0.020	−0.051	−0.154	−0.256	−0.359
0.359	2358	162	74	6	1	1
0.445	1131	413	189	15	3	3
0.528	816	188	86	7	2	1
0.615	415	63	29	3	1	
0.712	215	27	12	1		
0.832	131	18	8	1		
0.946	88	13	6			
1.060	38	13	6			
1.170	16					
1.332	0.3					

100% DLS = 24.4 ksi

GP77-0840-34

FIGURE A-19
—30% AIR-TO-AIR ALTITUDE - LRS 70
OCCURRENCES PER 260 HRS

Max % DLS	Minimum % DLS					
	0.223	0.073	0.010	−0.100	−0.209	−0.286
0.405	2358	162	74	6	1	1
0.515	1131	413	189	15	3	3
0.644	816	188	86	7	2	1
0.748	415	63	29	3	1	
0.837	215	27	12	1		
0.936	131	18	8	1		
1.050	88	13	6			
1.157	38	13	6			
1.284	16					
1.415	0.3					

100% DLS = 18.8 ksi

GP77-0840-35

FIGURE A-20
+30% AIR-TO-AIR ALTITUDE - FS 303
OCCURRENCES PER 260 HRS

Max % DLS	Minimum % DLS					
	0.223	0.073	0.010	−0.100	−0.209	−0.286
0.405	2358	162	74	6	1	1
0.501	1131	413	189	15	3	3
0.585	816	188	86	7	2	1
0.674	415	63	29	3	1	
0.773	215	27	12	1		
0.884	131	18	8	1		
1.002	88	13	6			
1.115	38	13	6			
1.245	16					
1.381	0.3					

100% DLS = 18.8 ksi

GP77-0840-36

FIGURE A-21
—30% AIR-TO-AIR ALTITUDE - FS 303
OCCURRENCES PER 260 HRS

Max % DLS	Minimum % DLS					
	0.170	0.021	−0.052	−0.158	−0.262	−0.368
0.368	2358	162	74	6	1	1
0.473	1131	413	189	15	3	3
0.579	816	188	86	7	2	1
0.683	415	63	29	3	1	
0.788	215	27	12	1		
0.894	131	18	8	1		
0.998	88	13	6			
1.100	38	13	6			
1.195	16					
1.332	0.3					

100% DLS = 24.4 ksi

GP77-0840-37

FIGURE A-22
+1000 LB AIR-TO-AIR GW - LRS 70
OCCURRENCES PER 260 HRS

Max % DLS	Minimum % DLS					
	0.166	0.020	−0.051	−0.154	−0.256	−0.359
0.215	2358	162	74	6	1	1
0.322	1131	413	189	15	3	3
0.431	816	188	86	7	2	1
0.544	415	63	29	3	1	
0.656	215	27	12	1		
0.763	131	18	8	1		
0.854	88	13	6			
0.944	38	13	6			
1.010	16					
1.070	0.3					

100% DLS = 24.4 ksi

GP77-0840-38

FIGURE A-23
F-4E(S) MILDEST AIRCRAFT - TRUNCATED σ_{MAX}
AIR-TO-AIR - LRS 70
OCCURRENCES PER 260 HRS

Max % DLS	Minimum % DLS			
	0.160	0.020	−0.051	−0.154
0.215	5829	206	55	3
0.322	3261	608	162	9
0.431	2080	195	52	3
0.544	1136	75	20	1
0.656	636	29	8	1
0.763	385	19	5	
0.854	144	9	2	
0.944	17	6	2	
1.010	4			
1.070	0.2			

100% DLS = 24.4 ksi

GP77-0840-39

FIGURE A-23 (Continued)
F-4E(S) MILDEST AIRCRAFT - TRUNCATED σ_{MAX}
AIR-TO-GROUND - LRS 70
OCCURRENCES PER 490 HRS

Max % DLS	Minimum % DLS				
	0.148	0.020	−0.051	−0.154	−0.256
0.215	747	49	13	1	
0.322	221	143	39	2	1
0.431	110	46	13	1	
0.544	35	17	5		
0.656	12	7	2		
0.763	5	5	1		
0.854	2	2	1		
0.944	1	1			
1.010	1				
–	–				

100% DLS = 24.4 ksi

GP77-0840-40

FIGURE A-23 (Concluded)
F-4E(S) MILDEST AIRCRAFT - TRUNCATED σ_{MAX}
NON-TACTICAL - LRS 70
OCCURRENCES PER 250 HRS

Max % DLS	Minimum % DLS					
	0.166	0.020	−0.051	−0.154	−0.256	−0.359
0.364	2358	162	74	6	1	1
0.483	1131	413	189	15	3	3
0.596	816	188	86	7	2	1
0.705	415	63	29	3	1	
0.812	215	27	12	1		
0.916	131	18	8	1		
1.013	88	13	6			
1.095	38	13	6			
1.192	16					
1.332	.3					

100% DLS = 24.4 ksi
500 lb Increase in Air-to-Air GW
5% Increase in Air-to-Air Airspeed
10% Increase in Air-to-Air Altitude

GP77-0840-41

FIGURE A-24
SIMULTANEOUS VARIATION OF GW, AIRSPEED, MISSION MIX, AND ALTITUDE
LRS 70
AIR-TO-AIR SPECTRUM
OCCURRENCES PER 260 HRS

Max % DLS	Minimum % DLS			
	0.160	0.020	−0.051	−0.154
0.364	5829	206	55	3
0.466	3261	608	162	9
0.576	2080	195	52	3
0.684	1136	75	20	1
0.791	636	29	8	1
0.899	385	19	5	
1.004	144	9	2	
1.108	17	6	2	
1.206	4			
1.332	.2			

500 lb Increase in Air-to-Ground GW
3% Increase in Air-to-Ground Airspeed
100% DLS = 24.4 ksi

GP77-0840-42

FIGURE A-24 (Concluded)
SIMULTANEOUS VARIATION OF GW, AIRSPEED, MISSION MIX, AND ALTITUDE
LRS 70
AIR-TO-GROUND SPECTRUM
OCCURRENCES PER 490 HRS

Max % DLS	Minimum % DLS					
	0.160	0.020	−0.051	−0.154	−0.256	−0.359
0.359	8934	417	142	10	1	1
0.461	4613	1164	390	26	4	3
0.564	3006	429	151	11	2	
0.666	1586	155	54	4	1	
0.768	863	63	22	2		
0.871	523	42	14	1		
0.973	240	25	9			
1.076	43	16	6			
1.178	1					

100% DLS = 24.4 ksi

GP77-0840-43

FIGURE A-25
VARIATION OF MAX SPECTRUM STRESS
F-4E(S) SPECTRUM - LRS 70 - σMAX = 28.7 KSI
OCCURRENCES PER 1000 HRS

Max % DLS	Minimum % DLS					
	0.160	0.020	–0.051	–0.154	–0.256	–0.359
0.359	8934	417	142	10	1	1
0.461	4613	1164	390	26	4	3
0.564	3006	429	151	11	2	
0.666	1586	155	54	4	1	
0.768	863	63	22	2		
0.871	559	45	15	1		
0.973	262	27	10			
1.076	1					

100% DLS = 24.4 ksi

GP77-0840-44

FIGURE A-26
VARIATION OF MAX SPECTRUM STRESS
F-4E(S) SPECTRUM - LRS 70 - σMAX = 26.3 KSI
OCCURRENCES PER 1000 HRS

Max % DLS	Minimum % DLS					
	0.166	0.020	–0.051	–0.154	–0.256	–0.359
0.359	2358	162	74	6	1	1
0.474	1131	413	189	15	3	3
0.584	816	188	86	7	2	1
0.690	415	63	29	3	1	
0.795	215	27	12	1		
0.900	131	18	8	1		
0.994	88	13	6			
1.081	38	13	6			
1.180	16					
1.332	.3					

100% DLS = 24.4 ksi

GP77-0840-45

FIGURE A-27
+6% AIR-TO-AIR AIRSPEED - LRS 70
OCCURRENCES PER 260 HRS

Max % DLS	Minimum % DLS					
	0.166	–0.051	–0.154	–0.256	–0.359	–0.461
0.359	5048	406	37	4	3	2
0.461	1745	1040	93	11	7	4
0.564	1074	472	44	7	2	1
0.666	844	159	19	2	1	
0.768	688	77	9	1		
0.871	461	51	3			
0.973	312	38				
1.076	208	7				
1.178	104					
1.281	15					
1.395	1					

100% DLS = 24.4 ksi

GP77-0840-46

FIGURE A-28
FMS F-4E(S) SEVERE AIR-TO-AIR - LRS 70
OCCURRENCES PER 500 HRS

Max % DLS	Minimum % DLS			
	0.160	–0.051	–0.154	–0.256
0.359	3748	57	3	2
0.461	1978	168	9	5
0.564	1231	54	3	2
0.666	771	21	2	1
0.768	525	8	1	
0.871	331	5		
0.973	165	2		
1.076	49	1		
1.178	8			

100% DLS = 24.4 ksi

GP77-0840-47

FIGURE A-28 (Continued)
FMS F-4E(S) SEVERE AIR-TO-GROUND - LRS 70
OCCURENCES PER 300 HRS

Max % DLS	Minimum % DLS			
	0.148	−0.051	−0.154	−0.256
0.359	610	35	3	
0.461	210	107	6	2
0.564	97	36	2	1
0.666	33	13		
0.768	11	6		
0.871	6	3		
0.973	2	2		
1.076	2			

100% DLS = 24.4 ksi

GP77-0840-48

FIGURE A-28 (Concluded)
FMS F-E(S) SEVERE NON-TACTICAL - LRS 70
OCCURRENCES PER 200 HRS

Max % DLS	Minimum % DLS				
	0.138	–0.040	–0.119	–0.198	–0.278
0.437	13,694	805	393	103	5
0.516	7,354	1,318	720	103	5
0.595	3,982	1,202	655	154	7
0.675	1,097	1,790	851	154	8
0.753	1,113	920	459	103	5
0.833	495	624	328	51	2
0.912	330	385	225	50	
0.992	123	228	153		
1.071	40	34	15		
1.150	1				

100% Stress = 31.5 ksi
LRS 70

GP77-0840-49

FIGURE A-29
F-4E T-BIRD SOLO OCCURRENCES PER 1000 HRS

Max % DLS	Minimum % DLS					
	0.166	0.020	–0.051	–0.154	–0.256	–0.359
0.359	3220	222	101	8	2	1
0.461	1552	566	259	21	4	4
0.564	1066	245	112	9	3	1
0.666	554	84	39	4	1	
0.768	281	35	16	1		
0.871	150	20	9	1		
0.973	112	17	8			
1.076	62	17	8			
1.178	19					
1.332	0.3					

100% DLS = 24.4 ksi

GP77-0840-51

FIGURE A-30
F4E(S) SERIAL NO. 711072 AIR-TO-AIR - LRS 70
OCCURRENCES PER 260 HRS

Max % DLS	Minimum % DLS			
	0.160	0.020	– 0.051	– 0.154
0.359	7970	282	75	4
0.461	4470	834	222	12
0.564	2717	254	68	4
0.666	1513	100	27	1
0.768	831	38	10	1
0.871	440	22	6	
0.973	186	12	3	
1.076	28	9	3	
1.178	5			
1.332	0.2			

100% DLS = 24.4 ksi

GP77-0840-52

FIGURE A-30 (Continued)
F-4(S) SERIAL NO. 711072 AIR-TO-GROUND - LRS 70
OCCURRENCES PER 490 HRS

Max % DLS	Minimum % DLS				
	0.148	0.020	−0.051	−0.154	−0.256
0.359	1020	67	18	1	
0.461	303	196	54	3	1
0.564	143	60	17	1	
0.666	47	23	6		
0.768	16	9	2		
0.871	7	4	1		
0.973	3	3	1		
1.076	2	1			
1.178	1				

100% DLS = 24.4 ksi

GP77-0840-7

FIGURE A-30 (Concluded)
F-4E(S) SERIAL NO. 711072 NON-TACTICAL - LRS 70
OCCURRENCES PER 250 HRS

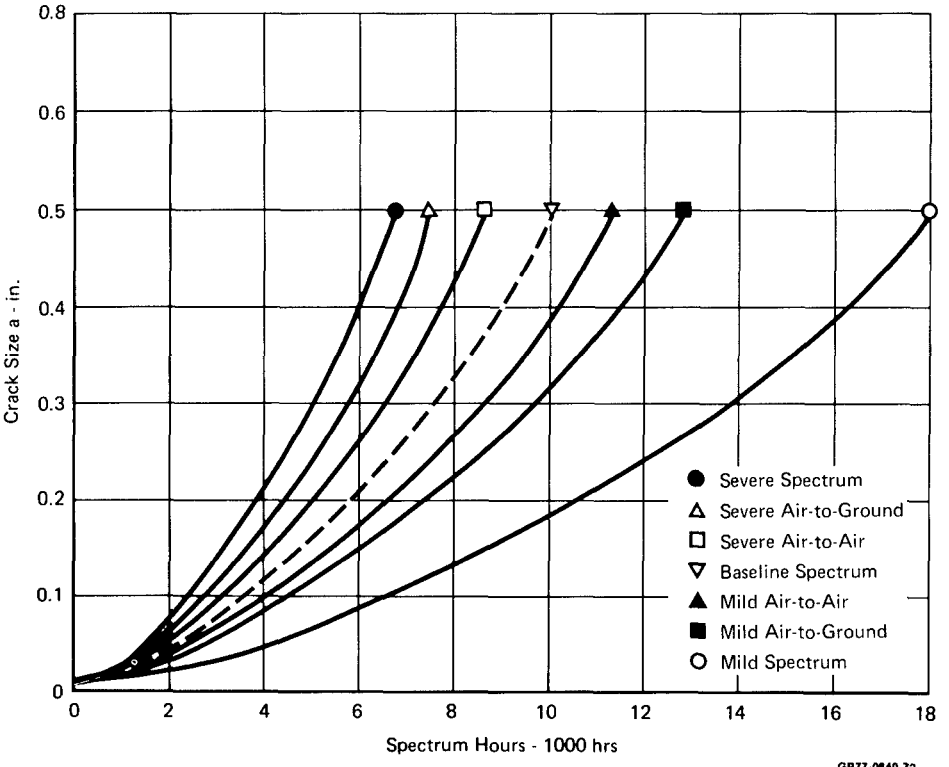

FIGURE A-31
LRS 70 MISSION PARAMETER VARIATIONS
Load Factor Exceedance

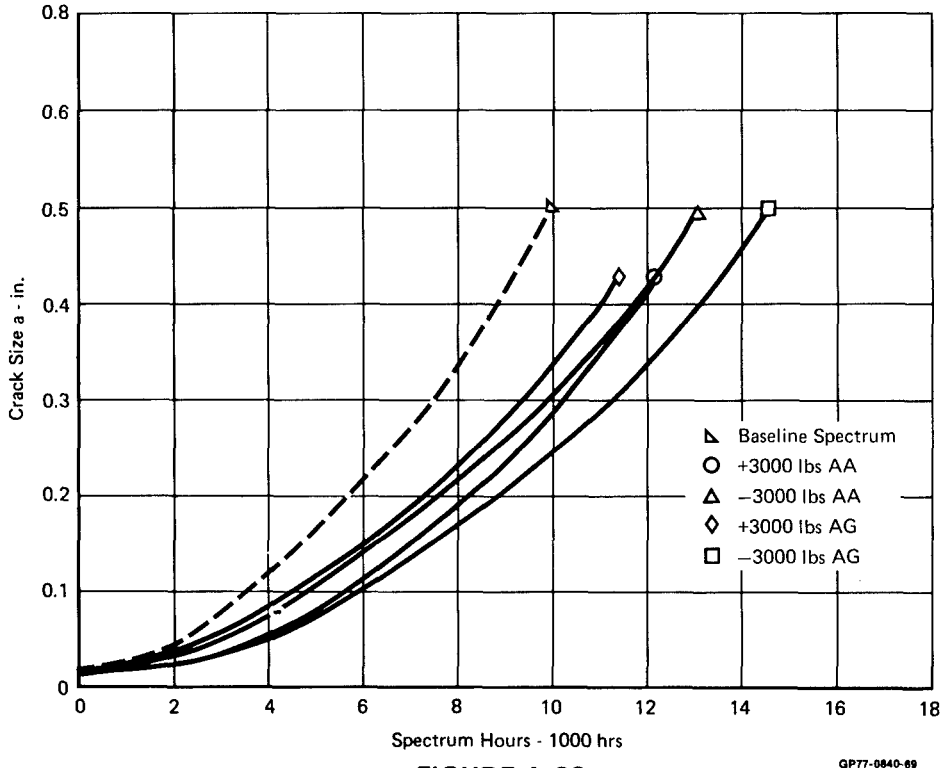

FIGURE A-32
LRS 70 (WING) GROSS WEIGHT VARIATIONS

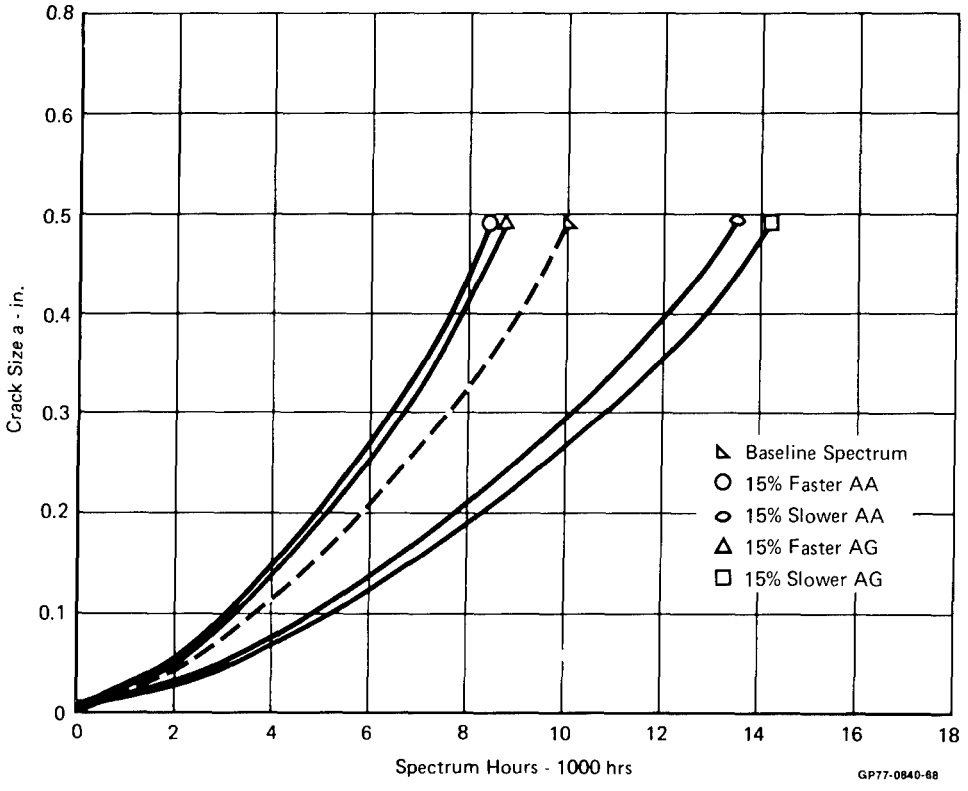

FIGURE A-33
LRS 70 (WING) AIRSPEED VARIATIONS

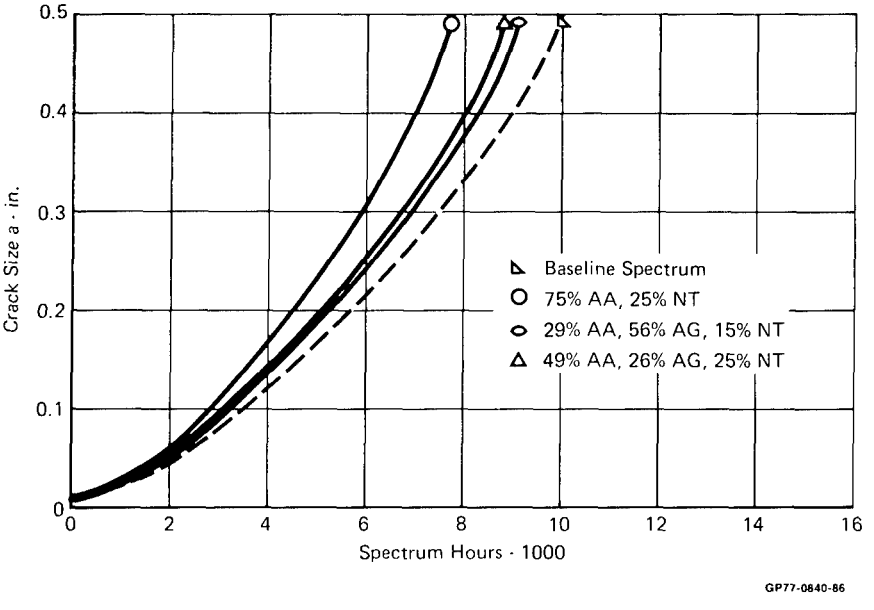

FIGURE A-34
LRS 70 (WING) MISSION MIX VARIATIONS

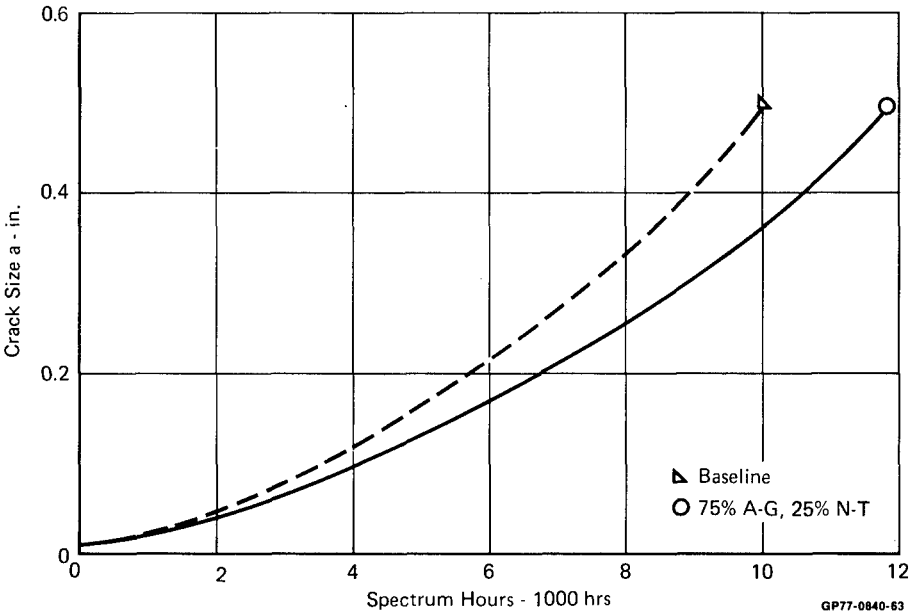

FIGURE A-35
LRS 70 MISSION PARAMETER VARIATIONS
75% Air-to-Ground, 25% Non-Tactical

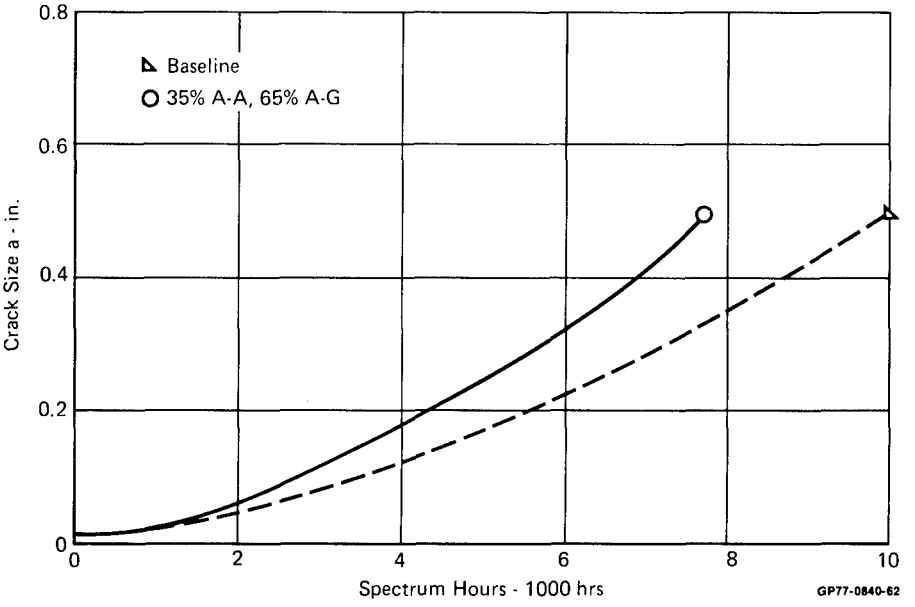

FIGURE A-36
LRS 70 MISSION PARAMETER VARIATIONS
35% Air-to-Air, 65% Air-to-Ground

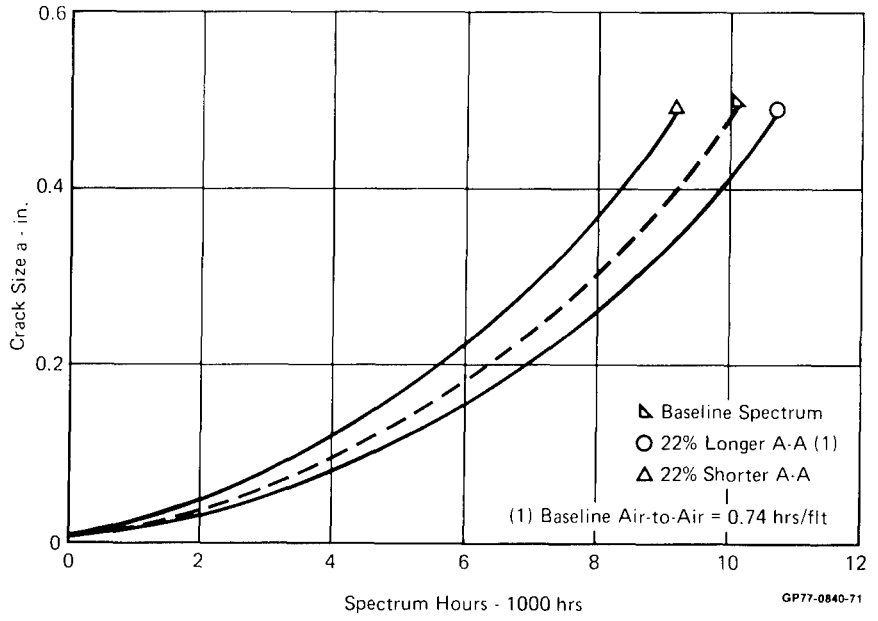

FIGURE A-37
LRS 70 (WING) MISSION DURATION VARIATIONS

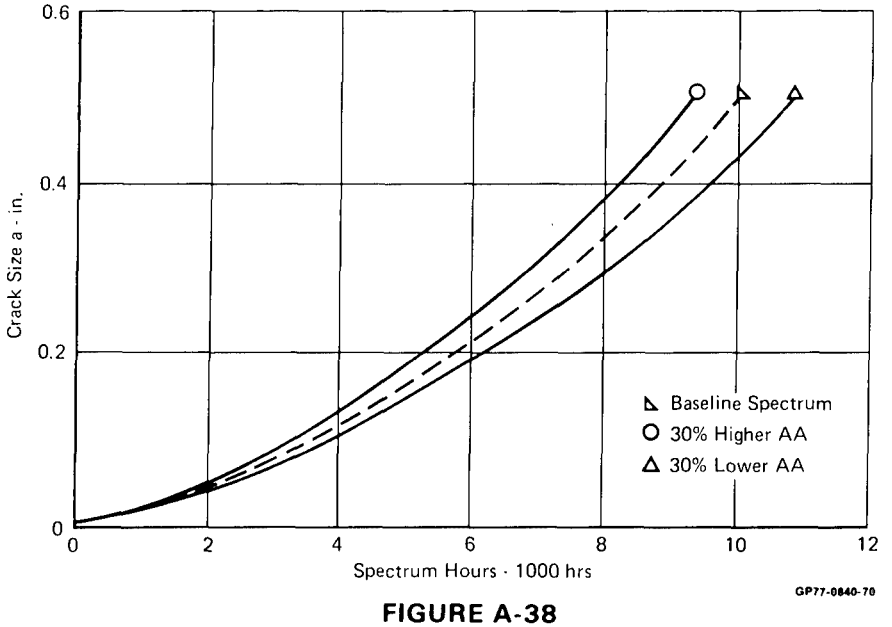

FIGURE A-38
LRS TO (WING) ALTITUDE VARIATIONS

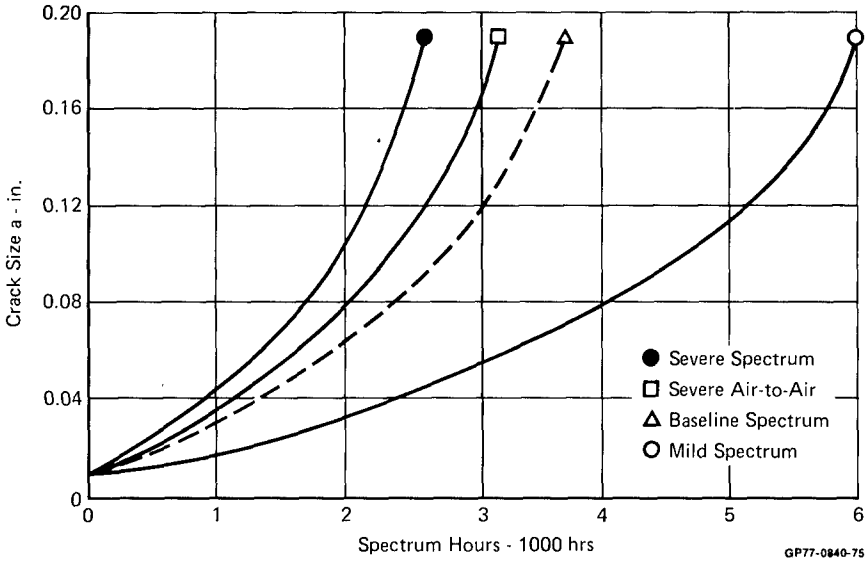

FIGURE A-39
FS 303 MISSION PARAMETER VARIATIONS
Load Factor Exceedance

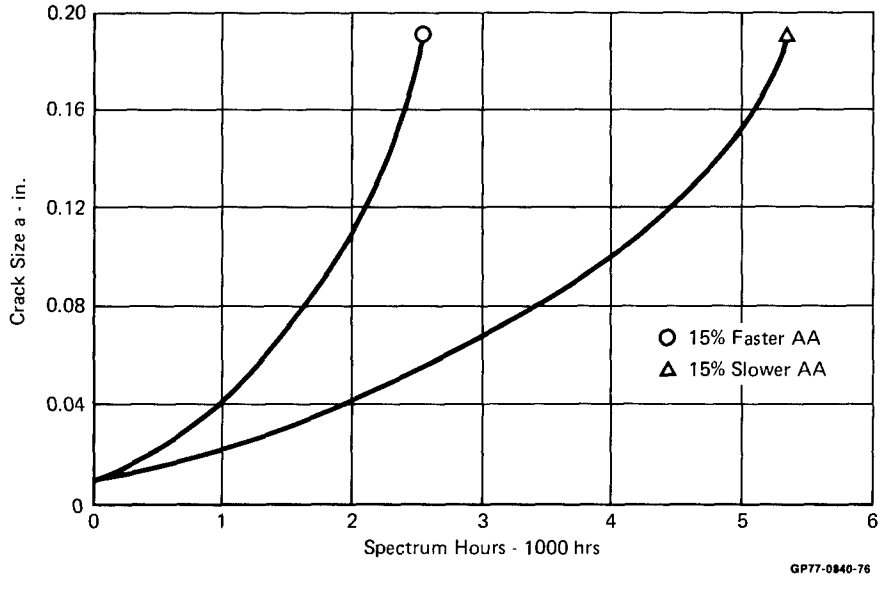

FIGURE A-40
FS 303 AIRSPEED VARIATION

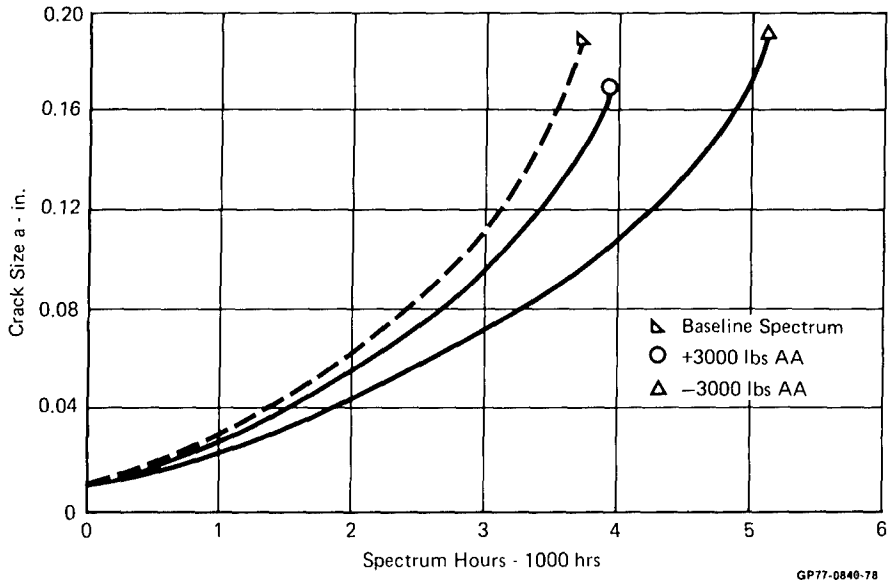

FIGURE A-41
FS 303 GROSS WEIGHT VARIATIONS

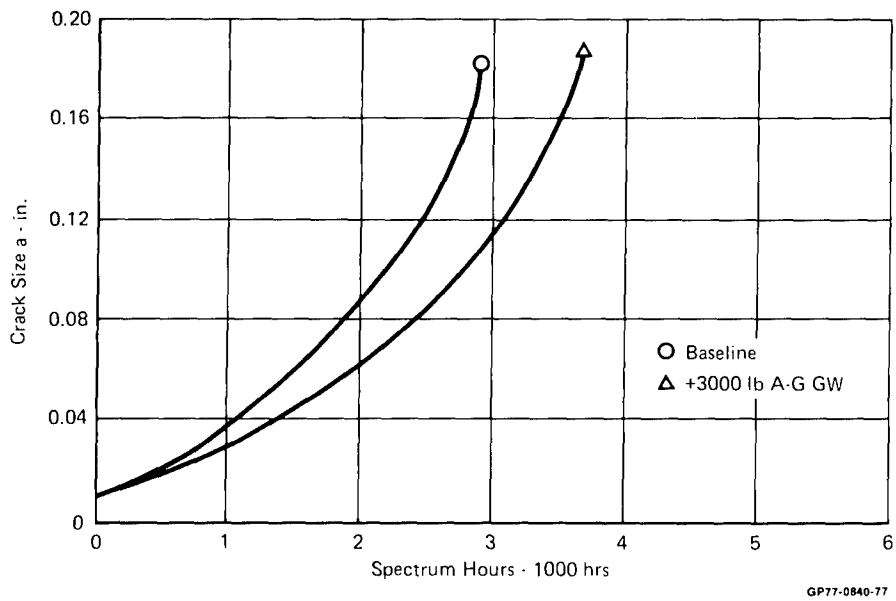

FIGURE A-42
FS 303 MISSION PARAMETER VARIATIONS
+3000 Lb Air-to-Ground Gross Weight

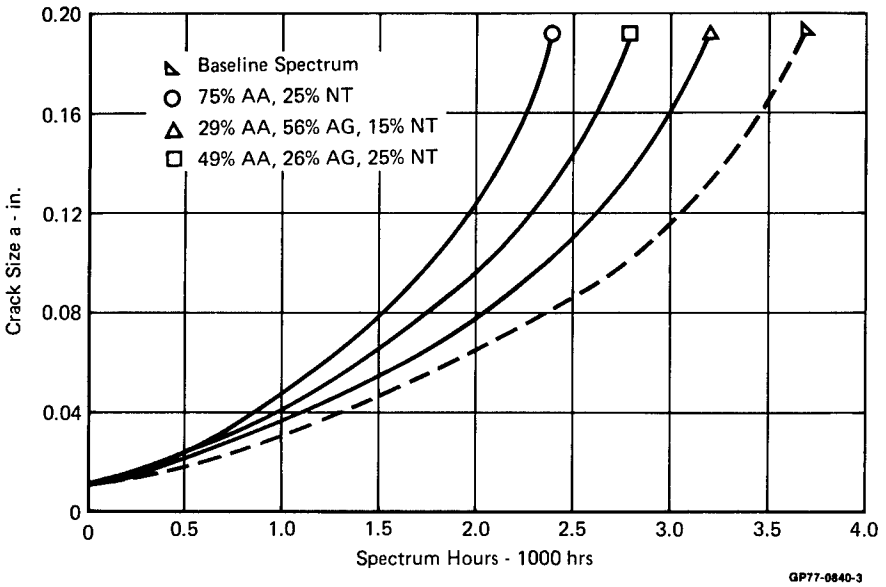

FIGURE A-43
FS 303 MISSION MIX VARIATION

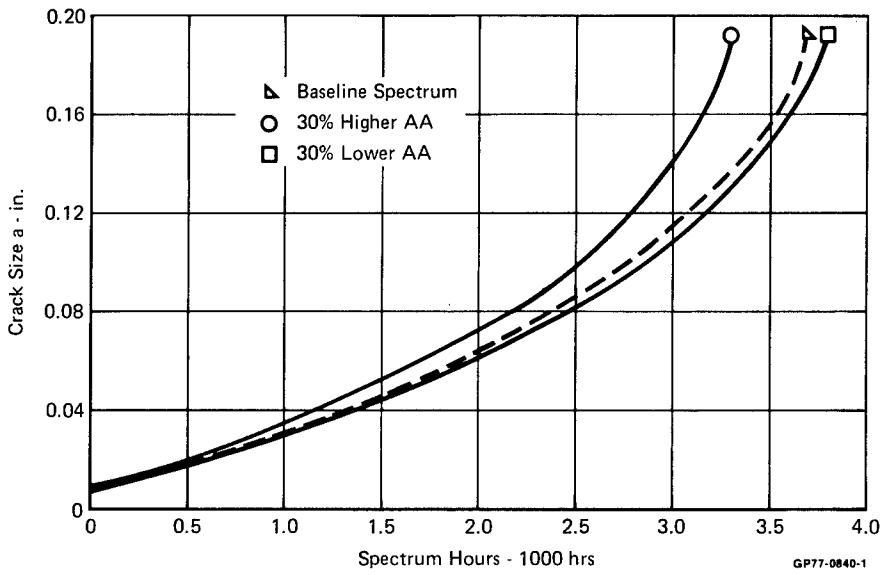

FIGURE A-44
FS 303 ALTITUDE VARIATION

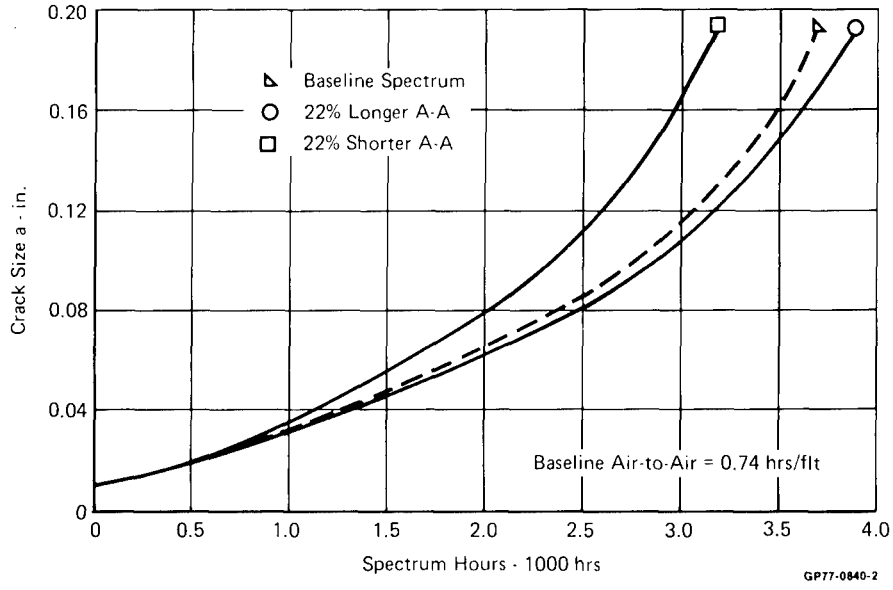

FIGURE 45
FS 303 MISSION DURATION VARIATION

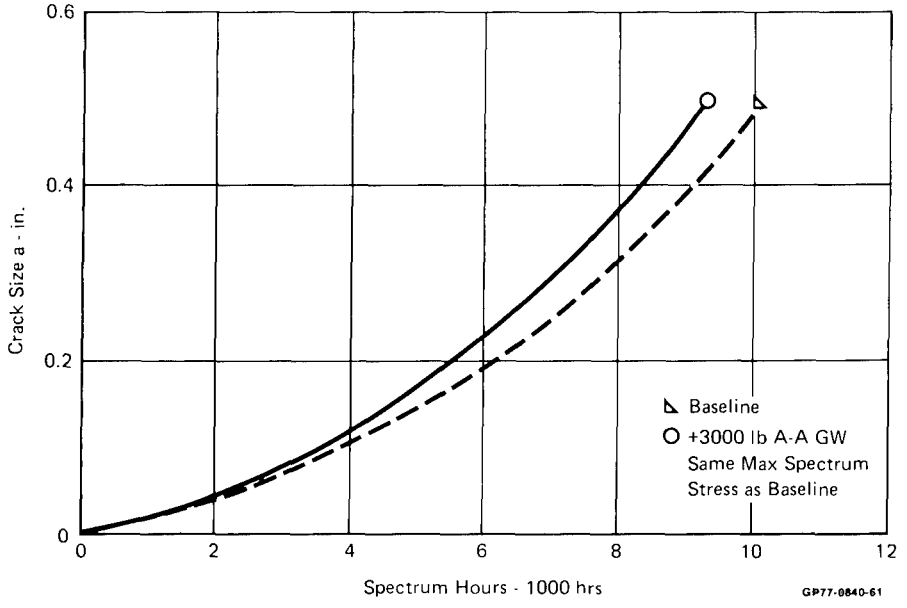

FIGURE A-46
LRS 70 MISSION PARAMETER VARIATIONS
+3000 Lb Air-to-Air Gross Weight

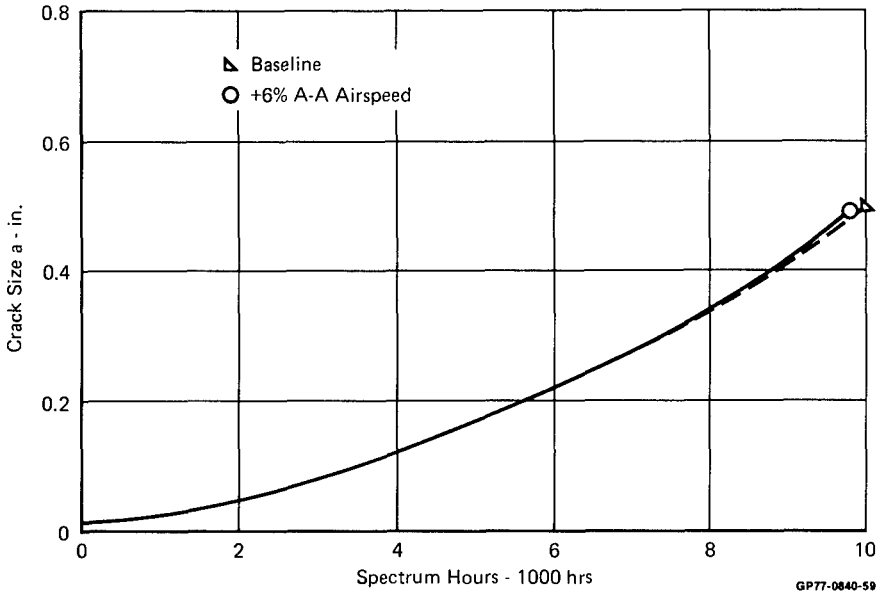

FIGURE A-47
LRS 70 MISSION PARAMETER VARIATIONS
+6% Air-to-Air Airspeed

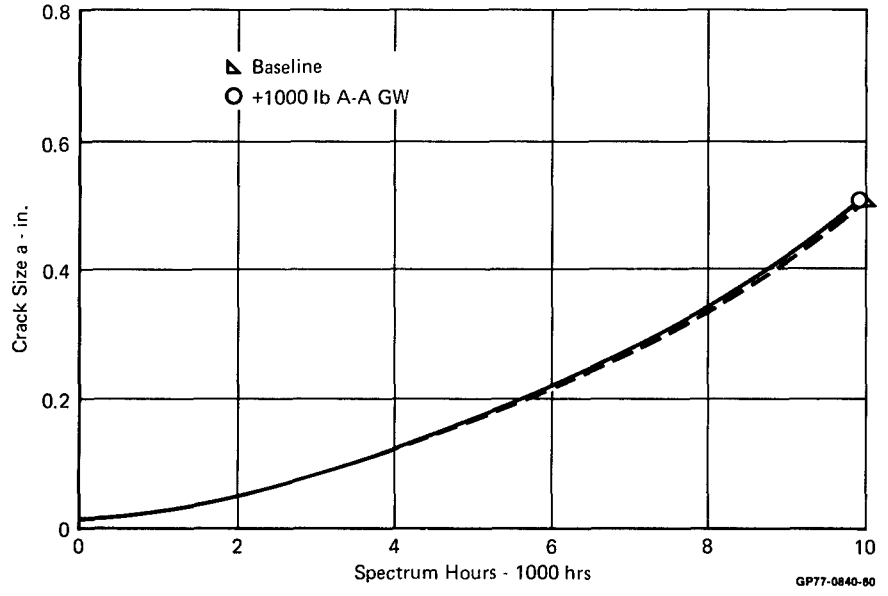

FIGURE A-48
LRS 70 MISSION PARAMETER VARIATIONS
+1000 Lb Air-to-Air Gross Weight

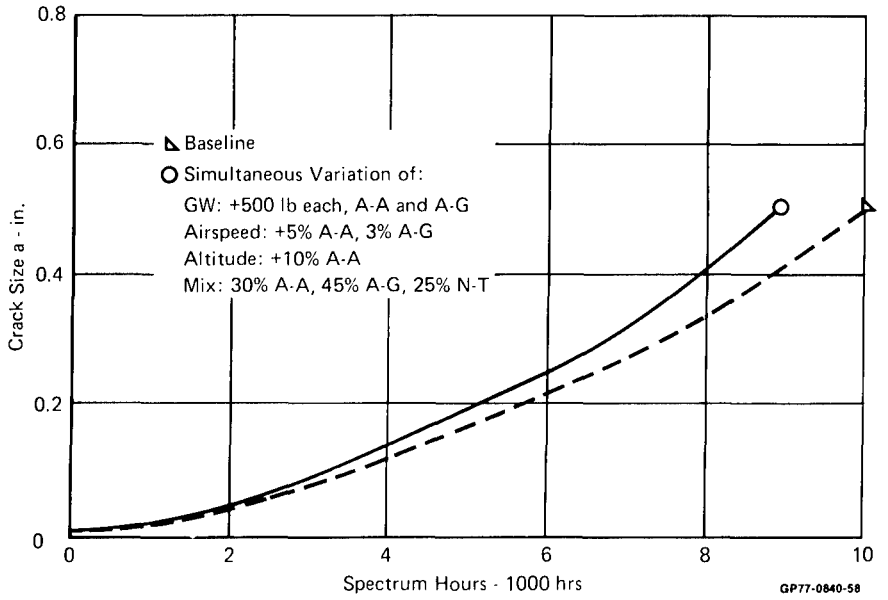

FIGURE A-49
LRS 70 MISSION PARAMETER VARIATIONS
Simultaneous Variation

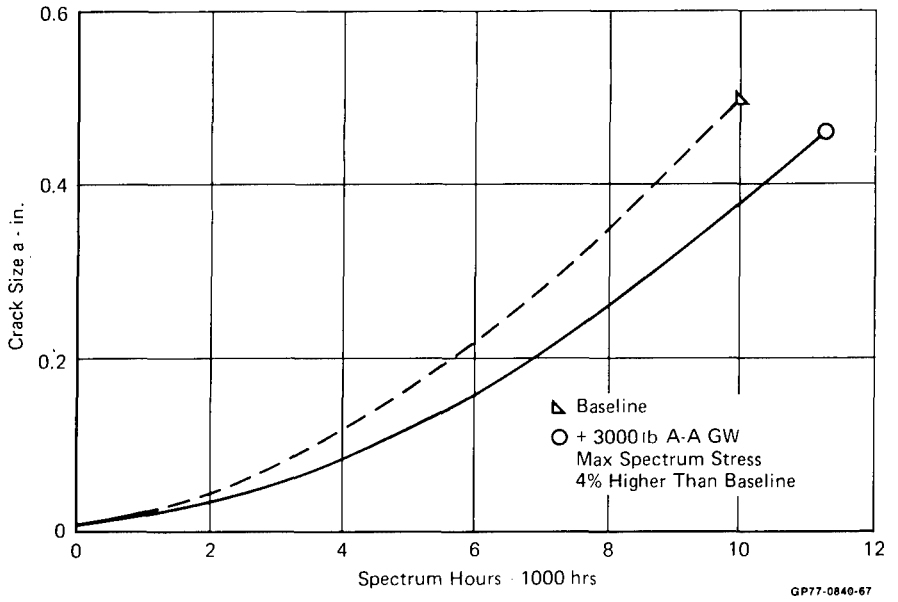

FIGURE A-50
LRS 70 MISSION PARAMETER VARIATIONS
+3000 Lb Air-to-Air Gross Weight

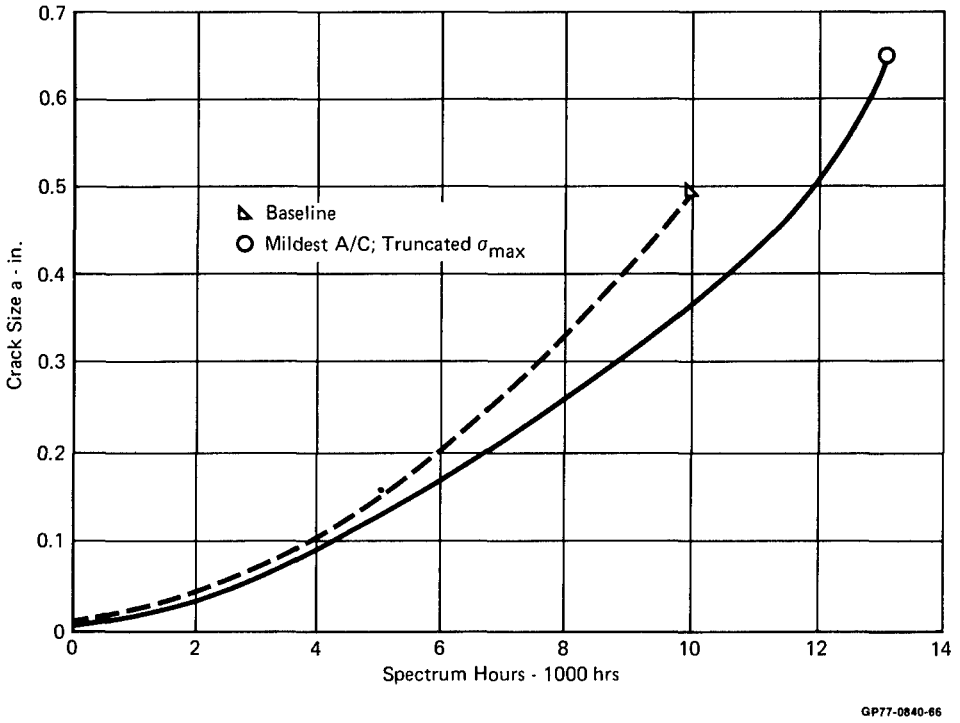

FIGURE A-51
LRS 70 MISSION PARAMETER VARIATIONS
Mildest Aircraft - Truncated σMax

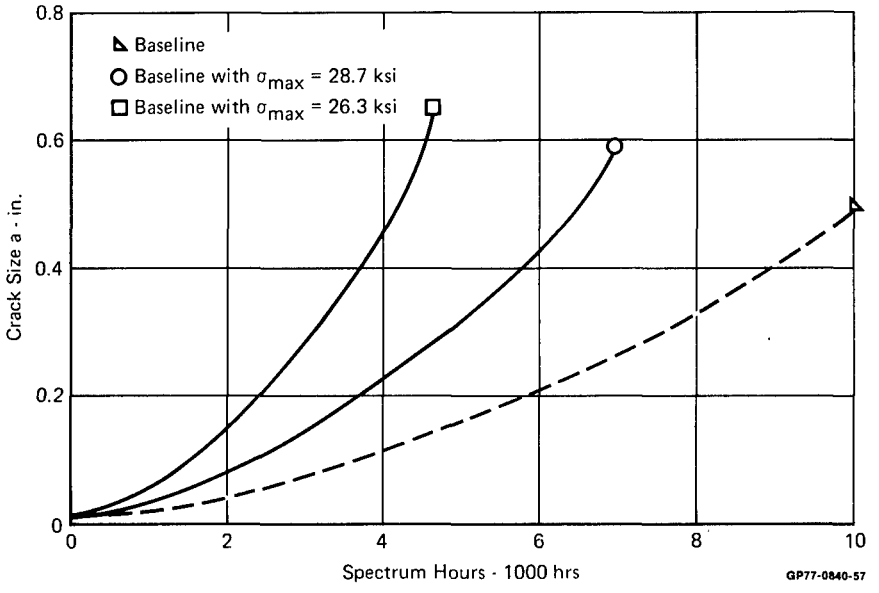

FIGURE A-52
LRS 70 MISSION PARAMETER VARIATIONS
Variation of Baseline σ_{Max}

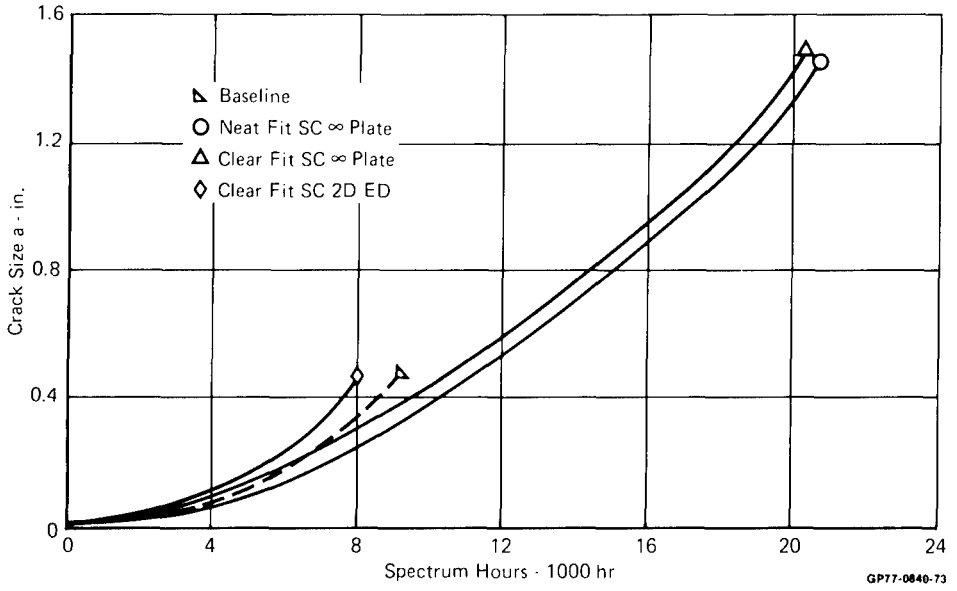

FIGURE A-53
LRS 70 GEOMETRIC K_T

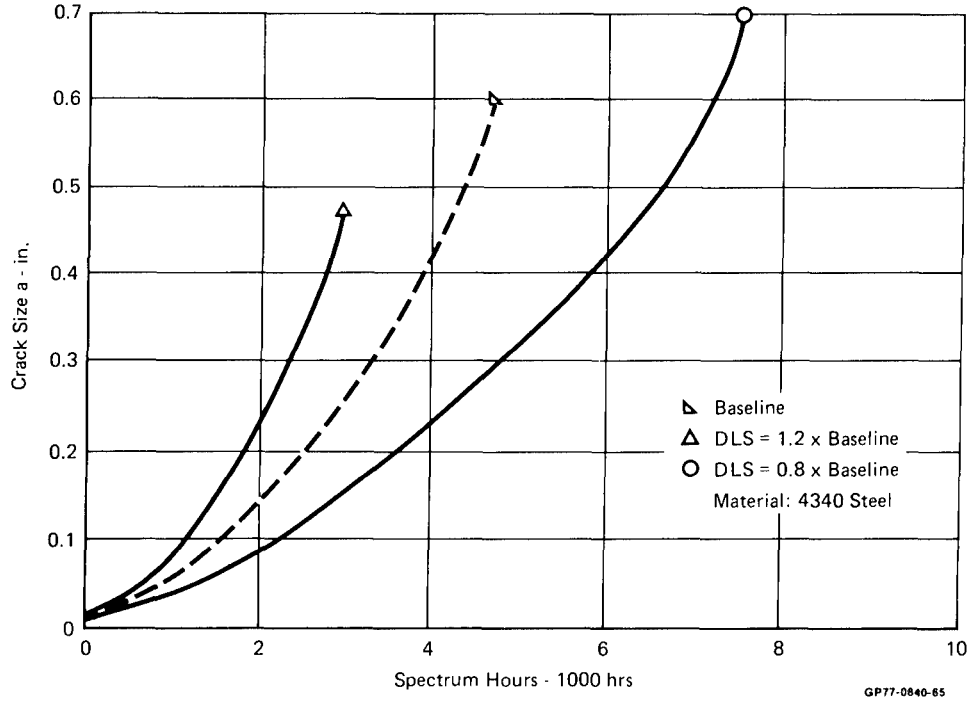

FIGURE A-54
LRS 70 WING MATERIAL VARIATION
DLS = 68.3 Ksi

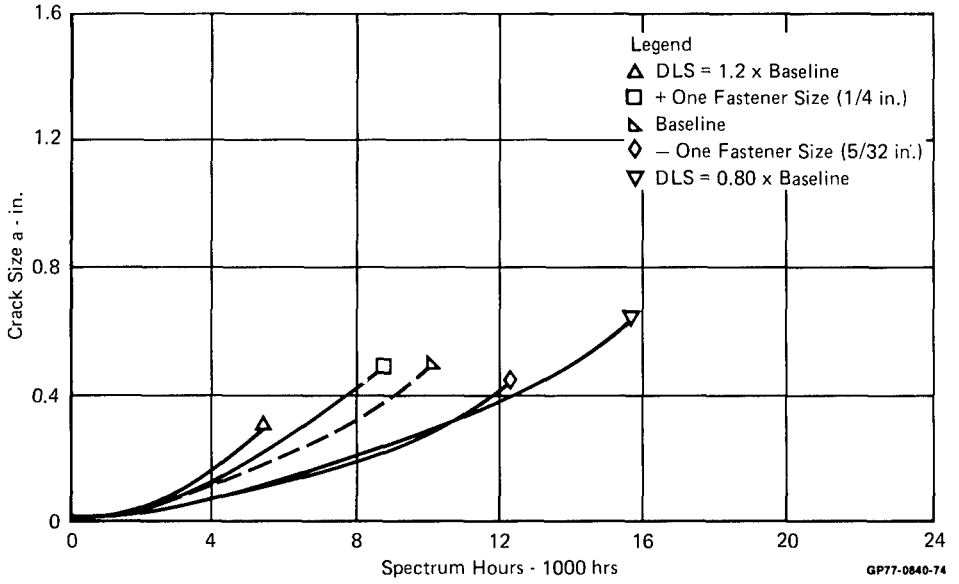

FIGURE A-55
LRS 70 DESIGN PARAMETER VARIATIONS

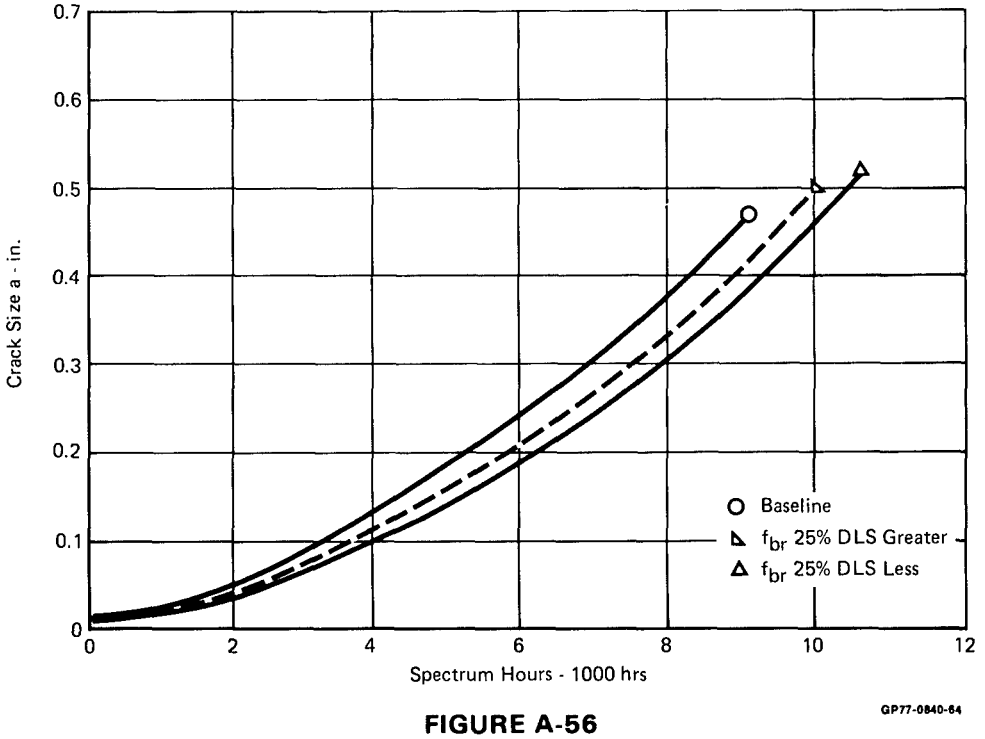

FIGURE A-56
LRS 70 BEARING STRESS

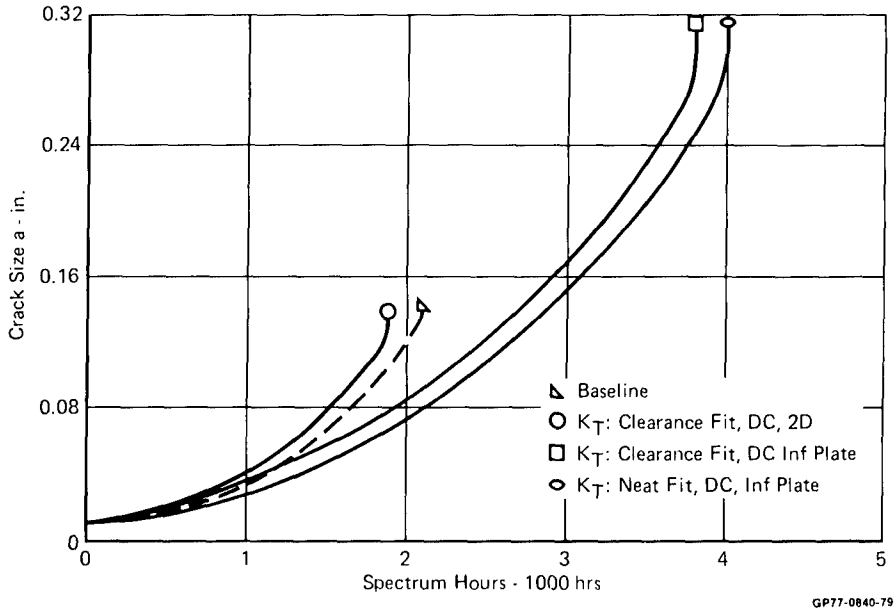

FIGURE A-57
FS 303 DESIGN PARAMETER VARIATIONS
K_T Variations

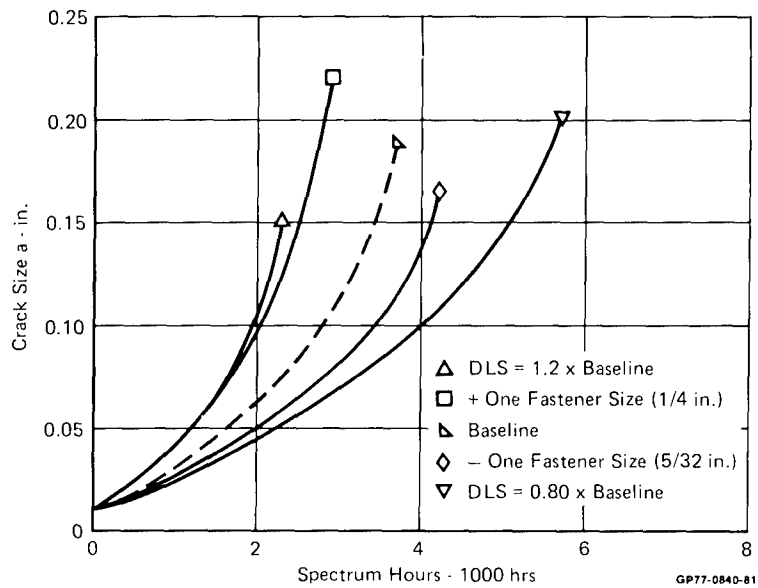

FIGURE A-58
FS 303 DESIGN PARAMETER VARIATIONS

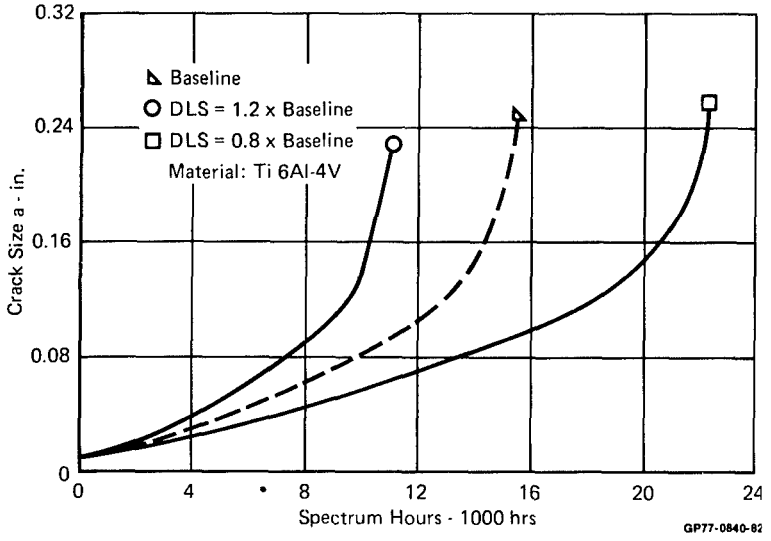

FIGURE A-59
FS 303 DESIGN PARAMETER VARIATIONS
Design Limit Stress
DLS = 30.1 Ksi

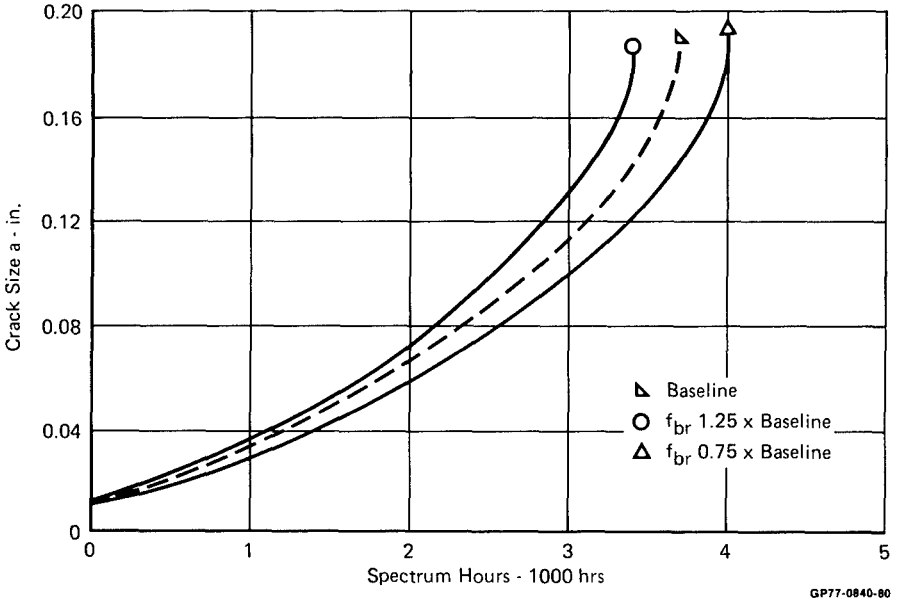

FIGURE A-60
FS 303 BEARING STRESS VARIATION

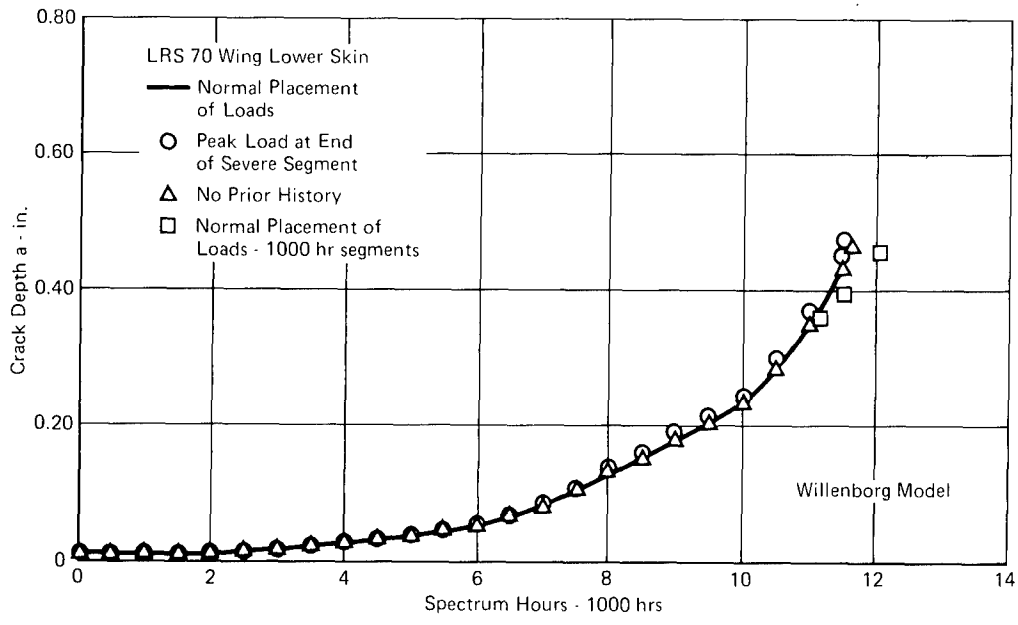

FIGURE A-61
SEQUENCE NO. 1
F-4 BASELINE→FMS SEVERE→FMS MILD

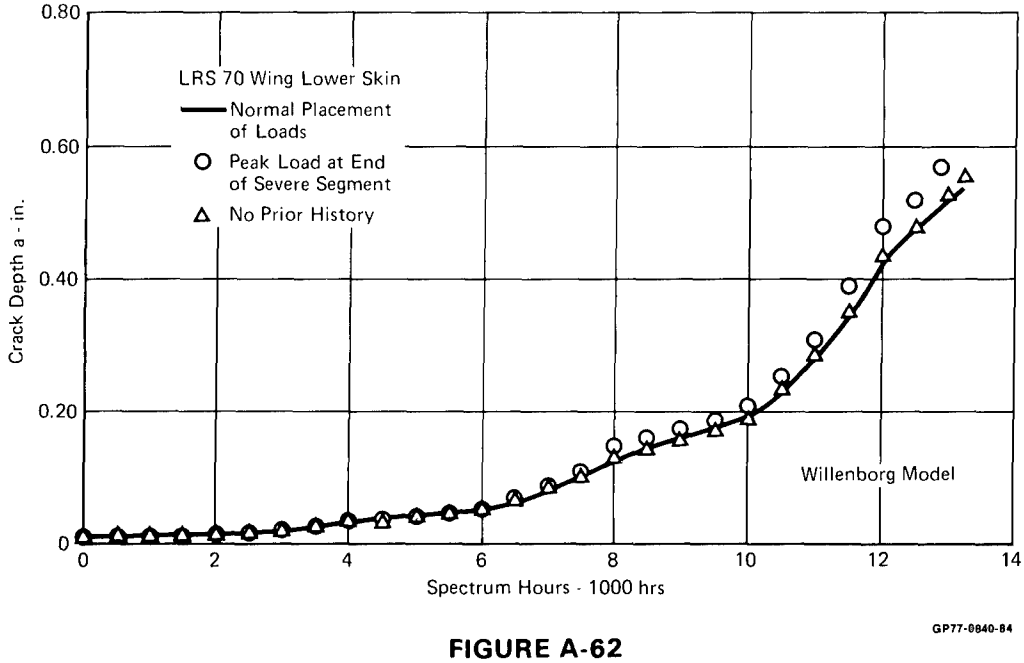

FIGURE A-62
SEQUENCE NO. 2
F-4 MILD→F-4 SEVERE→F-4 MILD

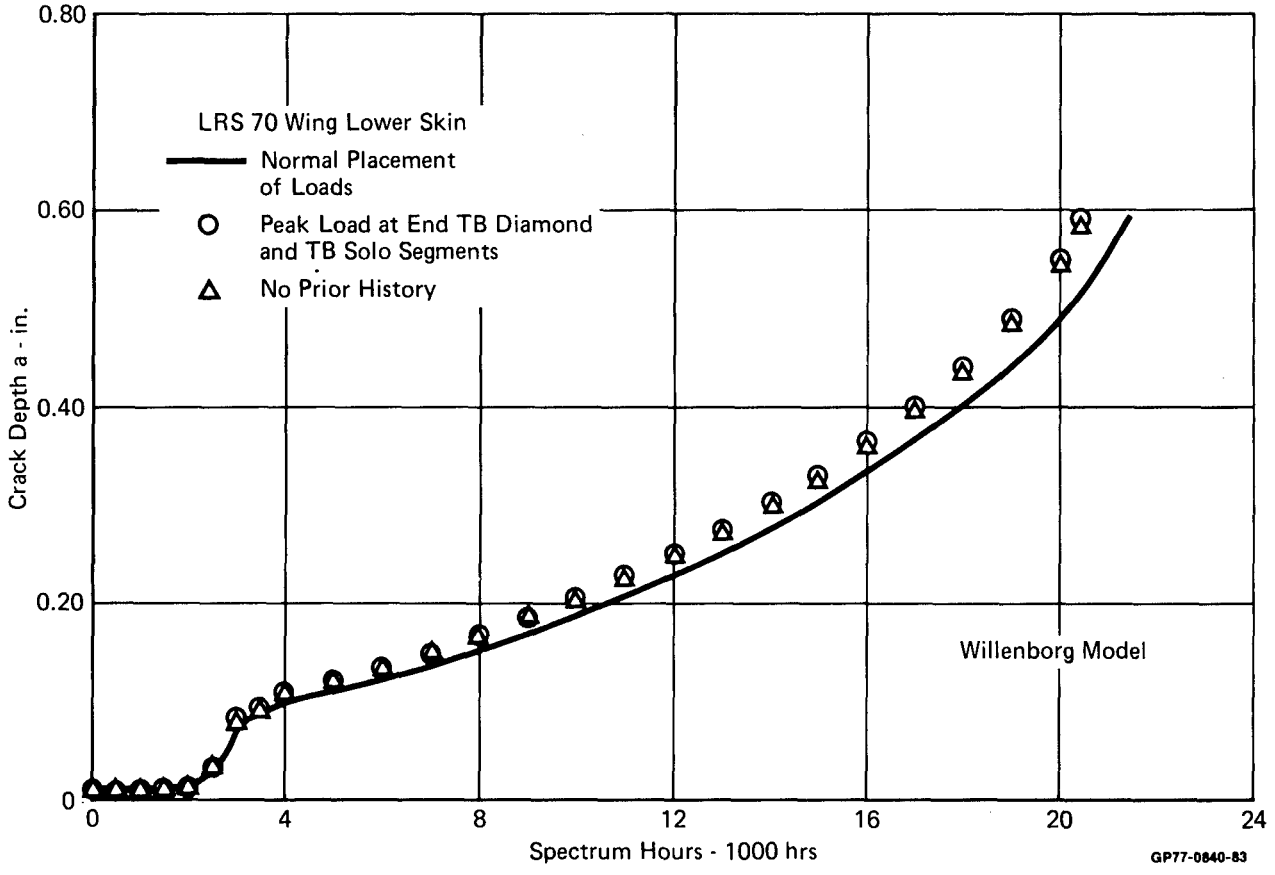

FIGURE A-63
SEQUENCE NO. 3
F-4 BASELINE→T-BIRD DIAMOND→T-BIRD SOLO→T-BIRD DIAMOND→F-4 BASELINE

☆U.S.Government Printing Office: 1977 — 757-080/176